CANADIAN THESES

THÈSES CANADIENNES

NOTICE

The quality of this microfiche is heavily dependent upon the quality of the original thesis submitted for microfilming. Every effort has been made to ensure the highest quality of reproduction possible.

If pages are missing, contact the university which granted the degree.

Some pages may have indistinct print especially if the original pages were typed with a poor typewriter ribbon or if the university sent us an inferior photocopy.

Previously copyrighted materials (journal articles, published tests, etc.) are not filmed.

Reproduction in full or in part of this film is governed by the Canadian Copyright Act, R.S.C. 1970, c. C-30.

AVIS

La qualité de cette microfiche dépend grandement de la qualité de la thèse soumise au microfilmage. Nous avons tout fait pour assurer une qualité supérieure de reproduction.

S'il manque des pages, veuillez communiquer avec l'université qui a conféré le grade.

La qualité d'impression de certaines pages peut laisser à désirer, surtout si les pages originales ont été dactylographiées à l'aide d'un ruban usé ou si l'université nous a fait parvenir une photocopie de qualité inférieure.

Les documents qui font déjà l'objet d'un droit d'auteur (articles de revue, examens publiés, etc.) ne sont pas microfilmés.

La reproduction, même partielle, de ce microfilm est soumise à la Loi canadienne sur le droit d'auteur, SRC 1970, c. C-30.

THIS DISSERTATION
HAS BEEN MICROFILMED
EXACTLY AS RECEIVED

LA THÈSE A ÉTÉ
MICROFILMÉE TELLE QUE
NOUS L'AVONS REÇUE

Canada

NL-339 (r.86/06)

ADAPTIVE FORWARD ERROR CONTROL CODING FOR KA-BAND SATELLITE LINKS

MUZIBUL HAYAT KHAN

A Thesis
In
The Department
of
Electrical Engineering

Presented in Partial Fulfillment of the Requirements
for the Degree of Doctor of Philosophy at
Concordia University
Montréal, Québec, Canada

July 1986

ISBN 0-315-32252-7

ABSTRACT

ADAPTIVE FORWARD ERROR CONTROL CODING FOR Ka-BAND SATELLITE LINKS

Muzibul Hayat Khan, Ph.D.
Concordia University, 1986

Adaptive fade margin is required to counter the severe but varying rain attenuation in Ka-band Satellite communications. In order to determine a suitable rain counter-measure, the effectiveness of Adaptive Forward Error Control Coding (AFEC) scheme is studied.

At first, rain attenuation characteristics in Ka-bands is investigated. A seasonal and diurnal change in rain attenuation pattern is observed in this frequency band. Due to the variable attenuation, dedicated resource rain counter-measure schemes are shown to be less efficient and not cost-effective compared to adaptive resource sharing schemes.

Implementation aspects of adaptive resource sharing schemes are studied and AFEC resource sharing is found to be best suited as a rain countermeasure scheme. Two AFEC schemes using convolutional codes and concatenated codes are proposed and their performance analyzed. The schemes can provide a progressively adaptive fade margin of 10.1 and 10.4 dB respectively in excess of systems fixed fade margin.

To improve the efficient use of shared resources of the system an AFEC scheme using double coding is introduced and its performance analyzed. In this

scheme a single codec is used repeatedly, as a result hardware cost reduces and its utilization increases. It is shown that convolutional and Golay double coding schemes can provide an adaptive fade margin of 10.8 dB and 8.1 dB respectively. Although concatenated codes have slightly better performance than double codes, hardware implementation and decoding complexity of the latter is significantly less.

For effective operation of double codes interleaving/deinterleaving is required. Analysis of suitable interleaving/deinterleaving is given. The results show that Block interleaving is advantageous for double coding using block codes.

Implementation complexity of a conceptual AFEC resource sharing scheme using Golay double coding is analyzed in light of time frame expansion, link condition monitoring, signalling , etc. It is concluded that the scheme can be adapted to the present DA-TDMA system technology.

DEDICATED TO MY PARENTS

ACKNOWLEDGEMENT

I owe a great debt of gratitude to Dr. V.K. Bhargava and Dr. T. Le-Ngoc for their guidance, encouragement and friendship during the research and throughout my graduate studies at Concordia University. I would also like to thank Dr. G.E. Seguin, Dr. D. Haccoun and Dr. J. Conan for many valuable discussions. Sincere thanks are extended to several colleagues for their useful discussions and assistances.

I would like to express my appreciation for the financial support provided by NSERC, Grant Number G-0878, awarded under their strategic grant program.

Mr. B.K. Datta deserves a special word of thanks for his help in typing the manuscript and preparation of figures on a very tight schedule.

I am grateful to Dr. A.L. Sher, Dr. S.M. Faruque and other friends for their indispensable encouragement and help.

I can only hint at the debt I owe to my wife Chumki and our parents, for the patience, faith, constant support and encouragement during my four years of graduate studies. And finally, a word for my son Kishore, whose innocent demands made the last part of the work even tougher, who also provided a lot of enjoyment during the enormous task of completing the thesis.

Table of Contents

List of Figures

List of Tables

CHAPTER ONE

INTRODUCTION

The problem of reliable communication over long distance has found an efficient solution via satellites. As the demand for satellite communication increases and technology develops, the number of satellites in orbit also increases. To serve these ever increasing demands, conventional C-band* satellite systems are joined by high frequency Ku-bands** systems. A NASA sponsored study in 1980 [1.1] showed that rapidly increasing demands for U.S. domestic satellite communications services would probably saturate the orbit space and frequency allocations at C- and Ku-bands near the end of this decade.

With the development of technology in recent years there has been tremendous improvement in the capability of transponders to handle more throughput. The capacity of a typical (36 MHz) transponder has grown from a few hundred circuits in the early 1970's to 1000 or more today. Within the next decade, individual transponder capacities of up to 3000 circuits are expected to be in operation through advanced modulation and source coding techniques.

The estimated capacity limit of domestic satellite using C- and Ku-band frequencies has also increased from the earlier estimate of 430 transponders to about 1200 transponders. It may be seen from Fig. 1.1 that the C- and Ku-bands will be saturated in the early 1990's. In fact, given current orbit spacing con-

---

* 3.7-4.2 GHz Down/ 5.925-6.425 GHz Up

** 10.95-11.2 GHz Down, 11.45-11.7 Down/ 14-14.5 GHz Up

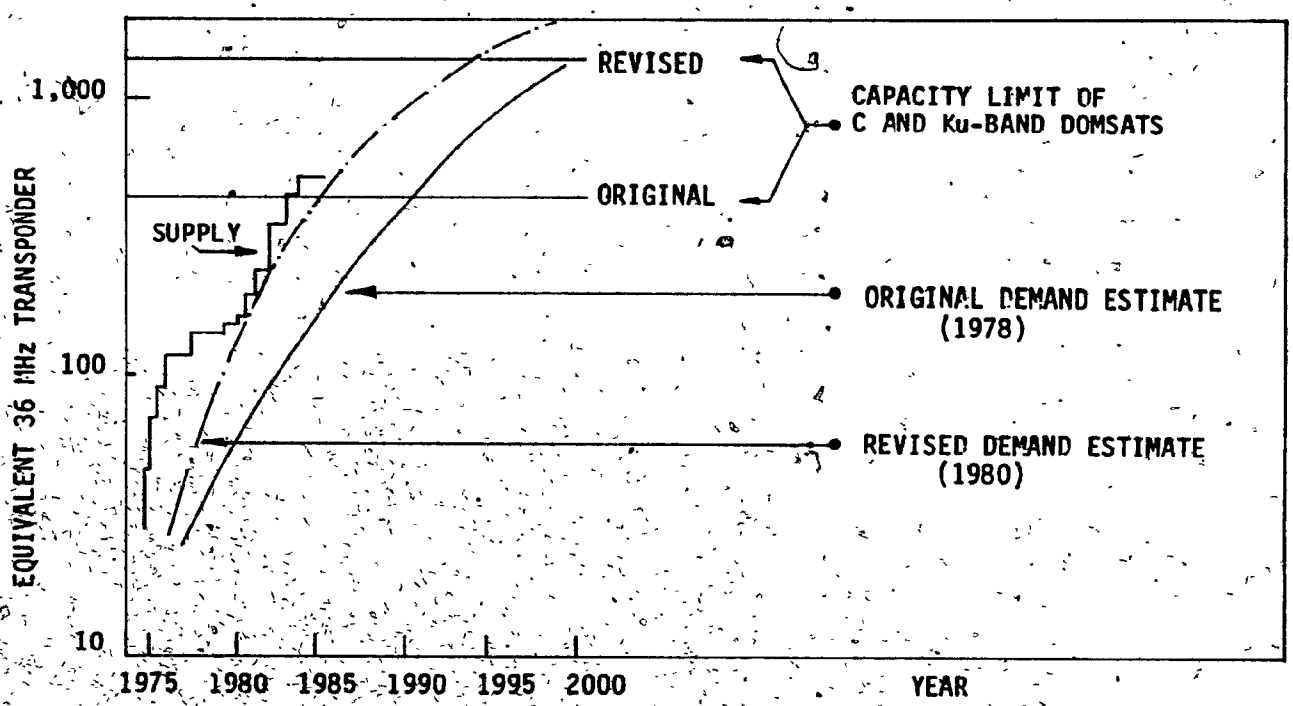

Fig. 1.1 U.S. domestic satellite demand and supply (from [1.1]).

straints (4^0 between C-band satellites and 3^0 between Ku-band satellites), the orbit space for existing and planned C-band domestic satellite is already saturated. Closer spacing currently under consideration by the CCIR (down to 2^0 at C-band) potentially offers additional orbit capacity but it is not expected that this would delay the saturation by more than a few years.

For this reason, the communication satellite technology program is focused on the Ka-bands*** which is the next higher frequency band above the C- and Ku-bands allocated for fixed domestic satellite service. The primary attraction of this band is the 2.5 GHz bandwidth available for communication purposes, which is five times that of either the C- or Ku-bands. This large bandwidth can accommodate the increased traffic capacity.

A distinct advantage of the high frequencies lies in their ability to generate multiple spot beams with small size antennas. For spot beams which serve spatially separated regions, the same frequency can be used without causing any interference. This, in conjunction with the size reduction of all RF systems on the spacecraft permitted by the higher frequencies, allows the construction of very high capacity satellites that require only modest weight and size increases when compared to current satellites. As a result, the potential cost per circuit may be considerably lower than that of current systems.

One of the major problem in communicating at these frequencies is the high level of attenuation encountered. Measured data obtained from the south-east portion of the United States indicates that rain attenuation exceeds 40 dB at the 30 GHz uplink frequency and 20 dB at the 20 GHz downlink frequency more than 0.1% of the time [1.1]. Hence, a high fade margin is required to meet the standard availability requirement of 99.99%.

*** 17.7-21.2 GHz Down/ 27.5-31 GHz Up

Keeping the high fade margin means lower satellite power for the communication link and as a consequence, a lower signal-to-noise ratio (SNR) for the same noise power. Hence, the available power will support fewer channels. Moreover, the rain attenuation encountered is not uniformly distributed. They have seasonal and diurnal variations which show that severe rain fade is an irregular but unavoidable phenomenon. This is because severe rain attenuation is associated with heavy downpours and thunderstorms [1.2]. During a thunderstorm, rain attenuation is much higher than its average value. These attenuation levels are too large to be overcome by power control alone.

The conventional method which is generally used to achieve reliable communications in the face of such high levels of rain attenuation is called site diversity, two antennas at two different sites supporting one ground station. The sites are connected by a terrestrial link. This is based on the fact that since rain cells are limited in extent to several miles, the probability that both terminals of an earth station simultaneously experience large rain attenuation is low. This can be diminished by increasing the distance between the terminals.

With the introduction of Ka-band satellite communication systems, it will be possible to offer various types of services such as customer premises services, public broadcasting services, individual communication system through satellite, etc. But site diversity cannot be implemented for such cases because the cost of such an arrangement will be prohibitive. Even for higher traffic links, maintaining site diversity is not an easy task because of the cost and complexity related in connecting two stations by radio-relay link or cable link.

Furthermore, conventional techniques of rain attenuation counter-measure using dedicated resources of large fixed link margin or the alternative of widely applied site diversity are fully used only during occasional heavy rainstorms (i.e.

$\approx$ 0.1% of the time). The rest of the time they do not utilize their full potential. To achieve a cost effective solution, it is necessary to use adaptive measures. These measures will help to overcome rain attenuation at the time of its occurrence. They will also change adaptively with the intensity of attenuation. To enhance the effectiveness of the above scheme a reserved pool of rain counter-measure resources can be created and shared among the users when needed.

Usually the earth stations of a satellite system are situated far apart from each other. Hence, at any instant of time, only a few earth stations will experience rain attenuation and require use of the resource pool. This minimizes the size of the required resource pool. Reduction in resource pool size increases the overall effective usable capacity of the system.

1.1 Thesis outline

The aim of this thesis is to survey and compare the effectiveness of dedicated rain counter-measure schemes and adaptive resource sharing rain counter-measure schemes for Ka-band satellite systems and investigate the performance and feasibility of a suitable scheme.

The thesis is presented in the following order:

In chapter two characteristics of rain attenuation are investigated. Different rain attenuation prediction models are illustrated to relate the effects of several parameters e.g. rate of rainfall, operating frequency of the communication link, slant path, elevation angle, etc., on the rain attenuation experienced by any particular earth station. Using these models, the link fade margins for earth stations can be determined.

Conventional dedicated resources rain counter-measures are also studied in this chapter.

In chapter three different adaptive resource sharing techniques are studied and their performances compared. Effective usable capacity of these schemes and their feasibilities in TDMA environment are also studied.

It is shown in this chapter that a scheme using Adaptive Forward Error Control Coding (AFEC) associated with information rate reduction techniques has satisfactory performance and less implementation complexity. This scheme is chosen for further studies.

In chapter four the general concept of an AFEC resource sharing scheme is studied. The result of the study suggests some rain counter-measure schemes where switching is done from a low gain code to a high gain code in order to achieve variable fade margin. Selection criteria for candidate codes and possible choices of codes for various AFEC schemes are also discussed here.

However, the above schemes require two different set of codecs, one gives low gain and the other (when used alone or in cases used jointly with the other one) gives high gain. But, due to infrequent occurrences of large rain attenuation, the schemes utilize their full resources only occasionally. In order to make efficient utilization of the resources, an AFEC scheme using double coding is introduced in this chapter. For double coding applications a single codec is used repeatedly for added gain.

In chapter five double coding gain, interleaving requirements and candidate double codes are studied. A conceptual implementation of an AFEC resource sharing scheme using Golay double coding for high speed applications is discussed.

Chapter six concludes with a summary of results and suggestions for further research.

1.2 Research contributions :

The major contribution of this research is a study of the rain attenuation problem and effective counter-measure for Ka-band satellite systems. In investigating the effectiveness of various counter-measure schemes their performance is compared with feasibility and implementation aspects considered.

Some specific contributions are summarized below :

* Survey of available literature on rain attenuation in Ka-bands to summarize the characteristics of rain fade experienced by the satellite links operating in this band.

* Survey of different rain counter-measure schemes to compare their performance, effectiveness and feasibility for high capacity TDMA applications.

* Investigation of an AFEC resource sharing concept, and a study of the code selection criteria and candidate codes for the scheme.

* Introduction of an AFEC scheme using Reed Solomon/ convolutional concatenated codes.

- As a logical continuation, introduction of another class of AFEC schemes using double coding. These schemes are shown to have significantly lower hardware complexity and decoding computations, and increased codec utilization.

- Investigation of double code performance, computation complexity and interleaving requirements.

- Conceptual implementation of an AFEC Golay double coding resource sharing scheme for high speed applications.

REFERENCES

[1.1] Sivo, J.N., "Advanced Communications Satellite Systems ," IEEE Journal on SAC, Vol. SAC-1, 1983, pp. 580-588.

[1.2] Ippolito, L.J., " Radio Propagation for Space Communications Systems ," Proc. of IEEE, Vol. 69, 1981, pp. 697-727.

CHAPTER TWO

CHARACTERISTICS OF RAIN ATTENUATION

The major concern in digital satellite communications is the bit error rate (BER) degradation due to the presence of hydrometeors, particularly rain, in the propagation path. The effect of rain can be summarized as follows:

a) Rain attenuates the transmitted signal on the earth-space (uplink) and space-earth (downlink) paths

b) Rain increases the apparent sky temperature (i.e. received noise) for the receiver of the downlink earth station

c) Rain also causes beam depolarization which then leads to increased levels of co-channel interference in systems employing orthogonal polarization.

The combined effect of these three factors represents an equivalent fade (i.e. reduction in the effective $\frac{E_b}{N_o}$) and, as a result increases the BER at the receiver. The objective of reliable communication is to maintain the BER below a certain threshold, otherwise outage will occur (i.e. the link is considered unavailable). For example, according to CCIR recommendation, the BER should be $\leq 10^{-4}$

and $\leq 10^{-6}$ for voice and data communications respectively.

Meteorological data collected through the years using actual propagation experiments, sun trackers, and radar reflectivity measurements indicate that attenuation due to rain in a satellite link depends on [2.1]:

a) Rate of rainfall at the earth station

b) Operating radio frequency of the communication link

c) Slant path and elevation angle

The evaluation of rain attenuation for satellite link system design requires a detailed knowledge of the attenuation statistics for each ground terminal location at the specific frequency of interest. Direct long-term measurements of path attenuation for all potential ground terminal locations in an operational satellite network are not feasible. Over the past several years extensive efforts have been undertaken to develop reliable techniques for the prediction of path rain attenuation for a given location and frequency [2.2, 2.3, 2.4, 2.5, 2.6].

Using the prediction models, the effect of rain attenuation on different earth stations is evaluated and valuable information regarding the determination of an adequate rain counter-measure which would provide necessary link availability is derived. Though rain attenuation varies from year to year, the prediction models can give conservative estimates of the attenuation.

Although at present time not a single prediction method has been accepted for world wide application by the world community, one of the most commonly used model is described here.

2.1 Rain attenuation prediction models

Crane Global Attenuation Model [2.3]

A prediction model for rain attenuation, recently developed by Crane, provides a completely self contained procedure which is applicable on a global basis. The global model is based upon the use of geophysical data to determine the surface point rain rate, point-to-point variations in rain rate, and the height dependence of attenuation given the surface point rate or the percentage of the year the attenuation value is exceeded.

Surface point rain rate data from the U.S.A and global sources was used to produce ten rain rate climate regions for the earth's land and water surface areas. Fig. 2.1 shows the resulting global map of the eight basic climate regions, including the ocean areas.

The Crane model relates the surface point rain rate R_p to a path averaged rain rate $\bar{R}$, through an effective path average factor, determined empirically from terrestrial measurements of rain rate at path lengths up to 22.5 km. The resulting relationship was modeled by a power law expression

$$\bar{R} = \gamma(D)\, R_p^{[1+\delta(D)]}, \quad [\text{mm/hr}] \tag{2.1}$$

where

D — horizontal path length

$\gamma(D)$, $\delta(D)$ are determined from a best fit analysis of the terrestrial path data.

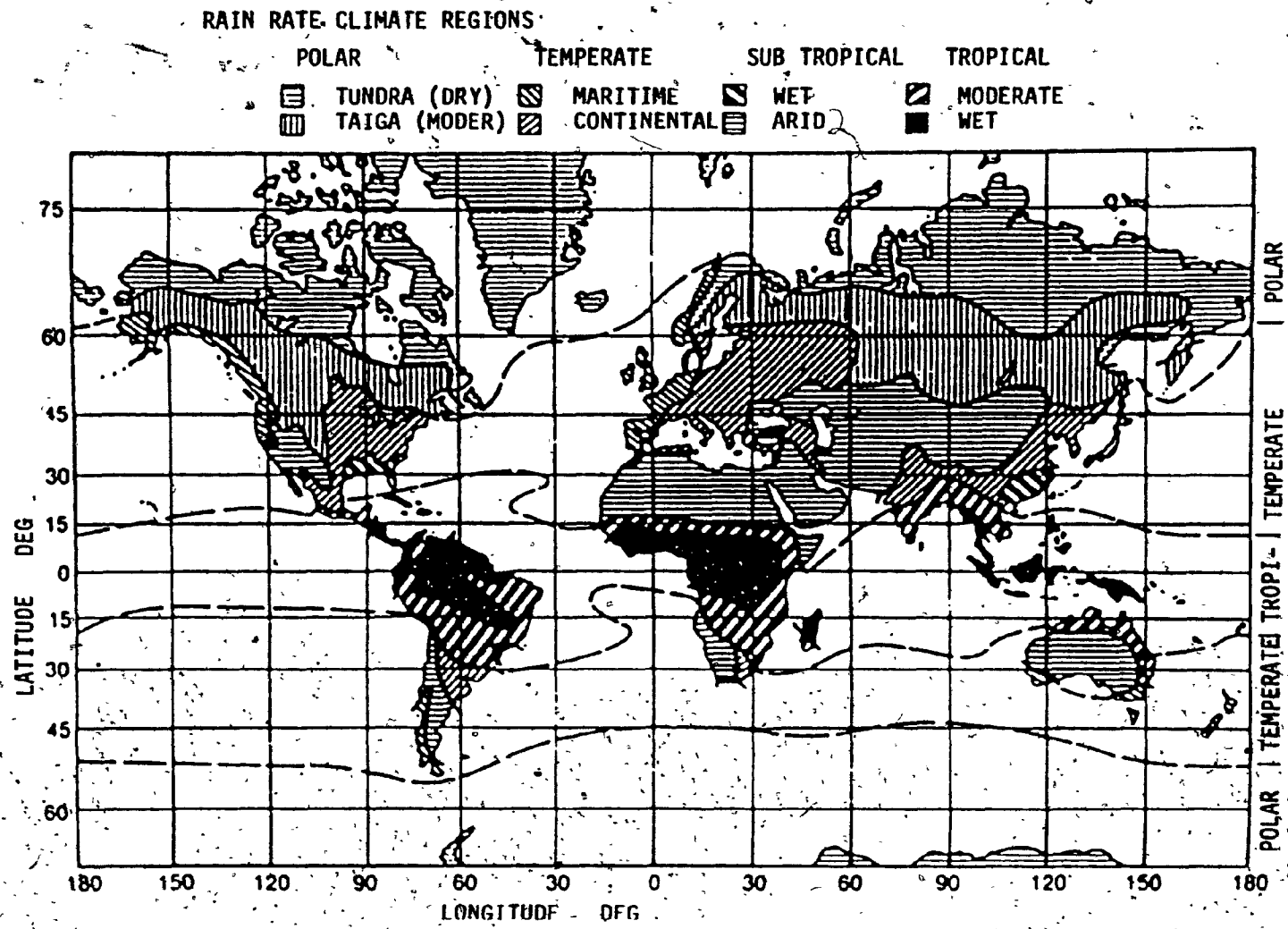

Fig. 2.1 Rain climatic regions for the global rain attenuation model (from [2.3]).

Relative path profile curves for rain rate as a function of D were determined by numerically differentiating γ and δ, then represented by two exponential functions over the range of D from 0 to 22.5 km. The resultant piecewise exponential expression for integrated attenuation for a slant path at an elevation angle Θ, as a function of the point rain rate R_p is:

$$A(R_p,D) = \frac{aR_p^b}{\cos\Theta}\left[\frac{e^{UbD}-1}{Ub}\right] \quad 0 \le D \le d$$

and (2.2)

$$A(R_p,D) = \frac{a\,R_p^b}{\cos\Theta}\left[\frac{e^{UbD}-1}{Ub} - \frac{X^b\,e^{Ybd}}{Yb} + \frac{X^b\,e^{YbD}}{Yb}\right]$$

$$d \le D \le 22.5 \text{ [km]}$$

where

U,X,Y empirical constants that depend on R_p

These constants are determined as follows:

$$U = \frac{1}{d}\ln\left[X\,e^{Yd}\right]$$

$$X = 2.3\,R_p^{-0.17}$$

$$Y = 0.026 - 0.03\,\ln(R_p)$$

$$d = 3.8 - 0.6\,\ln(R_p)$$

The annual attenuation distribution is generated from Eq. (2.2) as follows:

a) Select the rain rate distribution for the desired location from the rain climate region maps (Fig. 2.1) and Table 2.1

b) Determine the surface projected path length for each percent of the year value from

$$D = \frac{H - G}{\tan\Theta} \qquad (2.3)$$

where H is the 0^0 isotherm height found from the Fig. 2.2, G is the ground terminal elevation above sea level

c) Calculate the slant path attenuation for each percent of the year from Eq. (2.2), with the a and b coefficients selected for the frequency of interest (see Table 2.2)

The global model has yet to be extensively validated by direct measurements from regions of the world such as Europe or Asia. However as illustrated in [2.3] the results from over a dozen U.S.A and Canadian locations at frequencies from 11 to 30 GHz have shown very good correlation.

Table 2.1 Point rain rate distribution values (mm/h) versus percent of year rain rate is exceeded for the global model (from [2.3]).

PERCENT OF YEAR	RAIN CLIMATE REGION :										MINUTES PER YEAR	HOURS PER YEAR
	A	B	C	D_1	D_2	D_3	E	F	G	H		
0.001	28	54	80	90	102	127	164	66	129	251	5.3	0.09
0.002	24	40	62	72	86	107	144	51	109	220	10.5	0.18
0.005	19	26	41	50	64	81	117	34	85	178	26	0.44
0.01	15	19	28	37	49	63	98	23	67	147	53	0.88
0.02	12	14	18	27	35	48	77	14	51	115	105	1.75
0.05	8	9.5	11	16	22	31	52	8.0	33	77	263	4.38
0.1	6.5	6.8	7.2	11	15	22	35	5.5	22	51	526	8.77
0.2	4.0	4.8	4.8	7.5	9.5	14	21	3.8	14	31	1052	17.5
0.5	2.5	2.7	2.8	4.0	5.2	7.0	8.5	2.4	7.0	13	2630	43.8
1.0	1.7	1.8	1.9	2.2	3.0	4.0	4.0	1.7	3.7	6.4	5260	87.66
2.0	1.1	1.2	1.2	1.3	1.8	2.5	2.0	1.1	1.6	2.8	10520	175.3

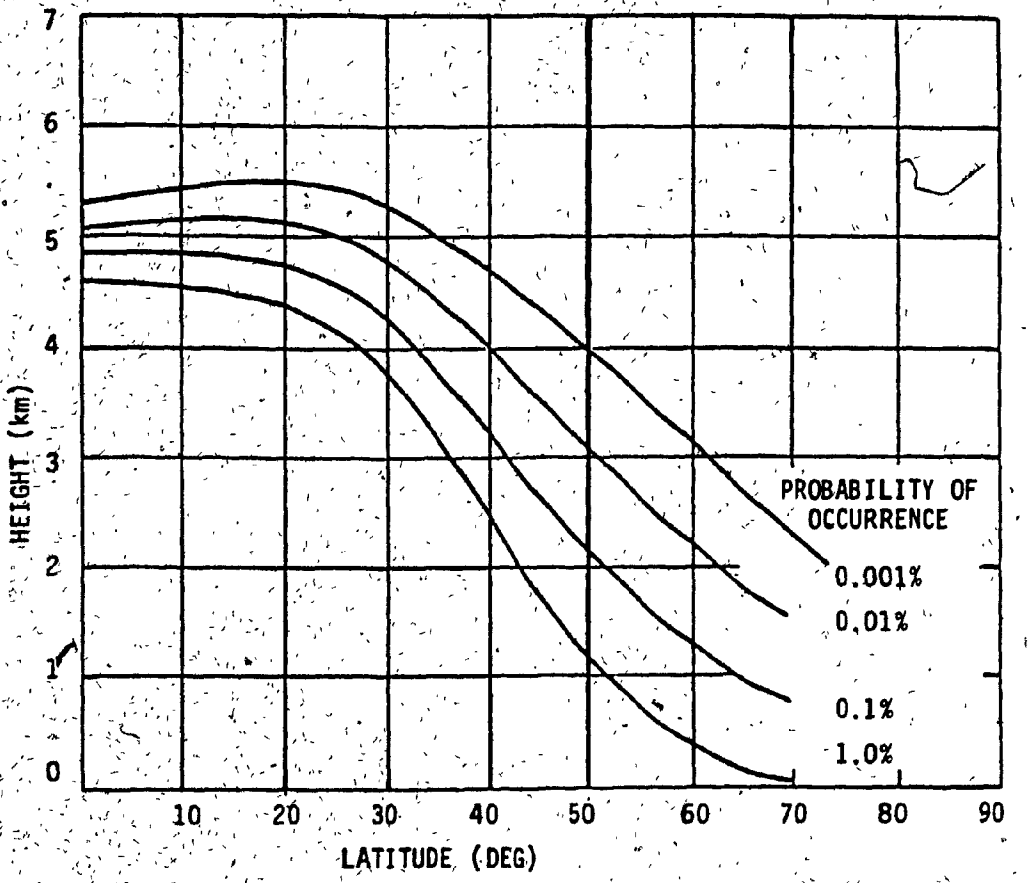

Fig. 2.2 The 0° isotherm height as a function of ground terminal location (latitude) and annual probability of occurrence (from [2.3]).

Table 2.2 Values for coefficients a and b. (LP_L for rain rate $\leq$ 30 mm/h, LP_H for rain rate $>$ 30 mm/h) (from [2.16]).

FREQ. (GHz)	a		b	
	LP_L	LP_H	LP_L	LP_H
10	1.17×10^{-2}	1.14×10^{-2}	1.178	1.189
11	1.50×10^{-2}	1.52×10^{-2}	1.171	1.167
12	1.86×10^{-2}	1.96×10^{-2}	1.162	1.150
15	3.21×10^{-2}	3.47×10^{-2}	1.142	1.119
20	6.26×10^{-2}	7.09×10^{-2}	1.119	1.083
25	0.105	0.132	1.094	1.029
30	0.162	0.226	1.061	0.964
35	0.232	0.345	1.022	0.907
40	0.313	0.467	0.981	0.864
50	0.489	0.669	0.907	0.815
60	0.658	0.796	0.850	0.794
70	0.801	0.869	0.809	0.784
80	0.924	0.913	0.778	0.780
90	1.02	0.945	0.756	0.776
100	1.08	0.966	0.742	0.774

2.2 Assessment of link fade margin

The required fade margin for a certain link can be determined from the knowledge of attenuation which the corresponding earth station experiences. As illustrated in detail in [2.2] with the help of such model it is possible to find the probability that attenuation A exceeds a margin M. This is expressed in the following manner [2.2] :

$$Pr\{A \geq M\} \approx P_0 \frac{1}{2} \operatorname{erfc}\left[\frac{\ln M - \ln A_m}{\sqrt{2}\, S_A}\right] \tag{2.4}$$

where

erfc(-) denotes complimentary error function

A_m median value of A

S_A standard deviation of ln A

P_0 probability that link is affected by rain

The above equation shows that rain attenuation has a log normal distribution, which means increment ΔA, of attenuation, A, in decibels is approximately linearly proportional to A.

$$\Delta A = h \cdot A \tag{2.5}$$

where

h a proportional parameter. It is a time varying random variable.

Experimental data also indicates [2.2] that the distribution of fade duration, τ, of rain attenuation exceeding a given threshold is approximately lognormal and that the average fade duration of any satellite link depends on the fade margin and operating frequency. The average outage decreases as the fade margin is increased. Knowledge of the fade duration distribution plays an important role in designing suitable fade counter-measures.

In Table 2.3 [2.7] comparative data of the average of required fade margin to achieve varying availability is illustrated for satellite links operating at different slant angles and frequencies. It is found that for a fixed slant angle, the fade margin requirement increases quite rapidly as the operating frequency is increased.

In general, attenuation level and radio frequency could be accurately related by

$$\frac{A_f}{A_{f_0}} = \left(\frac{f}{f_0}\right)^{1.72} \tag{2.6}$$

where

A_f attenuation at frequency f

A_{f_0} attenuation at frequency f_0

It is assumed that A_f and A_{f_0} have the same probability of occurrence for a given path length.

Table 2.3 Range of rain margin required [dB] (no margin greater than 20 dB considered) (from [2.7]).

ELEVATION IN DEGREES		10						20						90					
FREQ.-GHz		7	20	30	40	45	50	7	20	30	40	45	50	7	20	30	40	45	50
% AVAILABILITY	90	0	1	1	2	3	10	0	1	1	1	2	5	0	0	0	0	1	2
	95	0-1	1-6	1-12	2-20			0	1-3	1-5	1-9	2-12	5-18	0	0-1	0-2	0-2	1-3	2-4
	97	0-1	2-9	3-19				0	1-4	1-9	2-16	3-20		0	0-1	0-2	1-3	1-4	2-5
	98	0-1	2-11					0	1-6	1-13				0	0-1	0-3	1-4	1-6	2-8
	99	0-1	3-18					0-1	1-10					0	0-3	1-6	1-10	1-12	3-15
	99.5	0-2						0-1	2-16					0	0-5	1-13	1-20		
	99.9	1-3						0-2						0-1					

Considering the effects of increased rain attenuation and higher operating noise temperature encountered at higher frequencies, a Ka-band system would typically require 10 dB more of excess power than an equivalent Ku-band system to achieve even a low system availability of 99.5%.

In Figs. 2.3 and 2.4 (derived from Table 2.3) a typical satellite link availability vs. link margin is illustrated for uplink (30 GHz) and downlink (20 GHz) in Ka-bands. The fade margin required for a link availability of 99.5% is 20 dB for downlink while for uplink, the required margin exceeds 30 dB.

Experimental data shows that rain attenuation statistics have year to year variations. They also have seasonal and di-urnal variations, which indicate that severe rain attenuations are an irregular but unavoidable phenomenon, as illustrated in Figs. 2.5 and 2.6 [2.3, 2.8].

Fig. 2.5 illustrates that the magnitude of rain attenuation varies through the hours of the day and deep fades (or peak fades) are coincident with the peak telephone hours of the day. Statistics show that about 35 percent of rain outages will occur during telephone busy hours and the outage will interrupt all traffic on an satellite link at that time. Rain induced outages on satellite links have a higher service impact than multipath-fading-induced outages on terrestrial (4/6 GHz) radio relay links even if the two systems are engineered for equal total outage time. This is because multipath fading occurs mostly during the early morning hours of low telephone activity [2.1].

From Fig. 2.6 it is seen that the magnitude of rain attenuation varies through the months of the year. This results from the fact that severe rain attenuation is associated with heavy downpours and thunderstorms. During a thunderstorm rain attenuation is much higher than its average value while at other times the value is much lower.

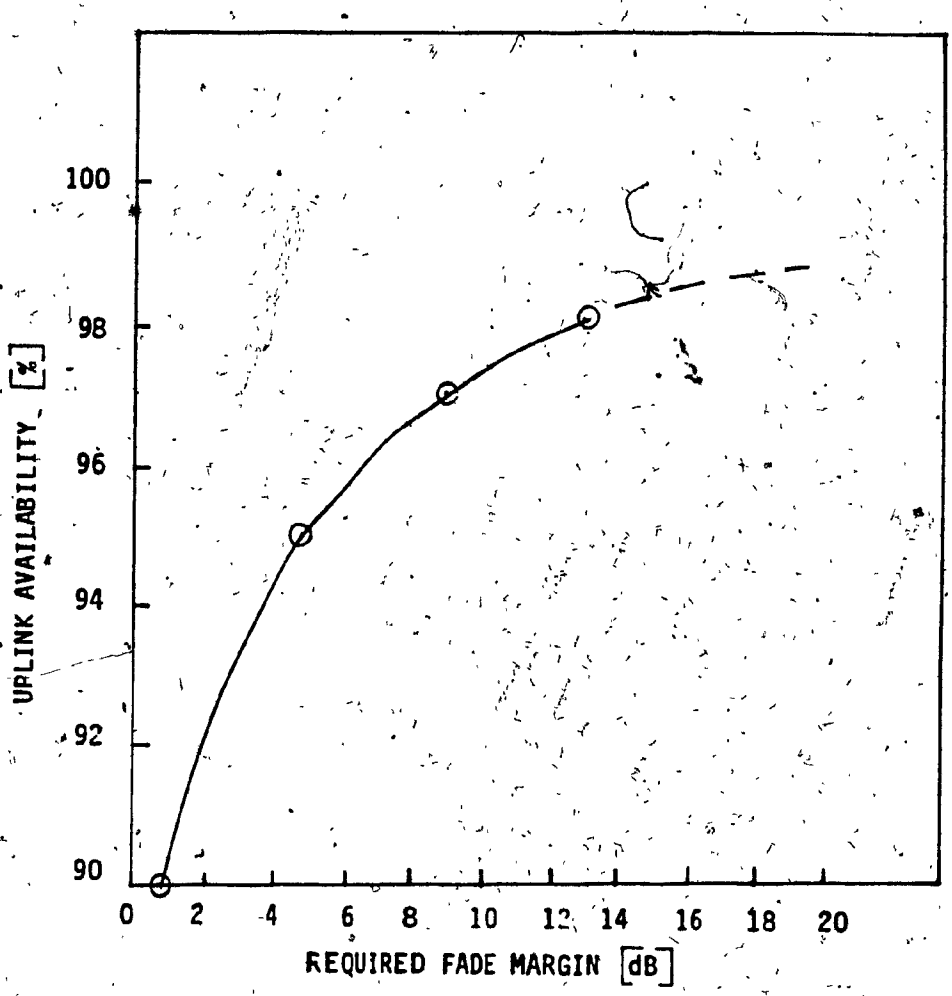

Fig. 2.3 Ka-Band uplink availability vs. fade margin (derived from Table 2.3).

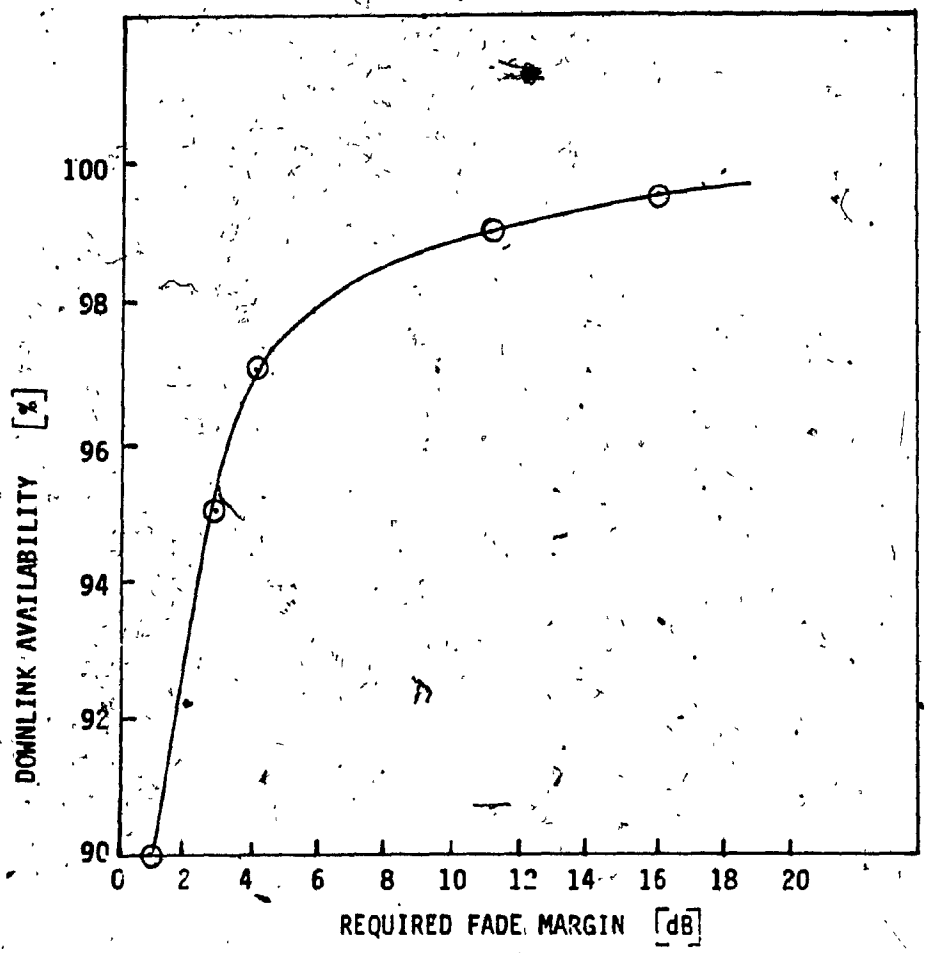

Fig. 2.4 Ka-Band downlink availability vs. fade margin (derived from Table 2.3).

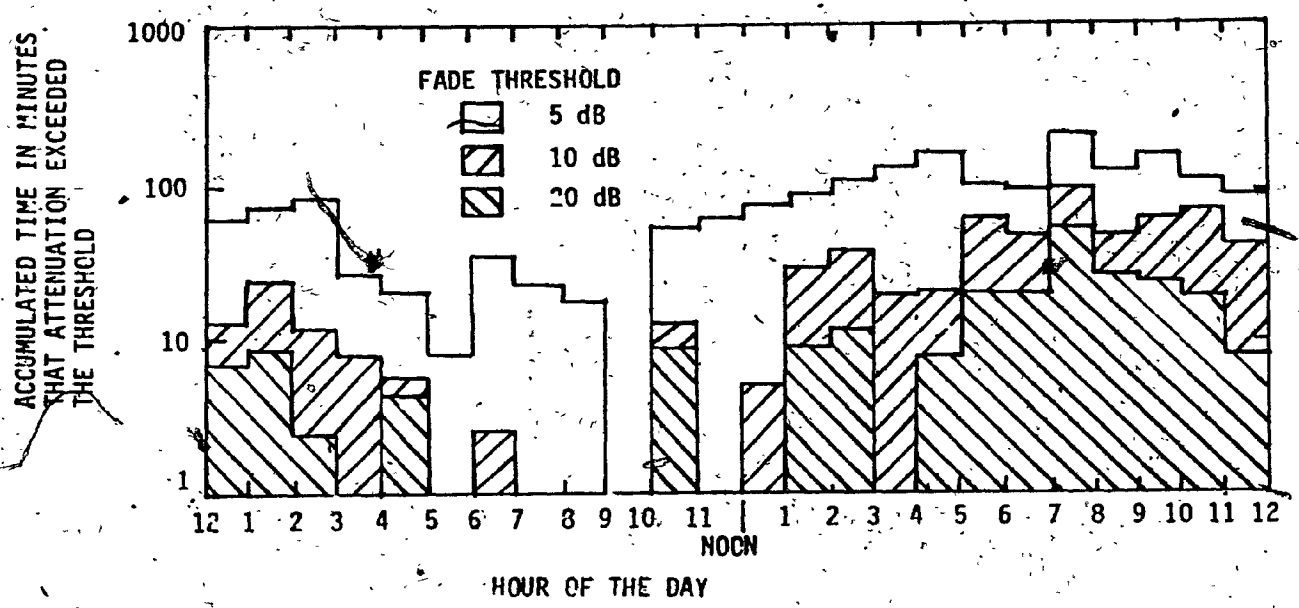

Fig. 2.5 Diurnal variation of 19 GHz rain attenuation statistics measured from the COMSTAR (D1)-to-Palmetto path (June 1976 to July 1977) (from [2.1]).

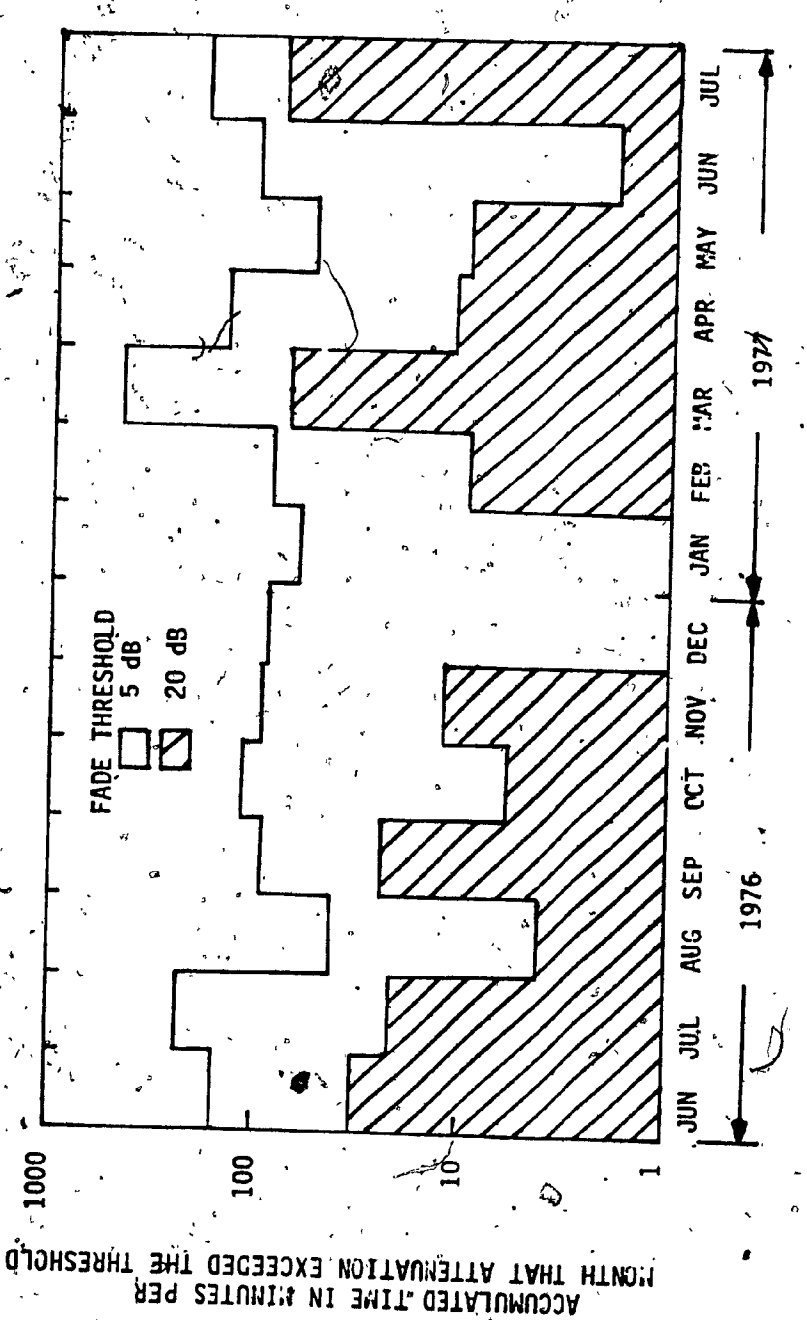

Fig. 2.8 Monthly variation of 19 GHz rain attenuation statistics measured from COMSTAR (D1)-to-Palmetto path (June 1976 to July 1977) (from [2.1]).

2.3 Conventional rain attenuation counter-measures

To date, most commercial satellite communication systems have employed the 6/4 GHz bands where the BER degradations associated with rainfall tend to be moderate (for instance, signal attenuation is typically below 3-4 dB for 99.99% of the time) [2.1]. These satellite systems have also been noise rather than interference limited. As a result, the techniques employed to counteract the effects of rain have been rather simple. Since the degradations were moderate, these simple ("brute force") techniques have proved to be cost effective. The rain counter-measure techniques generally used are of two types:

a) Link Margin

The most frequently encountered approach is simply to add a " rain margin " to the uplink and downlink power budgets (the amount of margin depending on the transponder back-off). This can be done either by increasing satellite and earth station antenna gains (larger antennas with more difficult pointing problems), reducing system noise temperatures (more expensive or cooled LNAs), or increasing transmitter power. Where antenna gains and LNA temperatures are limited by other technical (or economic) factors, link margin effectively means power margin.

However, in Ka-bands the attenuation levels are sometimes too large to be overcome by power margins.

b) Site diversity

The conventional method generally used to achieve reliable communications

in the face of such high levels of rain attenuation is called site-diversity or two different sites supporting one ground station. The sites are connected by a terrestrial link.

This is based on the fact that as the rain cells are limited in extent to several miles, the probability that both terminals of an earth station simultaneously experience large rain attenuation can be reduced by increasing the distance between the terminals [2.9].

The advantage which two ground stations allow over a single site can be expressed with the aid of a useful concept called "diversity gain". Diversity gain gives the performance at two ground sites relative to a single site. The ground site with the least attenuation is always chosen. Hodge [2.10, 2.11] developed an empirical model for diversity gain

$$G = a\left(1 - e^{-b\,d}\right), \quad [\text{dB}] \tag{2.7}$$

where

d site separation [km]

A single site attenuation [dB]

$$a = A - 3.6\left(1 - e^{-0.24A}\right) \quad [\text{dB}]$$

$$b = 0.46\left(1 - e^{-0.26A}\right) \quad [\text{km}]$$

However, it has been noticed [2.12] that under certain circumstances Eq. (2.7) may give unacceptable results, e.g., if availability requirements are greater

than 0.999 and single site attenuation is large, it is unreasonable to expect rain attenuation to disappear.

According to the Christopher model [2.12] the diversity gain has been incorporated into the required fade margin A_R (given a fixed probability of outage p). This is given by:

$$A_R = \left(\frac{\beta}{\left[1 - \frac{\beta}{\sqrt{1-\rho^2}} + \frac{1}{\sqrt{1-\rho^2}} \right]} \right) \ln \left(\frac{C_1}{p} \right) \qquad (2.8)$$

where

β variance of log A

ρ correlation co-efficient of rain attenuation on two sites

$$C_1 = \left(\frac{1}{1 - \frac{\rho}{\sqrt{1-\rho^2}}} \right) \exp \left(\frac{A_e}{\beta} + \frac{\left(\beta(1-\sqrt{1-\rho^2}) + A_e \right)}{\beta\sqrt{1-\rho^2}} \right)$$

$$A_e = A_M + \beta \ln \phi$$

ϕ fraction of time for which noticeable rain fall occurs

A_M fade margin [dB] in any single site

In Fig. 2.7 [2.13] a model relation between the rain auto-correlation function and distance is illustrated. It is shown that at a distance of 8 km the auto-correlation co-efficient equals 0.2, which corresponds to the optimum separation

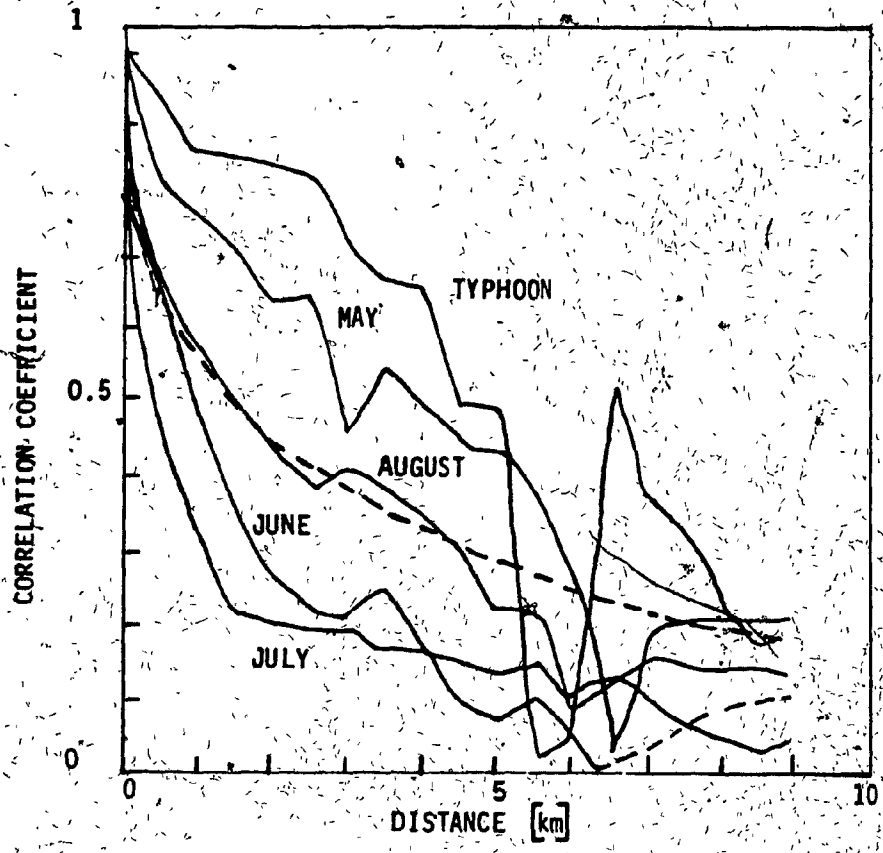

Fig. 2.7 Dependence of rain auto correlation function and distance (from [2.13]).

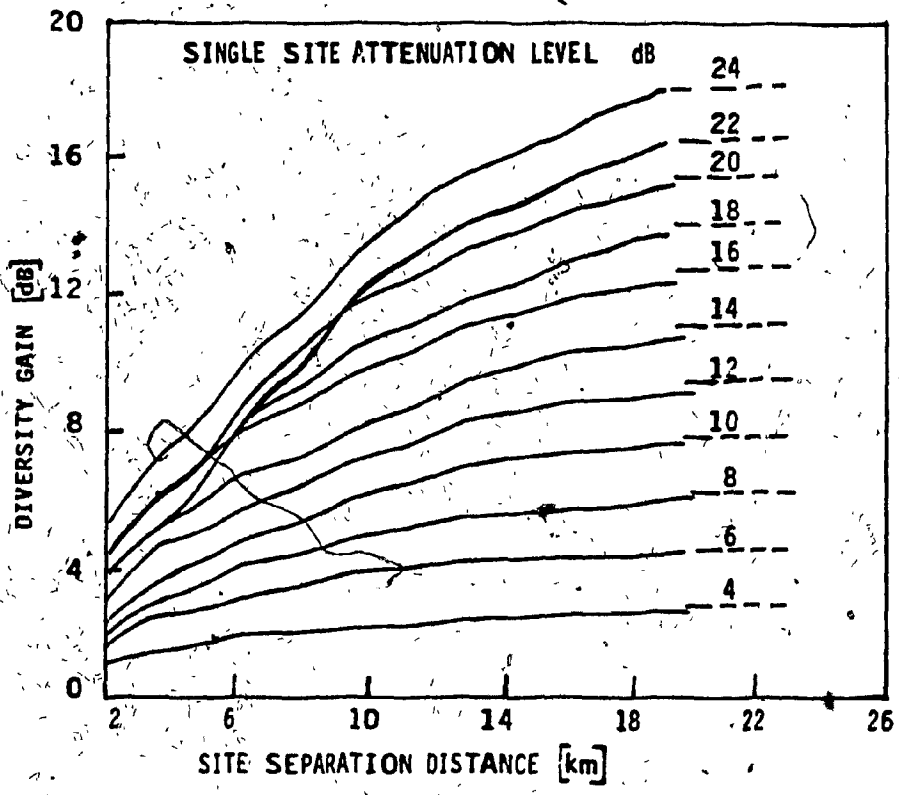

Fig. 2.8 Diversity gain versus site separation (from [2.14]).

distance for this particular case.

An estimate of reliability available with site diversity can be made using the model of Goldhirsch [2.14]. As shown in Fig. 2.8 diversity gain is related to single site attenuation and site separation. For example, a pair of sites 10 km apart will have a diversity gain of 9 dB relative to a single site suffering 16 dB attenuation.

With the introduction of Ku and Ka-band satellite communication systems it will be possible to offer various types of services such as customer premises service (CPS), public broadcasting services, individual communication system through satellite, etc. But site diversity cannot be implemented for such cases because the cost of such an arrangement will be prohibitive. Even for trunk communications, maintaining site diversity is not an easy task because of the cost and complexity related to connecting two site diversified stations by radio-relay link or cable link [11]. Moreover, due to seasonal and di-urnal variations of rain attenuation, the permanently dedicated resources of large fixed link margin or the alternative of widely applied site diversity are fully used only during occasional heavy rain storms (or equivalently, the system is severely overdesigned for upwards of 99.9% of the time) [2.1].

REFERENCE

[2.1] Ippolito, L.J., " Radio Propagation for Space Communications Systems," Proc. of IEEE, Vol. 69, 1981, pp. 697-727.

[2.2] Lin, S.H., Bergman, H.J., and Pursely, M.V., " Rain Attenuation on Earth -Satellite Paths -Summary of 10-year Experiments and studies," B.S.T.J, Vol. 59,1980, pp. 183-228.

[2.3] Crane, R.K., " A global model for rain attenuation model for earth-satellite paths," IEEE Pub. 78 CH 1354-4 AES, Arlington, VA, September 1978, pp. 391-395.

[2.4] Rice, P.L., and Holmberg, N.R., " Cumulative time statistics of surface point-rainfall rates , " IEEE Trans. on Communications, Vol. COM-21, 1973.

[2.5] Dutton, E.J., and Dougherty, H.T., " Modelling the effects of cloud and rain upon satellite-to-ground system performance , " Office of Telecommunications, Boulder, CO, OT Rep. 73-5, 1973.

[2.6] Dutton, E.J., " Earth space attenuation prediction procedure at 4 to 16 GHz, " Office of Telecommunications, Boulder, Co, OT Rep. 77-123, 1977.

[2.7] Bond, F.E., " Future Trends in Commercial and Military Systems ", Proc. of ICC, 1983, pp. D1.1.1-D1.1.6.

[2.8] Arnold, H.W., Cox, D.C., and Rustako, A.J., " Rain Attenuation at 10-30 GHz Along Earth-Space Paths; Elevation Angle, Frequency, Seasonal and Di-urnal Effects," IEEE Trans. on Communication, Vol. 29, 1981, pp. 716-721.

[2.9] Ippolito, L.J., Kaul, R.D., and Wallace, R.G., A Propagation Effect Handbook for Satellite Systems Design, NASA Headquarters, Washington, D.C, 1980.

[2.10] Hodge, D.B., " Radar Studies of Rain Attenuation and Diversity gain ," Mc Gill University, Montreal, Sci. Rep. MW-87, 1976.

[2.11] Hodge, D.B., " The Characteristics of MM-Wave length Satellite-to-Ground Space Diversity Links ," IEE Conf. Pub. 98, Conf. on Propagation of Radio waves at Freq. above 10 GHz, 1973.

[2.12] Christopher, P. " Atmospheric Attenuation for Correlated Satellite Communication Ground Sites," Proc. of ICC, 1983, pp. F1.6.1-F1.6.7.

[2.13] Morita, K., and Higuti, I., " Statistical Studies on Rain Attenuation and Site Diversity Effect on Earth-to-Satellite Links in Microwave and Millimeter Wavebands," Trans. of the IECE of Japan, Vol. 61, 1978, pp. 425-432.

[2.14] Goldhirsch, J. and Katz. I. " Useful Experimental Results for Earth-Satellite Rain Attenuation Modeling;" IEEE Trans. on Antennas and Propagation, Vol. 27, 1979, pp. 413-415.

[2.15] Sivo, J.N. " Advanced Communications Satellite Systems," IEEE Journal on SAC, Vol. 1, 1983, pp. 580-588.

[2.16] Mazur, B. Adaptive Forward Error Correction Techniques, Report on DSS Contract OST 81-00249, Miller Communication Systems Ltd., Ottawa, Canada, 1982.

CHAPTER THREE

ADAPTIVE RESOURCE SHARING CONCEPT

3.1 Introduction

From earlier discussions it is seen that satellite links in Ku- and Ka-bands are affected by severe rain attenuation which have seasonal and di-urnal variations. Hence maintaining high link availability requires a large fade margin but only for a small fraction of the overall time period. For example, in a typical earth station a fade margin of 11 dB is required to maintain a downlink availability of 99%. To increase the availability by another 0.9% (to 99.90%) the margin required is 20 dB. Whereas, to increase the availability by another 0.09% (to 99.99%), which is the standard for satellite links, the required fade margin exceeds 30 dB [3.1]. As a consequence conventional techniques of rain attenuation counter-measure using dedicated resources of large fixed link margin or the alternative of widely applied site diversity are fully used only during occasional heavy rainstorms. Hence, the measures are underutilized and not cost-effective, as a large portion of the system power is always kept on reserve, even when not required.

To achieve a cost effective solution, it is necessary to look for adaptive rain attenuation counter-measures. As the word adaptive means, these measures will help to overcome rain attenuation at the time of its occurrence. Moreover, they will change adaptively with the intensity of attenuation. In times of no rain

these measures will not be used and thus all the resources can be utilized fully for information transmission.

Usually, the types of adaptive measures to be used depends on the multiple access scheme of the system. Multiple access is known as the scheme for sharing a satellite transponder among users. It may be defined as the technique by which a number of earth stations form communication links through one or more satellite RF channels. In this chapter different adaptive resource sharing concepts will be discussed and the probability of rain outage for resource sharing systems will be analyzed.

3.2 Multiple access schemes

There are three basic multiple access schemes as illustrated in Fig. 3.1.

a) Frequency Division Multiple Access (FDMA) - In this scheme each uplink RF carrier occupies a defined frequency slot in the satellite transponder.

b) Time Division Multiple Access (TDMA) - In this scheme each uplink carrier operates only during specific time slots to access the satellite transponder.

c) Code Division Multiple Access (CDMA) - Here each uplink occupies the same frequency band at the same time, but uses different codes.

A detailed discussion of various multiple access schemes is given in [3.2]. It can

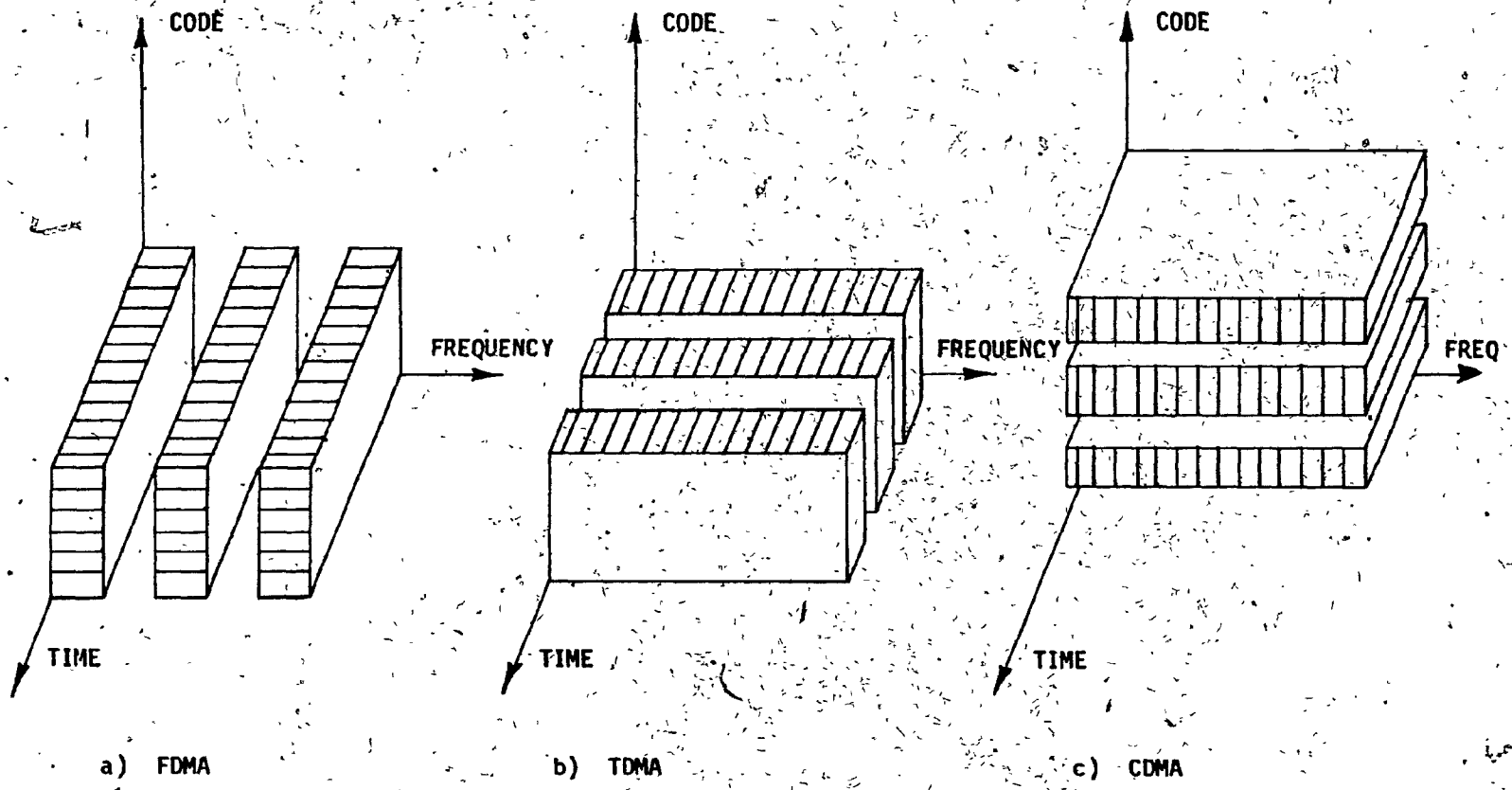

Fig. 3.1 Conceptual presentation of a) FDMA b) TDMA c) CDMA

be said that for large system, significantly higher capacities are achieved using TDMA rather than CDMA or FDMA. As illustrated in Fig. 3.2, TDMA has definite advantages over FDMA and CDMA when the number of users increases.

The other advantages of TDMA systems are:

a) They can easily be configured, which means changes in the burst plan, adding new stations or dropping some stations, etc., can be done in real time.

b) They can be programmed for large changes in the capacity assignment according to the requirements or demand.

These characteristics are very important for the efficient utilization of satellite capacity in a multi-user environment.

In Fig. 3.3 a TDMA time frame is illustrated. The frame is divided into non-overlapping time slots which are occupied by accessing signals (known as traffic burst) from different earth stations. The frame in this case begins with a reference burst RB_1. RB_2 is a second reference burst for redundancy. RB_1 and RB_2 are used as frame markers. The locations of traffic burst are referenced to the time of occurrence of RB_1 or RB_2. Each stations traffic is synchronized so that at the time of arrival at the satellite its traffic burst is confined within the specified timeslot.

In Fig. 3.4 a typical TDMA satellite transponder is illustrated. Here the received uplink bursts are amplified by a low noise amplifier (LNA), down converted to downlink frequency, amplified by the high power TWTA and

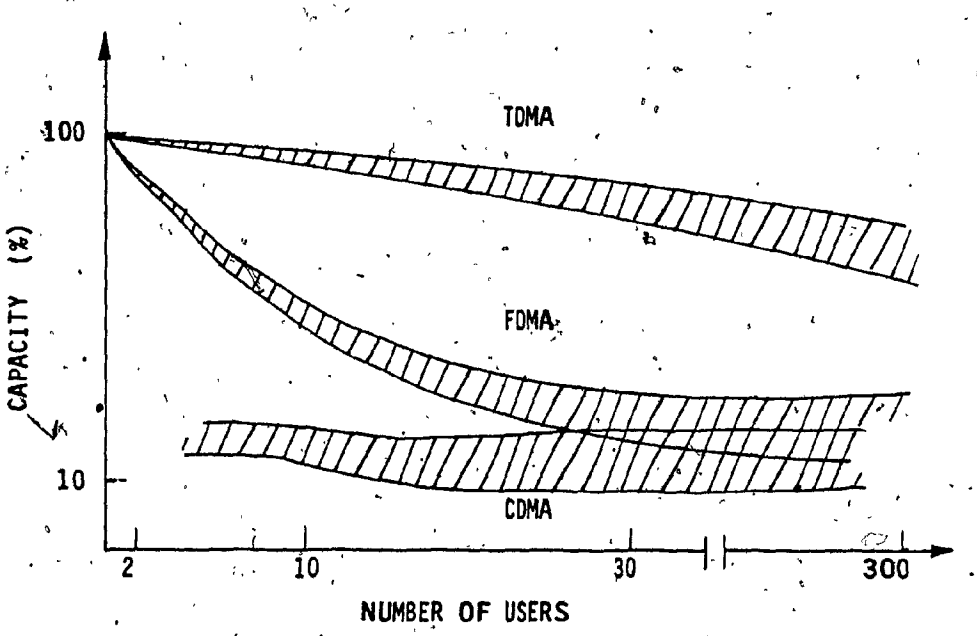

Fig. 3.2 Comparison of throughput for a uniform network, versus number of users (from [3.2]).

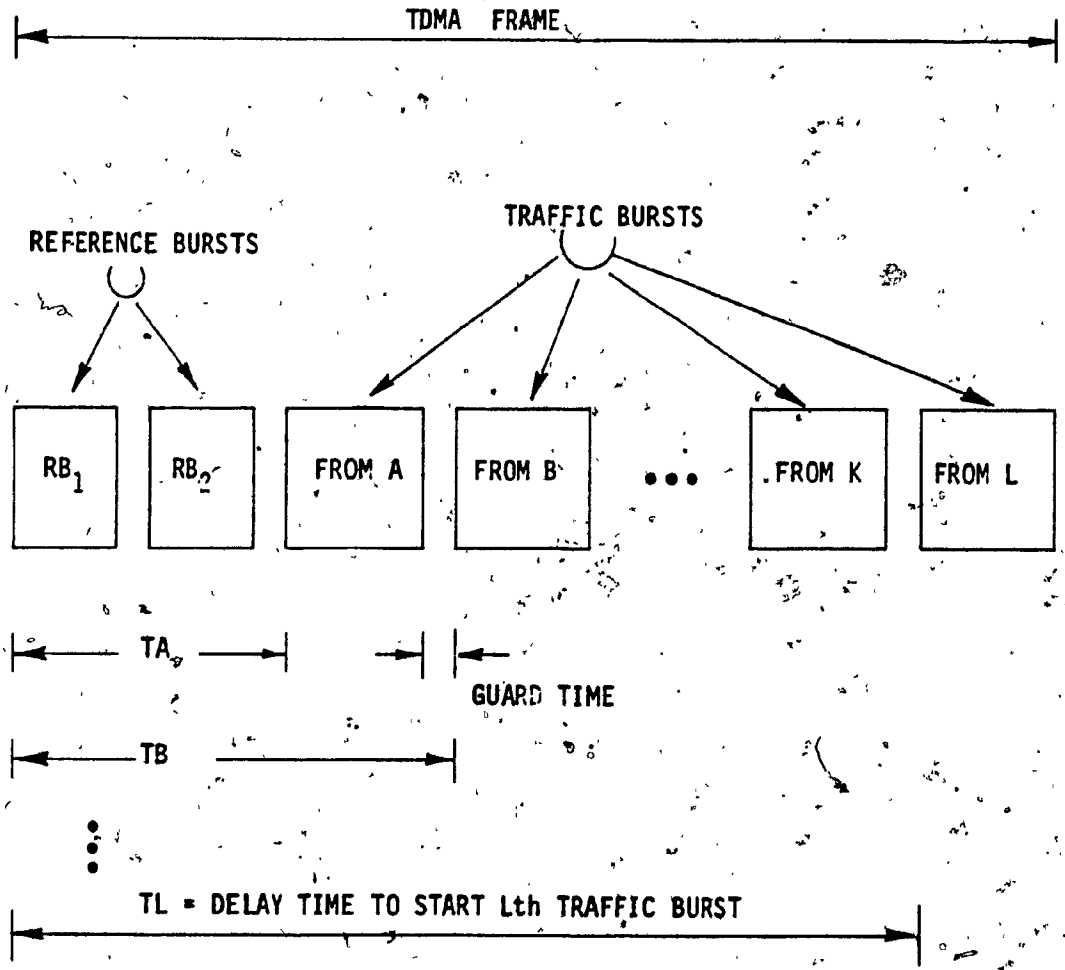

Fig. 3.3 A typical TDMA format

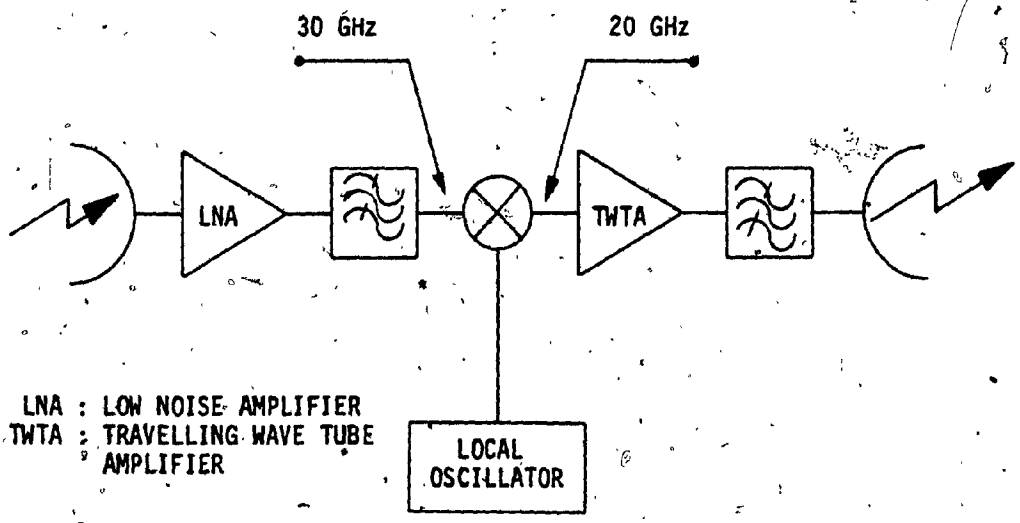

Fig. 3.4 Block diagram of an active satellite transponder

retransmitted to earth stations. At any one instant of time there is only one carrier present in TWTA. Hence, the TWTA nonlinearities are of no major concern and it can be operated in saturation mode (without input backoff). For this reason, TDMA can provide a higher capacity than multi-carrier FDMA and CDMA schemes.

In Ka-bands 2.5 GHz bandwidths are allocated for communication purposes, which is five times that of either the C or Ku-bands. Hence high capacity satellite systems will be established in these bands. For such high capacity links, TDMA is most suitably applied.

Most TDMA satellite transponders are currently used only as active repeaters without on-board signal processing. For digital satellites having on-board signal processing capability, the uplink RF burst is first demodulated to baseband signals, regenerated, then remodulated and transmitted to earth stations. This improves the system BER performance and isolates uplink from downlink. The baseband processor simplifies the task of on-board traffic routing, FEC switching, etc., and provides a flexible and efficient reconfiguration of downlink resources. It also offers flexibility to the implementation of resource sharing schemes.

It is believed that for future TDMA satellite transponders, on-board signal processing capability will be a common feature. In Fig. 3.5 a block diagram of such a regenerative satellite repeater having an on-board processor is illustrated.

In the following, some adaptive rain counter-measures suitable for TDMA applications will be discussed. Note that for these cases, the satellite transponders are assumed to be active repeaters.

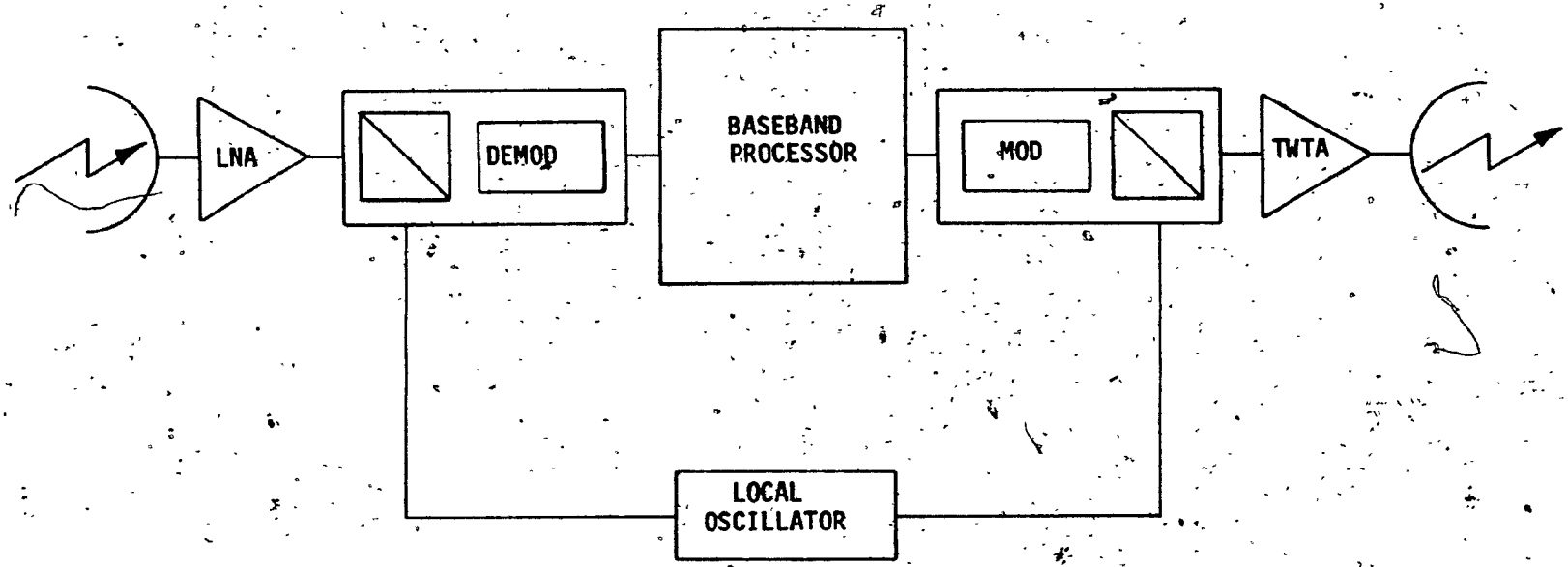

Fig. 3.5 Block diagram of regenerative satellite transponder

3.3 Adaptive Up-link power control

Rain fades on the Uplink can be effectively compensated by adaptively increasing the transmit power of the earth station [3.3]. The power control concepts can be categorized as follows :

1) Constant satellite power (CSP) sharing.

2) Adaptive satellite power (ASP) sharing.

A brief description of each is given below:

Constant satellite power sharing (CSP)

With this technique, the transmitter power of each earth station is adjusted to maintain constant carrier-to-noise ratio at the satellite output.

Assume a hypothetical satellite communication scenario illustrated in Fig. 3.6 where earth station #1 is linked to earth stations #3, #4, and #5 via satellite. In case of rain attenuation in earth station #1, its uplink and downlink CNR is degraded. The downlink CNR to the earth stations #3, #4, and #5 are also affected.

Under CSP control earth station #1 will increase the uplink transmit power to restore the necessary CNR for those downlinks. Moreover, the downlink CNR degradation to earth station #1 will not be changed.

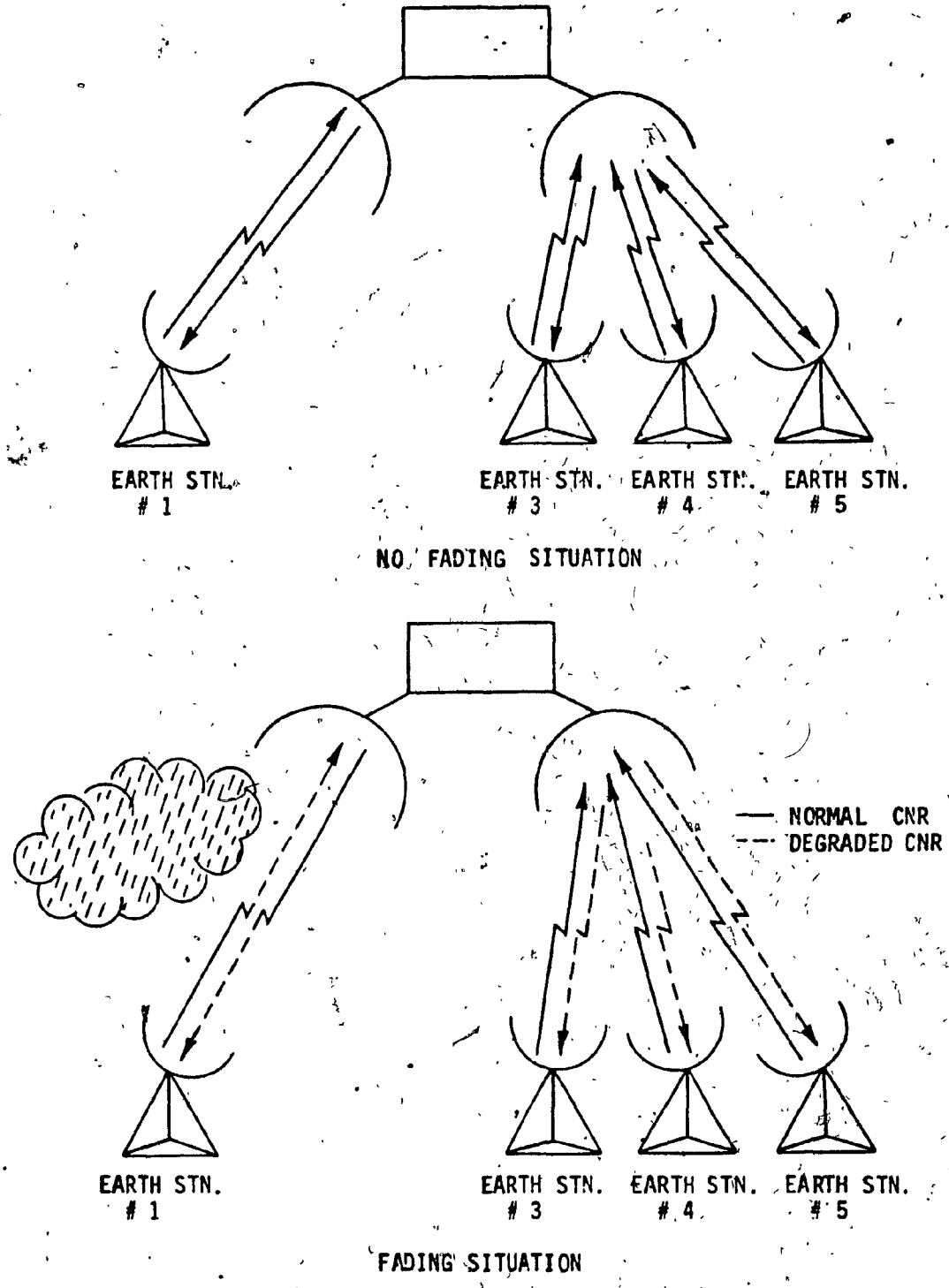

Fig. 3.6 Satellite link scenario.

Adaptive satellite power sharing (ASP)

Under ASP control, the transmitter power at each individual earth station is adjusted continuously such that the fade margin throughout the network is maximized. Compared to CSP, the present control also adjusts the downlink to earth station #1 (in Fig. 3.6) through uplink power adjustments of earth stations #3, #4, and #5. Thus, any change in environmental condition at a terminal triggers many simultaneous changes in transmit power throughout the earth stations of the network. Hence, ASP requires a complex monitoring and control mechanism.

An understanding of the operation of the above two control concepts may be obtained by examining a hypothetical CNR matrix (see table 3.1 and 3.2) where one earth station has suffered an attenuation due to rain.

Table 3.2 illustrates the effect of rain at earth station #1 which causes CNR degradation of 3.3 dB. It is evident that CNR for downlink at the affected earth station (i.e, the first column) and the CNR for downlink to earth stations #3, #4, and #5 have suffered CNR degradation of $\approx$ 3.3 dB (i.e, the first row) as a result.

Examining the effect of the above mentioned two control schemes in this situation reveals the following.

1) CSP would restore the CNR of the uplink from the affected Earth station. As a consequence, the CNR values of the first row will return to their previous values, but the CNR values of the first column will remain same.

2) ASP control would adjust all the uplink powers such that the affected downlinks will be restored to their previous values.

Table 3.1 Link margin for no fade situation

TRANSMITTING EARTH STATION	SIGNAL-TO-NOISE RATIO FOR RECEIVING EARTH STATIONS				
	1	2	3	4	5
1			6.0	7.8	7.4
2			6.8	8.5	8.1
3	6.6	7.5		6.8	6.4
4	7.5	8.4	6.1		7.4
5	7.0	7.9	5.6	7.2	

Table 3.2 Link margin during attenuation of $\approx$ 3.3 dB at earth station No. 1

TRANSMITTING EARTH STATIONS	SIGNAL-TO-NOISE RATIO FOR RECEIVING EARTH STATIONS				
	1	2	3	4	5
1			2.8	4.6	4.1
2			7.2	8.9	8.5
3	3.2	7.7		7.1	6.7
4	4.2	8.6	6.4		7.6
5	3.7	8.2	5.9	7.6	

However, in the process some downlinks will have a higher CNR than before.

With the advent of regenerative satellite repeaters the uplink and downlink will be isolated from each other. As a result rain counter-measure have to be applied to both links independently.

For uplinks, power control methods discussed so far could be suitably used. Usually high power amplifiers can be set up in earth stations to obtain excess power as weight and power supply will not be a problem.

Unlike earth stations, the satellites are usually power limited. Because of weight and size constraints for satellite based TWTAs and solar panels, very little excess power is available. As a consequence downlink power control as a rain counter-measure is not feasible. Also, uplink power control may not be attractive for some very limited groups of satellite users, e.g. users having mobile stations or earth stations at remote (inaccessible) sites, as in many cases these earth stations are power limited. Hence, it is necessary to find adaptive rain counter-measures alternative to power control to overcome the CNR degradation. These measures make use of various time and frequency resources to improve the effective fade margin for both uplink and downlink. These measures are:

a) Adaptive forward error correcting coding.

b) Adaptive rate reduction.

c) Adaptive utilization of lower frequency band back-up.

Some of these measures can also be combined together to form effective

hybrid schemes. In the following, brief descriptions of the measures are given.

3.4 Adaptive forward error correcting coding (AFEC)

Forward error correction (FEC) techniques have been used in communication systems to reduce the probability of error under low SNR.

In coding, the greater the number of redundant symbols, the higher the error correcting or detecting capability of the code. But, redundant bits increase the transmission bandwidth. In a bandwidth-limited system, the use of FEC causes a reduction in the satellite capacity whenever coding is used.

In order to maintain a constant system capacity with or without FEC, the following two schemes are used :

1) In-band adaptive coding: FEC is applied at the voice circuit level and to accomodate the extra bandwidth required for such coding, the voice encoding rate is lowered [3.4,3.5]. In this method quantization noise is traded off with bit error degradation at the individual circuit level.

2) FEC using Reserved Capacity: In this scheme an extra capacity is reserved to allow bandwidth expansion by FEC.

In-band adaptive coding usually requires the use of high rate codes, hence, the gain obtained is not sufficient to counter rain attenuation in Ka-bands. With, the latter scheme, any rate code can be used to obtain high gain provided the Reserved Capacity is available. In the following, the effective usable capacity for the latter scheme is derived.

Assume that the total number of available satellite channels without a reserved pool is N. If in a system using AFEC a pool of capacity required for K channels is reserved for coded symbols, then the total number of usable channels will be reduced to:

$$N_a = N - K + K\,r = N - K\,(1 - r) \tag{3.1}$$

where

r the code rate

K r number of channels that can be created out of the reserved pool and used by the unattenuated channels.

In the case of coding the unattenuated channels change places with the channels which require coding (see Fig. 3.7 and 3.8). In Fig. 3.7 the TDMA frame format having reserved slots for AFEC and switching of coded traffic to reserved slots is illustrated. In Fig. 3.8 a conceptual block diagram of a transmitter section with AFEC switching is shown.

Let F be the fraction of the total number of channels which require coding simultaneously to meet the propagation reliability. The pool size, expressed in number of channels is

$$K = \frac{F N_a}{r} \tag{3.2}$$

where

F N_a number of channels which need to be simultaneously protected

The value of K can be determined by knowing the required system outage

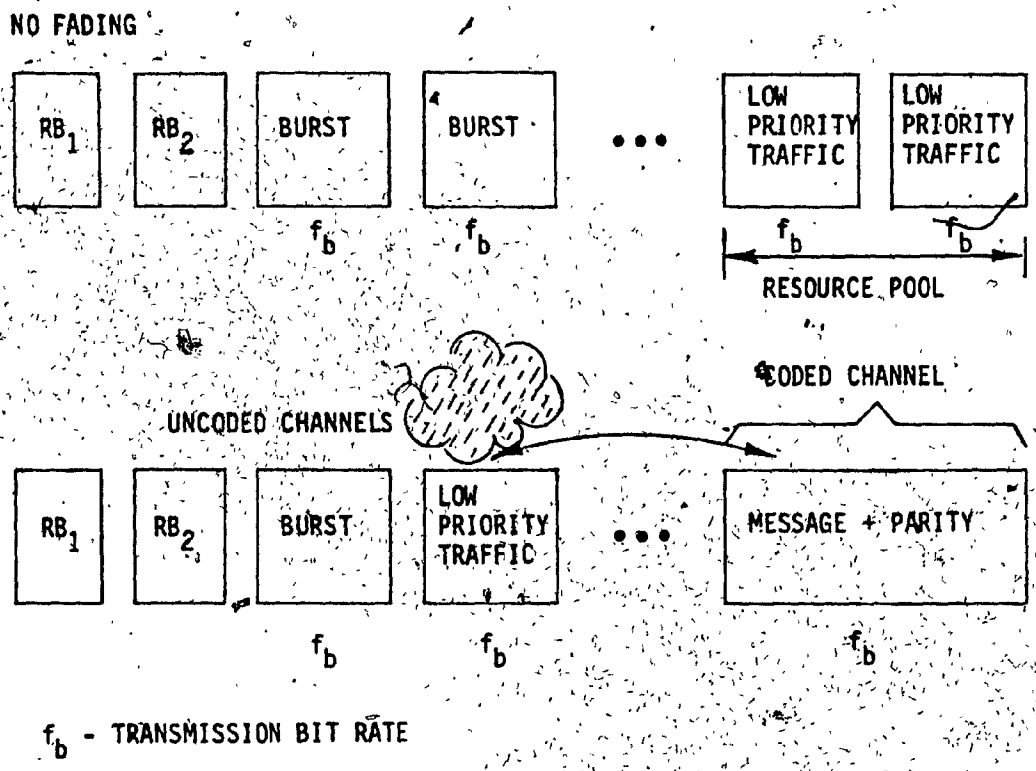

Fig. 3.7 Conceptual TDMA frame format for AFEC resource sharing

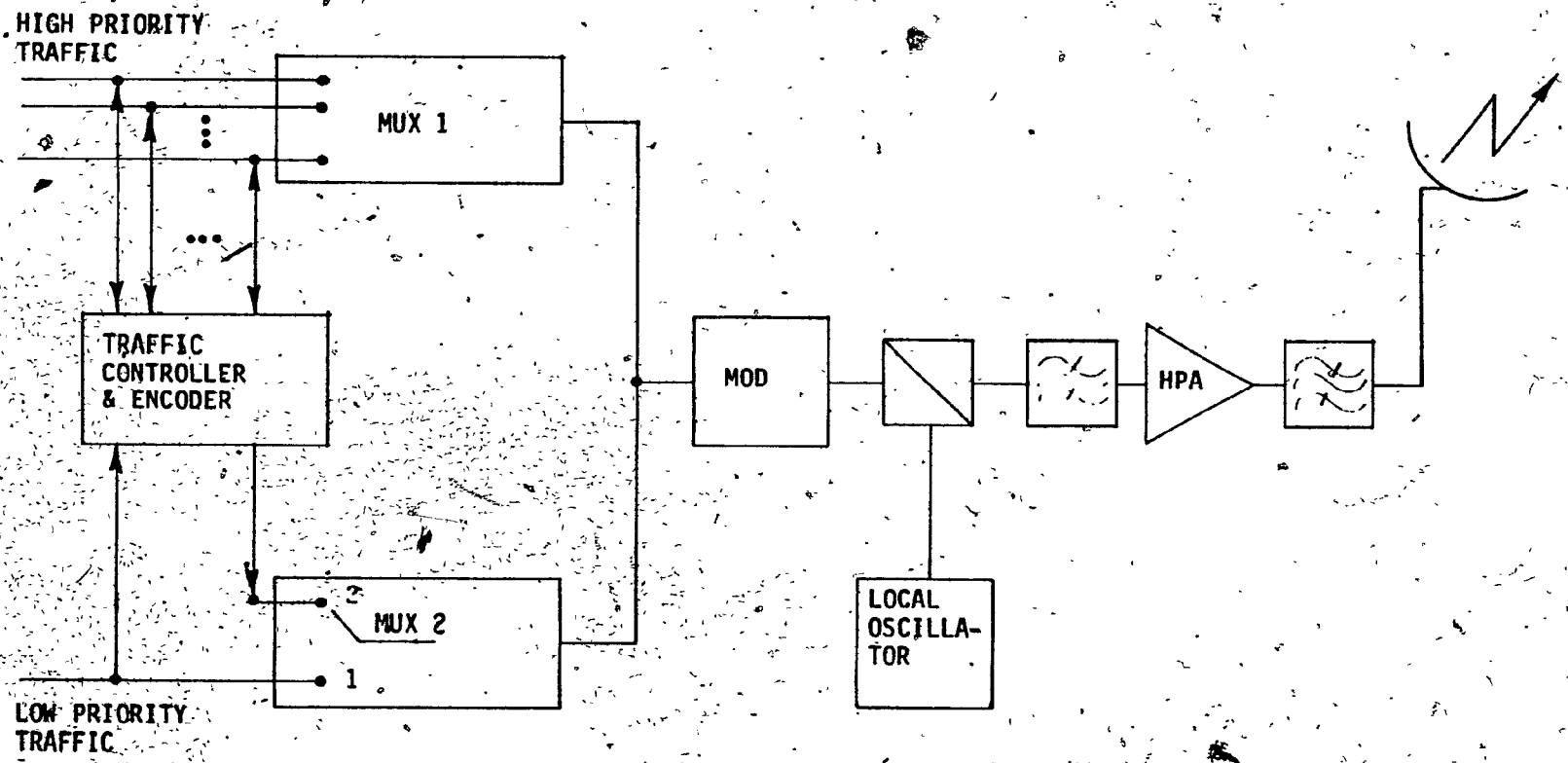

MUX 2 IS FOR RESERVED SLOTS

POS 1 UNFADED SITUATION
POS 2 FADED SITUTAION

Fig. 3.8 Conceptual block diagram of a transmitter with AFEC switching

performance. The analysis of the system performance for a given K is given in appendix 3A.

The relative effective usable capacity is derived as:

$$\frac{N_a}{N} = \frac{N - \frac{FN_a}{r} + FN_a}{N} \qquad (3.3)$$

$$= \frac{1}{1 + F(\frac{1}{r} - 1)}$$

The fraction of the total capacity lost is given by:

$$f_L = 1 - \frac{N_a}{N} \qquad (3.4)$$

$$= \frac{F(\frac{1}{r} - 1)}{1 + F(\frac{1}{r} - 1)}$$

Coding gain can be achieved at the cost of code rate reduction. However, as illustrated in Fig. 3.9 the increase in coding gain is not linearly proportional to the continuous decrease in the code rate. By decreasing the code rate the system gets complex and bandwidth gets expanded but the gain obtained is relatively small.

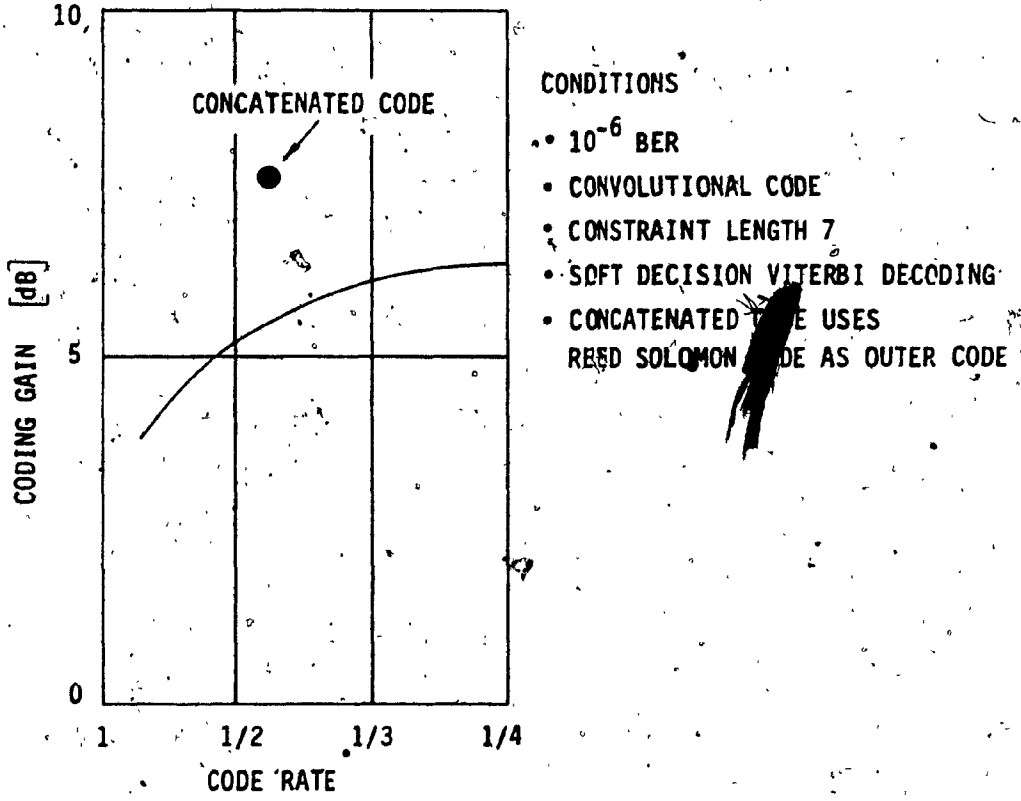

Fig. 3.9 Coding gain (from [3.1]).

3.5 Adaptive rate reduction

In a TDMA system, it is possible to increase the effective fade margin in a channel experiencing rain attenuation by reducing the transmission bit rate of that channel, as illustrated in Fig. 3.10 [3.1]. With the reduction of transmission bit rate the signal bandwidth reduces, signal power remaining constant. If the filter bandwidth can also be reduced in accordance with the transmission bit rate reduction, the signal-to-noise ratio improves. The gain is proportional to the ratio of the standard transmission bit rate to the reduced transmission bit rates.

To make the change possible a reserved portion of the frame is set aside to accomodate this reduced-rate burst.

By reasoning in a way similar to [1], the relative effective usable capacity is given by:

$$C_{ARR} = \frac{1}{1 + F(R_D - 1)} \tag{3.5}$$

where

R_D ratio of the standard transmission bit rate to the reduced transmission bit rate which is equivalent to the time frame expansion.

The gain versus capacity depicted in Fig. 3.11 shows that capacity falls rapidly when the gain due to rate reduction exceeds 10 dB [3.1].

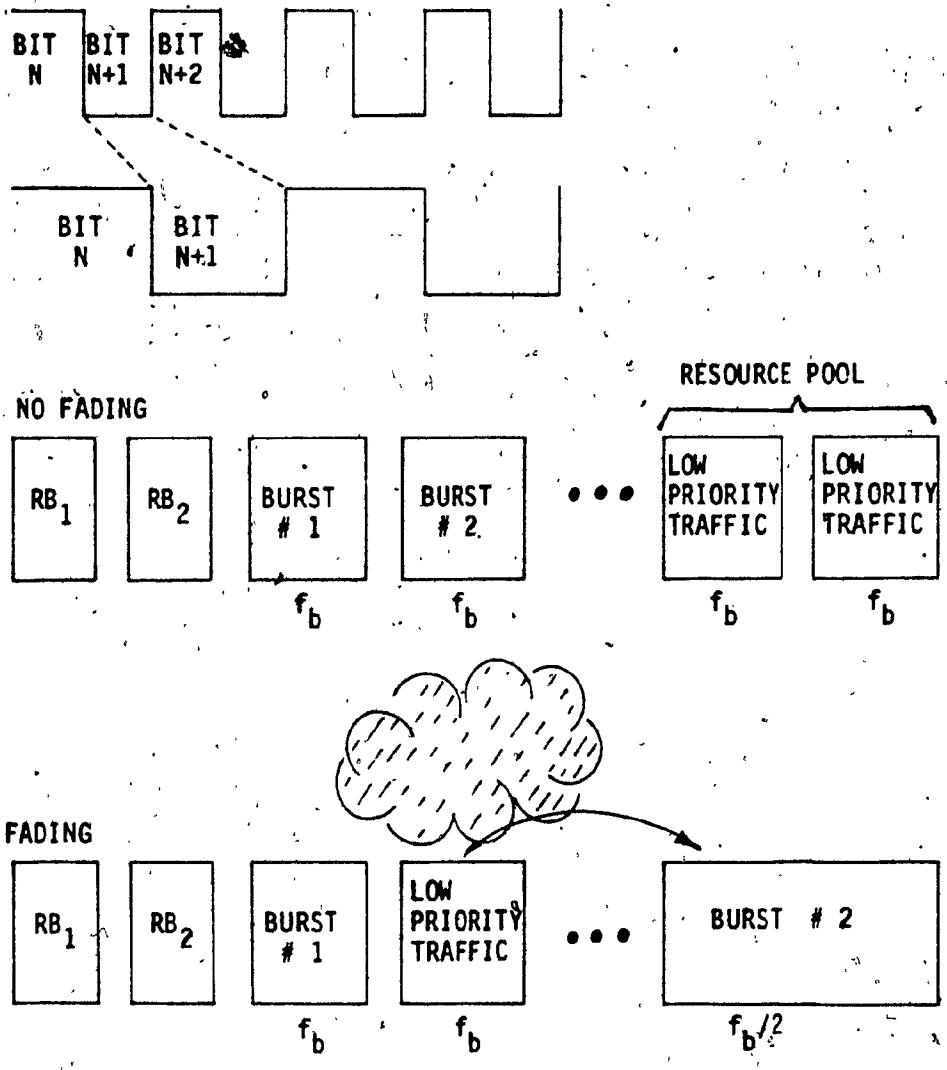

Fig. 3.10 Illustration of adaptive rate reduction and use of reserved pool (from [3.1]).

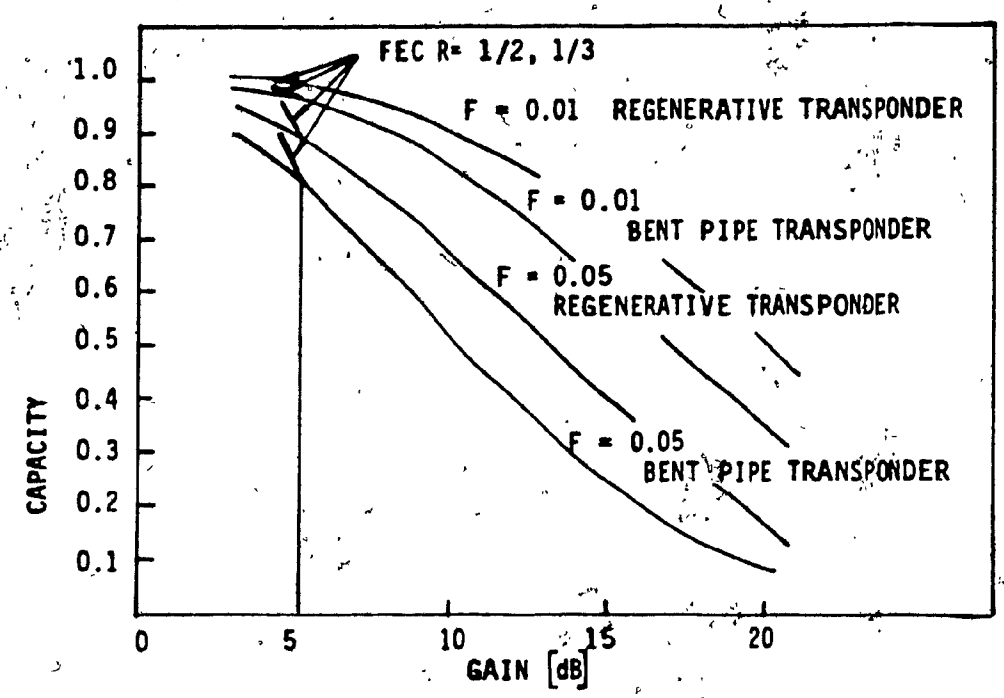

Fig. 3.11 Gain versus capacity for using rate reduction techniques (from [3.1]).

3.6 Adaptive utilization of lower frequency band back-up

The rain attenuation in C and Ku-bands is lower than that in Ka-bands by more than 10 dB for high rain rates. Hence, transmission in Ka-bands requires a larger fade margin than in lower frequency bands for the same availability.

In order to maintain the low fade margin and high availability, during severe rain attenuation, the affected traffic in the Ka-band can be transmitted in a lower frequency band. As soon as the rain attenuation improves, traffic can be reinstalled in their original slots as shown in Fig. 3.12 [3.1].

At time 'a' the attenuation experienced at station 1 becomes greater than the available Ka-band rain margin. Station 1 then switches to C or Ku-band, while all other stations operate at 30/20 GHz. In this example, the rain becomes so heavy at point 'b' that the C-band or Ku-band link is out. This condition rarely occurs, and its frequency is the same as for C-band or Ku-band satellite communications. At time 'c' the low frequency link is restored. At time 'd', attenuation at station 2 switches from high frequency band, etc. Thus, the scheme adaptively switches from a high frequency band to a low frequency band during fades and back to the original frequency band when the rain attenuation is not severe.

Thus using the lower frequency band allocation, or a portion thereof, as a backup for high capacity Ka-bands, allows a satellite capacity several times higher than that of the low frequency band with a nearly equal propagation reliability.

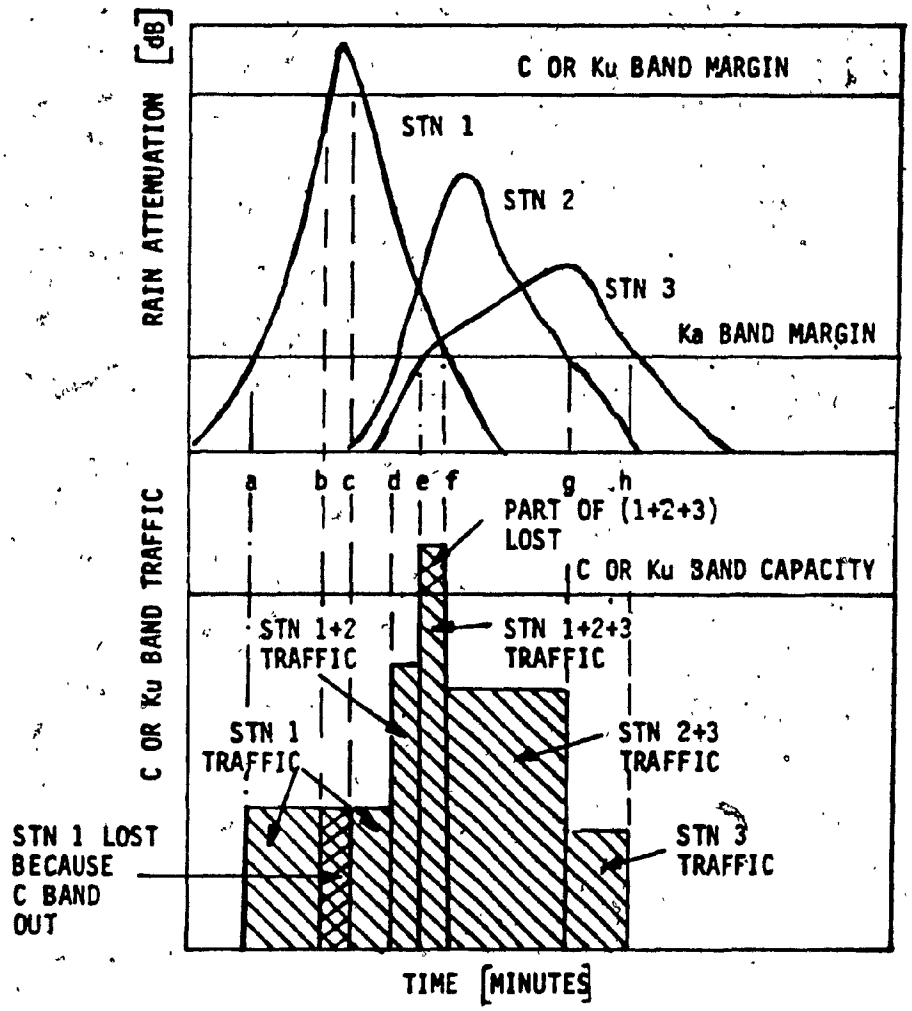

Fig. 3.12 C and Ku-Band frequency back-up (from [3.1]).

3.7 Allocation of Reserved Pool in TDMA Frame

In a TDMA environment both AFEC and ARR schemes require a reserve pool of additional slots in each TDMA time frame, which is only a small fraction of the total time frame, to be shared by all earth stations. This is known as resource sharing reserved pool. There are two typical resource sharing reserved pool TDMA frame formats

1) Common Burst Resource Pool (CBR): In this format (see Fig. 3.13 a) a small pool of reserved slots in the TDMA frame is made available on a burst basis, to be used with those sub-bursts which require protection.

2) Common Frame Resource Pool (CFR): In this format (see Fig. 3.13 b) the reserved pool is shown as being time slots at the end of the frame. These slots are made available to protect some fixed number of channels which experience simultaneous occurrences of fade.

There exist two variations in the use of CFR [3.6].

a) Bursts to degraded users are expanded and succeeding user bursts delayed (see Fig. 3.14)

b) All bursts are confined to their slots. Only the expanded portion of the burst to the degraded user is allocated in the reserved pool as a separate burst (see Fig. 3.15)

The first variation requires no additional overhead (for burst preamble) but requires rescheduling of the frame implying a change in the timing signal. The

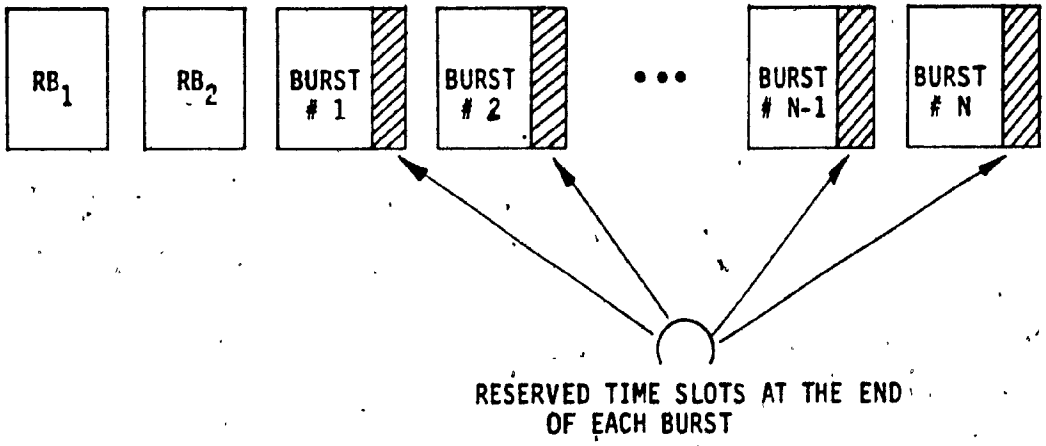

Fig. 3.13a TDMA frame format with reserved time slots at the end of each burst (from [3.6]).

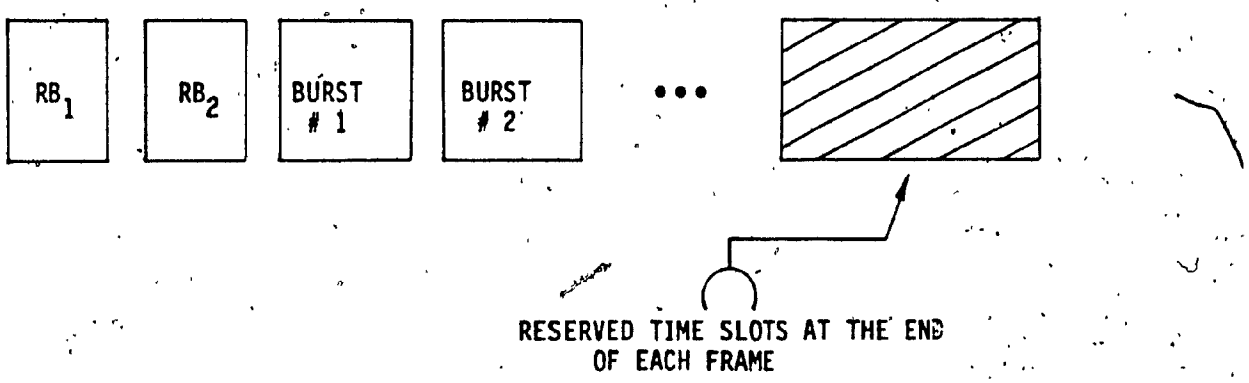

Fig. 3.13b TDMA frame format with reserved time slots at the end of each frame (from [3.6]).

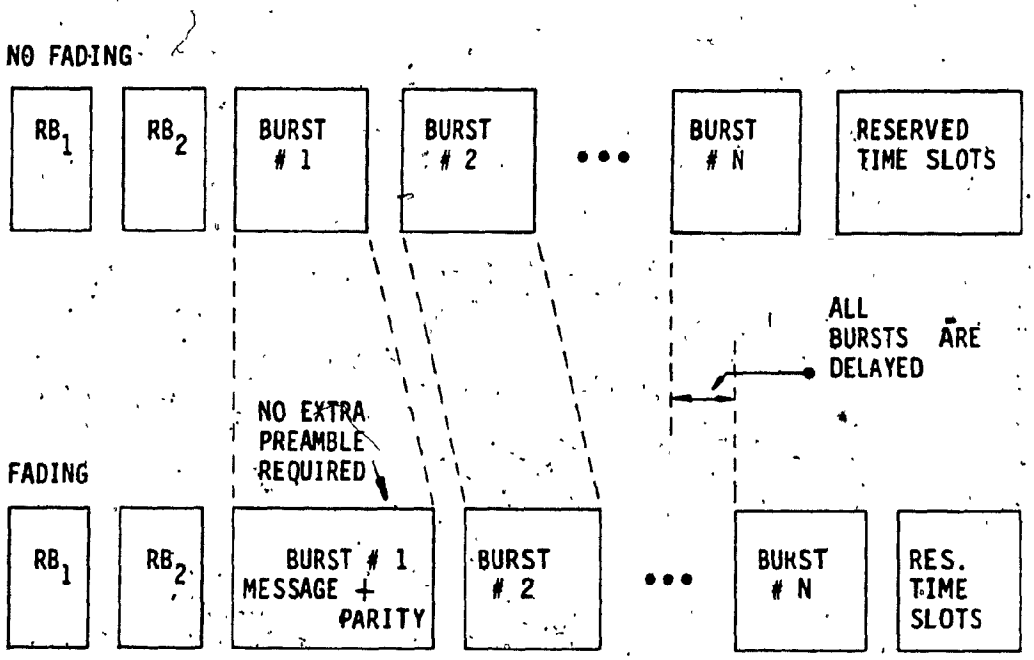

Fig. 3.14 A variant of TDMA reserved time slot allocation (bursts delayed) (from [3.6]).

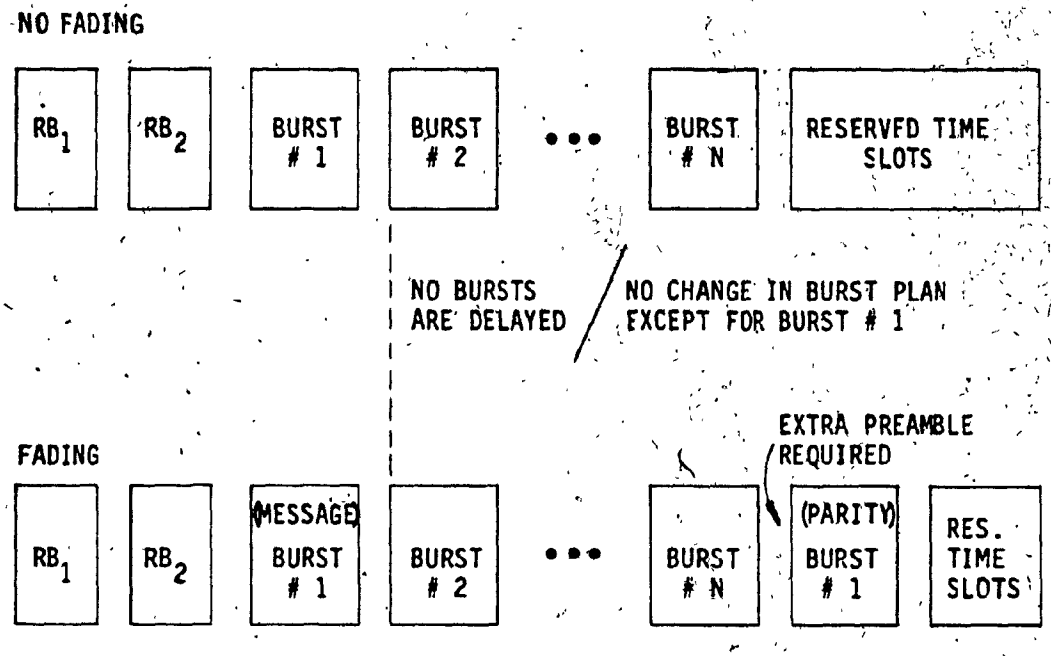

Fig. 3.15 A variant of TDMA reserved time slot allocation (no delay of bursts) (from [3.6]).

second variation minimizes the impact on other users, since frame rescheduling is not required. However, overhead is increased due to the additional guard time and burst preamble required. As a result, TDMA throughput is reduced due to increased overhead.

An alternative TDMA format mixes the features of CBR and CFR. In this format, a smaller pool of time slots is reserved at the end of each frame (see Fig. 3.16). In this manner, the station experiencing uplink degradation will transmit its burst in the reserved slot (at the end of frame) as well as the original slot. Other stations, with traffic destined for the degraded station will use the reserved slot at the end of its burst as well as the original sub-burst. This scheme combines the advantages of the various formats discussed above and minimizes their disadvantages.

In the last scheme, reserved slots at the end of each burst are allocated such that the burst can be protected from low fades. For high fades, the reserved slots at the end of the frame are also used for transmission purposes. As a result, less overhead is required. However, the disadvantage of this scheme is that reserved slots at the end of each burst can only be used for that particular burst and are not available to other bursts. This leads to inefficient use of resources.

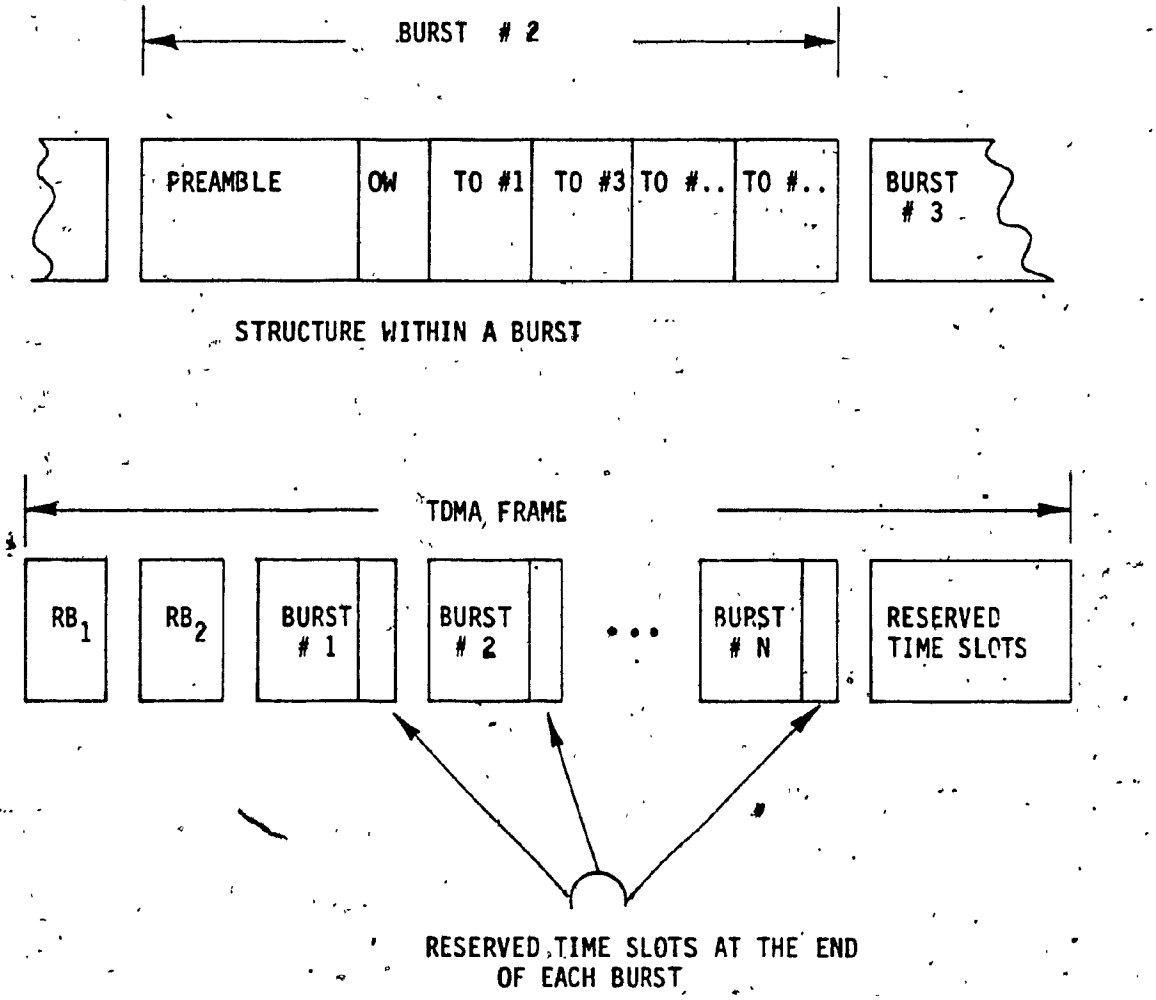

Fig. 3.16 A TDMA format with reserved time slots at the end of each bursts and frame (from [3.6]).

3.8 Discussion and evaluation

From Fig. 3.9 it is found that the gain achieved for a rate 1/2 code is 5 dB. By further reduction of the code rate to say 1/4 the increased gain achieved is only $\approx$ 1 dB. Decreasing the code rate results in bandwidth expansion and increases the reserved pool size. This reduces the effective usable capacity.

In rate reduction techniques the gain is proportional to the rate reduction. For example, a rate reduction of about 4 times can provide a gain of 5 dB [3.1]. For a higher rate reduction a bigger reserve pool is necessary, reducing the effective usable capacity.

Through adaptive FEC or rate reduction it is possible to compensate for rain attenuation of varying degrees. But, as the fade depth increases, the effective usable capacity decreases. Hence, adaptive FEC or rate reduction techniques are useful for relative low fades (e.g. in the range of 6 dB).

On the other hand, low frequency band back-up gives a better protection against deep fades. But for smaller fades which are more frequent, switching to low frequency band is unnecessary. However, transponder switching is very difficult to realize as it involves a change in the whole RF section.

All the adaptive techniques described above are not competing, but rather complement to each other. A combination of these techniques can result in a better performance. For example the combined coding and rate reduction scheme proposed in [3.7] can give an effective usable capacity exceeding 85 percent of that possible if it never rains. The scheme proposes use of rate 1/2 convolutional codes with a large channel signalling alphabet to permit a high rate of information transfer during clear-air conditions. When the fade depths exceed the built-in fade margin, the signalling alphabet is reduced and enough time slots are bor-

rowed from a resource sharing reserved pool to maintain the data rate at the faded site. Thus, depending on the depth of fade exceeding link margin, coding and rate reduction as well as rate reduction alone is used. The performance of this coding and rate reduction scheme was found to be much superior to the scheme using coding alone.

Another combined scheme of adaptive coding (rate 1/2), burst rate reduction and variable rate modulation (QPSK-BPSK) proposed in [3.8] has a high effective usable capacity with less complexity. The scheme proposes an adaptive coding strategy consisting of a rate 1/2 hard-decision decoded block or convolution code providing an equivalent 5 dB carrier-to-noise ratio gain (2 dB from the code plus 3 dB due to holding burst rate constant with burst length doubled) and a QPSK/BPSK switch capability (giving a further 3 dB carrier-to-noise ratio gain and burst-length doubling). The total equivalent coding gain for this scheme when both parts are simultaneously applied is at least 8 dB. However, the implementation of a QPSK/BPSK switch to the TDMA system warrants further investigation.

The third scheme, which is a slightly different version of coding and variable rate reduction, has been proposed in [3.9] for NASA's Advanced Communication Technology Satellite (ACTS) Systems. This scheme proposes a rate 1/2 coding and burst rate reduction to obtain 10 dB of gain; 4 dB is to be achieved by coding and the remaining 6 dB by rate reduction (quadrupling the coded burst length).

It is also possible to expect better results by combining frequency band back-up and adaptive FEC, or frequency band back-up and adaptive rate reduction. The two following hybrid schemes :

1) Combining burst rate reduction, coding and lower frequency band back-up

2) Combining variable rate modulation and coding, burst rate reduction and lower frequency band back-up

were described and their performance compared in [3.10]. It has been shown that the utilized capacity of scheme 1 (for an outage of 0.05 percent and fade margin of 2.5 dB), exceeds 99 percent of the effective usable capacity possible if it never rains. For scheme 2 similar performance is achievable at a fade margin of 1.5 dB. For higher outage objectives the loss of effective utilized capacity is higher for scheme 2.

A comparative performance study of these schemes and those given in [3.7] and [3.8] is also done in [3.10]. Scheme 1 was found to have a higher effective usable capacity than the scheme given in [3.7].

Compared with the scheme in [3.8], scheme 2 requires 6 dB less fade margin to achieve the same availability. Moreover, the requirement of variable transmission rate in many of the schemes mentioned above is very difficult to realize in practice. As the transmission rate is reduced, a series of changes has to be done in the receiver RF section for proper reception.

The major changes are:

- synchronous reduction of modem clock rate
- modification of clock recovery and symbol timing recovery circuits
- reduction of filter bandwidth in accordance with the reduced transmission bit rate to suppress noise.

It is difficult to make a RF section which can facilitate all those changes in real time within a high speed TDMA environment. One alternative could be to have separate RF sections for different transmission rates, which is again contrary to the concept of resource sharing.

On the other hand, by employing baseband coding and information rate reduction, added gain can be achieved while the transmission rate remains constant. Hence, no change in the RF section is required. This simplifies the adaptive FEC application and makes it attractive for further study as a potential rain counter-measure. In the following chapter, selection of proper codes and the effectiveness of Adaptive Forward Error Control coding as a rain counter-measure will be analyzed.

APPENDIX 3A

Analysis of Rain Outage Using Adaptive Resource Sharing

In the following section the outage of a satellite system which use resource sharing schemes as a rain-countermeasure is analyzed. The approach taken closely follows the method given in [3.11].

Rain attenuation characteristics were discussed in detail in Chapter 2. It was found that for earth stations which are situated in geographical proximity, the occurrence of rain attenuation at one earth station is dependent on that of other earth stations. Moreover, severe rain attenuation is experienced during thunderstorm activity period. Hence the probability that attenuation experienced by an earth station exceeds a given level during thunderstorm activity is much higher than the yearly average value. A bias term α_{SDCF} known as seasonal and di-urnal factor is used for accounting the higher probability of attenuation during thunderstorm activity. The value of α_{SDCF} is determined as follows:

$$\alpha_{SDCF} = \frac{h_1}{h_2} \tag{3A.1}$$

where

h_1 total number of hours in a year

h_2 total number of hours of thunderstorm activity

Rain attenuation measurements in different places at midlatitude regions show that periods of thunderstorm activity are typically restricted to a four-month interval lasting from June through September and to 6 hours out of every-day (1 to 7 PM) [3.12]. Hence, for these places the value of the rain correlation factor α_{SDCF} equals 12.

Assume that the whole satellite coverage area has been divided into a small number of regions with the rain fade statistics assumed uniform for each region. Within each region there are a number of earth stations. Let p_1 (a) be the yearly average probability that attenuation exceeds level 'a' at earth station #1. Also assume

$$\Pr\left\{A_1 > a \mid t \in TH\right\} = \alpha_{SDCF}\, p_1(a)$$
$$\Pr\left\{A_1 > a \mid t \in TH\right\} = 0 \qquad (3A.2)$$

where

t is a given instant of time

TH represents the thunderstorm activity period

The event that attenuation exceeds level 'a' at earth station #1 and level 'b' at earth station #2 may be assumed to be independent if the sites are widely

separated. Thus, the probability that attenuation at earth station #1 exceeds level 'a' and attenuation at earth station #2 exceeds 'b' simultaneously at time $t \in TH$ is given by

$$\Pr\left\{A_1 > a, A_2 > b \mid t \in TH\right\} = \left[\alpha_{SDCF}\, p_1(a)\right]\left[\alpha_{SDCF}\, p_2(b)\right] \quad (3A.3)$$

$$= \alpha^2_{SDCF}\, p_1(a)\, p_2(b)$$

Eq. (3A.3) can be easily generalized to the case of an arbitrary number of widely separated sites.

For two closely spaced sites, attenuation at the two sites may be produced by the same storm. Hence, another degree of attenuation event correlation known as site diversity factor α_{SDF} is assumed in addition to the seasonal and di-urnal correlations. In determining the α_{SDF} the following assumptions are made :

a) If a fade of level $a \geq a_o$ has occurred at some earth station, the probability that a fade of level $b \geq a_o$ is simultaneously occurring at a neighbouring earth station is given by C(b) i.e.

$$\Pr\left\{A_2 \geq b \mid A_1 \geq a, t \in TH\right\} = C(b) \quad (3A.4)$$

where

C(b) is assumed to be a fade level dependent constant over the h-hour storm

window.

b) at this second earth station the yearly averaged probability of a fade of level $b \geq a_o$ is attributed exclusively to the h-hour intervals surrounding the events $a \geq a_o$ at the first earth station

Then

$$p_2(b) = k \frac{h}{h_1} C(b) \tag{3A.5}$$

where

h_1 the number of hours in a year

k the average number of events per year the attenuation level exceeds a_o

Now,

$$\Pr\left\{A_1 \geq a, A_2 \geq b \mid t \in TH\right\} =$$

$$\Pr\left\{A_1 \geq a \mid A_2 \geq b, t \in TH\right\} \Pr\left\{A_2 \geq b \mid t \in TH\right\} \tag{3A.6}$$

From assumption b) and Eq.(3A.5)

$$\Pr\left\{A_2 \geq b \mid A_1 \geq a, t \in TH\right\} = C(b)$$

$$= \frac{h_1}{kh} p_2(b) \tag{3A.7}$$

Assume $\alpha_{SDF} = \frac{h_1}{kh}\alpha_{SDCF}$ then

$$\Pr\left\{A_1 \geq a, A_2 \geq b \mid t \in TH\right\} = \alpha_{SDF}\,\alpha^2_{SDCF}\,p_1(a)\,p_2(b) \qquad (3A.8)$$

For L closely spaced sites, Eq. 3.10, generalizes to

$$\Pr\left\{A_1 \geq a_1, A_2 \geq a_2, \ldots, A_L \geq a_L\right\} =$$

$$\alpha^{L-1}_{SDF}\,\alpha^{L}_{SDCF}\,p_1(a_1)\,p_2(a_2)\,\cdots\,p_L(a_L) \qquad (3A.9)$$

Thus, if there is an attenuation event at some earth station, the probability of the same happening at a second earth station within the surrounding geographical region is α_{SDF} times higher than would be expected from di-urnal and seasonal correlation considerations alone. The minimum value $\alpha_{SDF} = 1$ implies that fades occur independently within the thunderstorm period.

To perform the system outage analysis it is important to determine how many simultaneous fades are expected. As the number of earth stations experiencing simultaneous fades increases, there is a high probability that requests for rain counter-measures by the earth stations will outnumber the available resources, resulting in an outage. Hence, in estimating the size of a resource sharing pool a conservative view (i.e. higher values of α_{SDCF} and α_{SDF}) is taken.

Now assume the following system scenario for the ease of analysis:

a) All earth stations in a given region have the same built-in fade margin, i.e. the N_i stations in region i are assumed to have a built-in fade margin

of a_1 (dB)

b) All earth stations carry the same volume of traffic

c) Extra fade margin provided by a resource sharing rain counter-measure is m dB

d) The resources available can handle K simultaneous fades

To start with the analysis of rain outage of a satellite system using resource sharing, choose any two regions and find the probability that a given earth station in region 1 is operational. Since the two regions are arbitrary, the solution applies equally well to other regions.

At any earth station within region 1 three disjoint events may occur at any point in time.

E1) the fade depth, F, may be less than a_1

E2) F may be between a_1 and $a_1 + m$ and

E3) F may exceed $a_1 + m$

Then, the probability that the station is operational

$$\Pr\left\{\text{oper.} \mid t \in TH\right\} = \sum_{i=1}^{i=3} \Pr\left\{\text{oper.} \mid E_i, t \in TH\right\} \Pr\left\{E_i \mid t \in TH\right\} \qquad (3A.10)$$

Clearly,

$$\Pr\left\{\text{oper.} \mid E_1, t \in TH\right\} = 1$$

$$\Pr\left\{\text{oper.} \mid E_1, t \in TH\right\} = 0$$

(3A.11)

$$\Pr\left\{E_1 \mid t \in TH\right\} = 1 - \alpha_{SDCF}\, p(a_1)$$

$$\Pr\left\{E_2 \mid t \in TH\right\} = \alpha_{SDCF}\, p(a_1) - \alpha_{SDCF}\, p(a_1 + m)$$

Thus,

$$\Pr\left\{\text{oper.} \mid t \in TH\right\} = 1 - \alpha_{SDCF}\, p(a_1) +$$

$$\alpha_{SDCF} \Pr\left\{\text{oper.} \mid E_2, t \in TH\right\} \left[p(a_1) - p(a_1 + m)\right] \qquad (3A.12)$$

The result obtained from Eq. (3A.12) is averaged over the entire year

$$\Pr\left\{\text{not oper.}\right\} = \frac{1}{\alpha_{SDCF}} \left[1 - \Pr\left\{\text{oper.} \mid t \in TH\right\}\right] =$$

$$p(a_1) - \Pr\left\{\text{oper.} \mid E_2\ t \in TH\right\} \left[p(a_1) - p(a_1 + m)\right] \qquad (3A.13)$$

Now it is necessary to determine

$$\Pr\left\{\text{oper.} \mid E_2, t \in TH\right\}$$

If during a thunderstorm event E_2 occurs, a particular earth station will be operational if J earth stations simultaneously requiring the reserved pool is less than or equal K (i.e. $J \leq K$). However, if $J > K$ then the above probability is $\frac{K}{J}$.

If event E_2 occurs at a particular earth station, the probability that n_1 additional earth stations in region 1 need to use the reserved pool, where $0 \leq n_1 \leq N_1 - 1$, is given by:

$$\Pr\left\{n_1 \text{ in Region 1} \mid E_2\right\} = \tag{3A.14}$$

$$\binom{N_1 - 1}{n_1}\left[(q_1)^{n_1}(1 - q_1)^{N_1 - n_1 - 1}\right]$$

where

$$q_1 = \alpha_{SDCF}\,\alpha_{SDF}\left[p(a_1) - p(a_1 + m)\right]$$

The probability that n_2 earth stations in region 2 need to use the reserved pool, where $0 \leq n_2 \leq N_2$, is independent of the event E_2 at a particular earth station in Region 1. Assume the following three events, for $n_2 \geq 1$

L_1 a particular set of $n_2 - 1$ earth stations in Region 2 need to use the reserved pool

L_2 an additional earth station in Region 2, not included in L_1, needs to use the reserved pool, and

L_3 none of the remaining $N_2 - n_2$ earth stations of Region 2 need to use the reserve pool

Then

$$\Pr\left\{L_1 \cap L_2 \cap L_3\right\} = \Pr\left\{L_1 \cap L_3 \mid L_2\right\} \Pr\left\{L_2\right\}$$

$$= \Pr\left\{L_1 \mid L_2\right\} \Pr\left\{L_3 \mid L_2\right\} \Pr\left\{L_2\right\}$$

$$= \left\{q_2^{n_2 - 1}\left(1 - q_2\right)^{N_2 - n_2} q_2\right\} \frac{1}{\alpha_{SDF}} \qquad (3A.15)$$

where

$$q_2 = \alpha_{SDCF}\, \alpha_{SDF} \left[p(a_2) - p(a_2 + m)\right]$$

Thus, for $n_2 \geq 1$

$$\Pr\left\{n_2 \text{ in Region 2} \mid E_2\right\} =$$

$$\frac{1}{\alpha_{SDF}} \binom{N_2}{n_2} \left[q_2^{n_2}\left(1 - q_2\right)^{N_2 - n_2}\right] \qquad (3A.16)$$

The probability that none of the earth stations in Region 2 need to use the reserved pool is given by:

$$\Pr\left\{0 \text{ in Region 2} \mid E_2\right\} = 1 - \sum_{n_2=1}^{N_2} \Pr\left\{n_2 \text{ in Region 2} \mid E_2\right\}$$

$$= 1 - \frac{1}{\alpha_{SDF}}\left[1 - (1 - q_2)^{N_2}\right] \qquad (3A.17)$$

where the binomial sum formula has been invoked.

Returning to Eq. (3A.12), for $t \in TH$, the probability that a particular earth station in Region 1 is operational, given attenuation between a_1 and $a_1 + m$ dB, is determined by the sum of the probabilities of the disjoint events defined by:

$$V_{n_1, n_2, S} = \Phi_{n_1} \bigcap \Phi_{n_2} \bigcap S \qquad (3A.18)$$

for $0 \leq n_1 \leq N_1 - 1 ; 0 \leq n_2 \leq N_2$

where

Φ_{n_1} n_1 additional earth stations in Region 1 need to use the reserved pool

Φ_{n_2} n_2 earth stations in Region 2 need to use the reserved pool, and

S the particular earth station of interest has been assigned time slots from the reserved pool.

Define the function

$$f(m) = \begin{cases} 1 & \text{for } m \leq K \\ \dfrac{K}{m} & \text{for } m > K \end{cases} \tag{3A.19}$$

Then, it can be concluded that

$$\Pr\left\{\text{oper.} \mid E_2, t \in TH\right\} = \tag{3A.20}$$

$$\sum_{n_1=0}^{N_1-1} \sum_{n_2=0}^{N_2} \left[f(1+n_1+n_2) \Pr\left\{n_1 \text{ in Region 1} \mid E_2\right\} \right.$$

$$\left. \Pr\left\{n_2 \text{ in Region 2} \mid E_2\right\} \right]$$

where

$$\Pr\left\{n_1 \text{ in Region 1} \mid E_2\right\}, \Pr\left\{n_2 \text{ in Region 2} \mid E_2\right\}$$

are given by Eqs. (3A.12, 3A.16, and 3A.17).

Substituting Eq. (3A.20) into (3A.13) yields the desired result for the yearly average probability that a particular earth station is unavailable versus the built-in fade margins a_1 and a_2.

Extending the above analysis to I regions, the following is obtained:

$$\Pr\left\{\text{not oper.}\right\} = p(a_1) - \Pr\left\{\text{oper.} \mid E_2, t \in TH\right\}$$

$$\left[p(a_1) - p(a_1 + m)\right] \tag{3A.21}$$

where

$$\Pr\left\{\text{oper.} \mid E_2, t \in TH\right\} =$$

$$\sum_{n_1=0}^{N_1-1} \sum_{n_2=0}^{N_2} \cdots \sum_{n_I=0}^{N_I} \left[f(1 + n_1 + n_2 + \cdots + n_I) \prod_{i=1}^{I} \Pr\left\{n_i \text{ in Region } 1 \mid E_2\right\}\right] \tag{3A.22}$$

and where for Region 1

$$\Pr\left\{n_1 \text{ in Region } 1 \mid E_2\right\} = \binom{N_1 - 1}{n_1} \left[q_1^{n_1} (1 - q_1)^{N_1 - n_1 - 1}\right] \tag{3A.23}$$

for $0 \leq n_1 \leq N_1 - 1$ and for Region 2 through I

$$\Pr\left\{n_i \text{ in Region } 1 \mid E_2\right\}$$

$$= \frac{1}{\alpha_{SDF}} \binom{N_i}{n_i} \left[q^{n_i}_i (1 - q_i)^{N_i - n_i}\right], \quad 1 \leq n_i \leq N_i$$

$$= 1 - \frac{1}{\alpha_{SDF}} \left[1 - (1 - q_i)^{N_i}\right], \quad n_i = 0 \tag{3A.24}$$

where for all i,

$$q_i = \alpha_{SDCF}\,\alpha_{SDF}\left[p(a_i) - p(a_i + m)\right]$$

Thus, the probability that a particular earth station experiences an outage depends on the following probabilities :

1) Probability of rain attenuation for the particular earth station exceeds the built in fade margin.

2) Probability that the reserved pool is unavailable for that particular earth station to use rain counter measures.

The first probability can be determined through long term rain attenuation measurement data or prediction models (see chapter 2) obtained for the site of the particular station. The second probability is more difficult to obtain and requires knowledge of the probability that the total number of other stations in the system which experience simultaneous fade in excess of the built in margin exceeds the capacity of reserved resources. However, the second probability can be found using (3A.22), (3A.23), and (3A.24).

The resource sharing pool size is determined so that the probability of an outage can be reduced to an acceptable level.

REFERENCES

[3.1] Bronstein, L.M., " The Enhancement of Propagation Reliability for Millimeter wave Satellite Communication Systems," Proc. of ICC, 1982, pp. 1B4.1-1B4.5.

[3.2] Bhargava, V.K., Haccoun, D., Matyas, R., and Nuspl, P.P., Digital Communications by Satellite, John Wiley & Sons, New York, 1981.

[3.3] Ince, A.N., Brown, D.W. and Midgley, J.A., " Power Control Algorithms for Satellite Communication Systems," IEEE Trans. on Communications, Vol.COM-24, 1976, pp. 267-275.

[3.4] Sundberg, C.E., and Rydbeck, N. " Redistribution of Transmitted Satellite Power in PCM/TDMA Systems by Adaptive Use of Error-Correcting Codes ", Proc. of ICC, 1975, pp. 28-6--28-10.

[3.5] --- " Analysis of Pulse Code Modulation with Error Correcting Codes for TDMA Satellite Communication Systems ", Proc. of the 2nd ICDSC, 1975, pp. 214-219.

[3.6] Lee, L. and Strickland. G, Final Contract Report on Adaptive FEC, Submitted to INTELSAT, contract INTEL 222, RCE 008, Item 26, 1982.

[3.7] Acampora, A.S., " The use of Resource Sharing and Coding to Increase the Capacity of Digital Satellite;" IEEE Journal on Selected Areas in Communications, Vol. SAC-1, 1983, pp. 133-142.

[3.8] Mazur, B., Crozier, S., Lyons, R., and Matyas, R. " Adaptive Forward Error Correction Techniques in TDMA," Proc. of the 6th ICDSC, 1983, pp. XII-8 - XII-15.

[3.9] Inukai, T. and Campanella, S.J. " ACTS TDMA Network Control," Proc. of the 10th AIAA Satellite Systems Conference, 1984, pp. 188-195.

[3.10] Khan, M.H., Le-Ngoc, T., and Bhargava, V.K. "Adaptive Forward Error Control for Digital Satellite Systems," IEEE Trans. on Aerospace and Electronic Systems, Vol. AES 21, 1985, pp. 547-558.

[3.11] Acampora, A.S., " Rain Margin Improvement Using Resource Sharing in 12-GHz Satellite Downlinks, " B.S.T.J, Vol. 60, 1981, pp. 167-192.

[3.12] Ippolito, L.J., " Radio Propagation for Space Communications Systems, " Proc. of IEEE, Vol. 69, 1981, pp. 697-727.

CHAPTER FOUR

AFEC TECHNIQUES IN RESOURCE SHARING

In the previous chapter different adaptive resource sharing schemes were studied. The implementation complexity of those schemes was also compared. It was concluded that adaptive FEC (AFEC) resource sharing schemes are the simplest to implement and could be efficiently used as a rain counter-measure.

In this chapter two efficient hybrid AFEC resource sharing schemes suitable for high capacity TDMA systems are proposed.

At first, selection criteria for potential AFEC schemes and the comparative performance of available candidate codes will be given. Then a variation of concatenated coding called double coding will be introduced and its performance analyzed.

4.1 General concept

In general three basic resources, power, bandwidth, and time can be varied to achieve additional fade margins (FM). In TDMA, transmission / reception is carried out using power and bandwidth resources on a time sharing basis. From the practical constraints of a TDMA system and satellite architecture the first two resources, (power and bandwidth) are not conveniently varied adaptively. However, the burst transmission time can be extended using extra reserved time slots in the TDMA frame.

As a result, for additional FM, the information rate is reduced along with coding so that the transmission rate and bandwidth remains unchanged. Total coding gain (TCG)* obtained by coding will increase the FM thus countering rain fade. Extra bits due to coding are transmitted through the reserved time slots. The reserved pool of time slots are used on a resource sharing basis and can be allocated for any transmission burst on demand.

To detect the occurrence and magnitude of rain fade, it is required to monitor received power or BER. Uplink monitor controls the uplink power control (UPC) while detection of degraded downlink leads to a request and subsequent allocation of rain counter-measures from the resource controller. The whole switching process is a complex one requiring a number of different operations like TDMA frame configuration, signalling to the receiving earth stations, codec assignment and data control, etc. Moreover, to cope with the rapidly changing link degradation (0.1 to 0.5 dB/sec) [4.1], detection and allocation of counter-measure has to be effected very quickly. In view of the complexity involved with each switching process, it is preferred to keep the number of switching to a minimum. Hardware and software aspects of the monitoring system, and switching and control mechanism will be discussed in detail in Chapter 5.

In Fig. 4.1 the general concept of AFEC is illustrated with three modem performance curves for high and low gain codes and no coding. Assume that in a normal operating condition the unfaded received power by the monitor is $C_{unfaded}$ [dBm], and the corresponding bit error rate is BER_0 for no coding. Usually BER_0 is much lower than the threshold bit error rate BER_T (e.g. 10^{-5}). With the occurrence of fades the received power is attenuated, resulting in a reduction of $\frac{E_b}{N_o}$ and an increase of BER. As rain attenuation approaches the fixed FM_0 (e.g.

* Total coding gain = net coding gain + gain due to information rate reduction

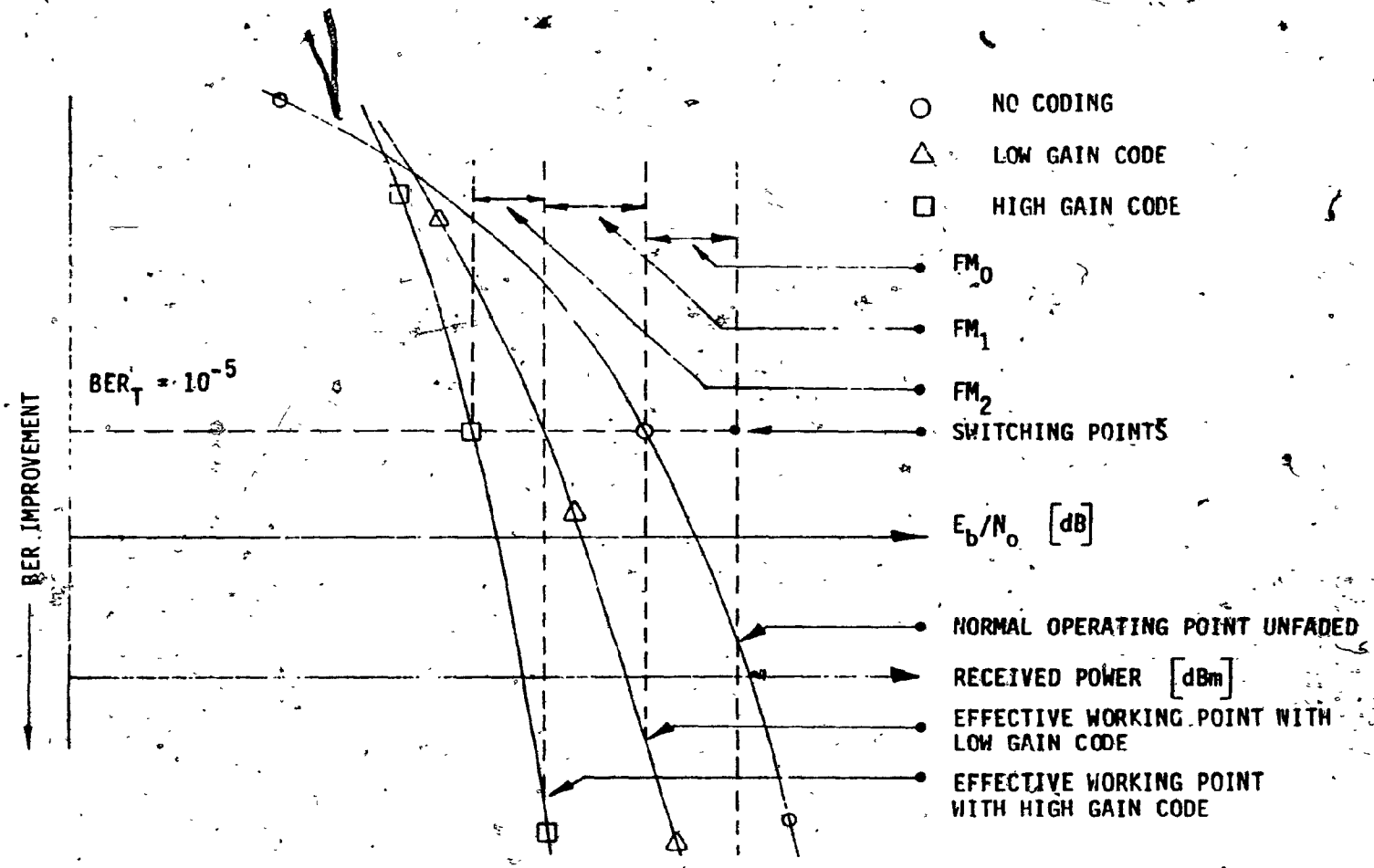

Fig. 4.1 AFEC concept

11 dB) the BER approaches the threshold BER_T. At this point the low gain code is introduced. The BER becomes BER_1, providing an additional fade margin FM_1 which is the TCG of the low gain code. Similarly, if the rain attenuation keeps increasing and approaches ($FM_0 + FM_1$) the high-gain codec is introduced to bring the operating BER to BER_2, providing an additional fade margin FM_2. Here ($FM_1 + FM_2$) represents the TCG of the high gain codec. In other words to keep the operating BER lower than the threshold BER_T, different codecs are introduced as follows.

a) for received power (C_{rcv}) higher than ($C_{unfaded} - FM_0$) no codec is used.

b) For received power within the range ($C_{unfaded} - FM_0$) to ($C_{unfaded} - FM_0 - FM_1$), the low gain codec is introduced.

c) For received power within the range of ($C_{unfaded} - FM_0 - FM_1$) to ($C_{unfaded} - FM_0 - FM_1 - FM_2$) the high gain codec is used.

Thus, an effective AFEC scheme can be realized by switching from no coding to a low / high gain code and vice versa in response to the rain attenuation.

In accordance with the fade margin requirement for a rapidly changing link, the codes to be used for AFEC resource sharing should have at least 5 and 9 dB of TCG at a minimum BER of 10^{-5}. The mean BER is derived from the BER of 10^{-4} and 10^{-6} which are recommended by CCIR as standard for voice and data transmission respectively [4.1].

For effective performance of an AFEC scheme the candidate codes have to satisfy the following criteria :

1) The codes have to be adaptive to switching from no coding to coding, or from one codec to another such that data transmission is uninterrupted

and lossless in the transition process. Moreover, extra hardware which does not constitute part of the sharable resource pool (e.g. separate sets of codecs, buffers and other accessories) should be kept to a minimum.

2) High capacity satellite systems of the future will operate at high data rates. Hence, less complex codes are preferable to be compatible with high speed operation.

3) The codes chosen should have enough coding gain (e.g. at least 5 to 9 dB or more) to counter severe rain fade situations.

4) High rate codes are preferable as they require a smaller TDMA reserved pool.

As can be seen, the criteria to select an ideal AFEC scheme are quite contradictory in nature and difficult to satisfy simultaneously. Thus, while choosing a suitable high/low gain code some criteria get preference over others.

In the following sections, theoretical possibilities and limitations of coding schemes, performance of suitable candidate codes and codec complexity will be discussed.

4.2 Overview of coding development and candidate codes for AFEC schemes

Shannon [4.2] inaugurated the study of the performance of coding schemes on a channel in which the input is a real signal of limited power, and the noise is additive, Gaussian, and white. His work established that for any fixed signal-to-noise ratio, $\frac{E_b}{N_0}$, there is a critical code rate, called capacity, such that given

sufficient delay and computing resources, it is possible to design a low rate code which attains any specified user error probability. He also discovered another critical code rate, R_0, below which the required decoding costs and complexity may be significantly less.

According to this theory, which was refined by many authors [4.3, 4.4, 4.5, 4.6], for binary block codes, the average sequence error probability over the ensemble of all codes of varying length and rate is given by

$$\overline{P_s} < 2^{-n(R_0 - r)} \tag{4.1}$$

where

r Code rate

n Length of code

From Eq. (4.1) it is evident that as long as $R_0 > r$ it is possible to drive the probability of error to zero provided that the code is long enough.

By letting the code rate equal $(R_0 - \epsilon)$, with ϵ very small, a bound on achievable coding gain can be derived as plotted in Fig. 4.2 [4.7]. The plot indicates the minimum possible value of $\frac{E_b}{N_0}$ for a given code rate for which Eq. (4.1) can still be driven to zero while keeping 'n' fixed to a finite value.

For example, it is known that with ideal PSK signalling and no coding an $\frac{E_b}{N_0}$ of 9.6 dB is required to produce an error rate of 10^{-5}. From Fig. 4.2 it is seen that an arbitrarily low error rate can be obtained for an $\frac{E_b}{N_0}$ of 2.54 dB with a

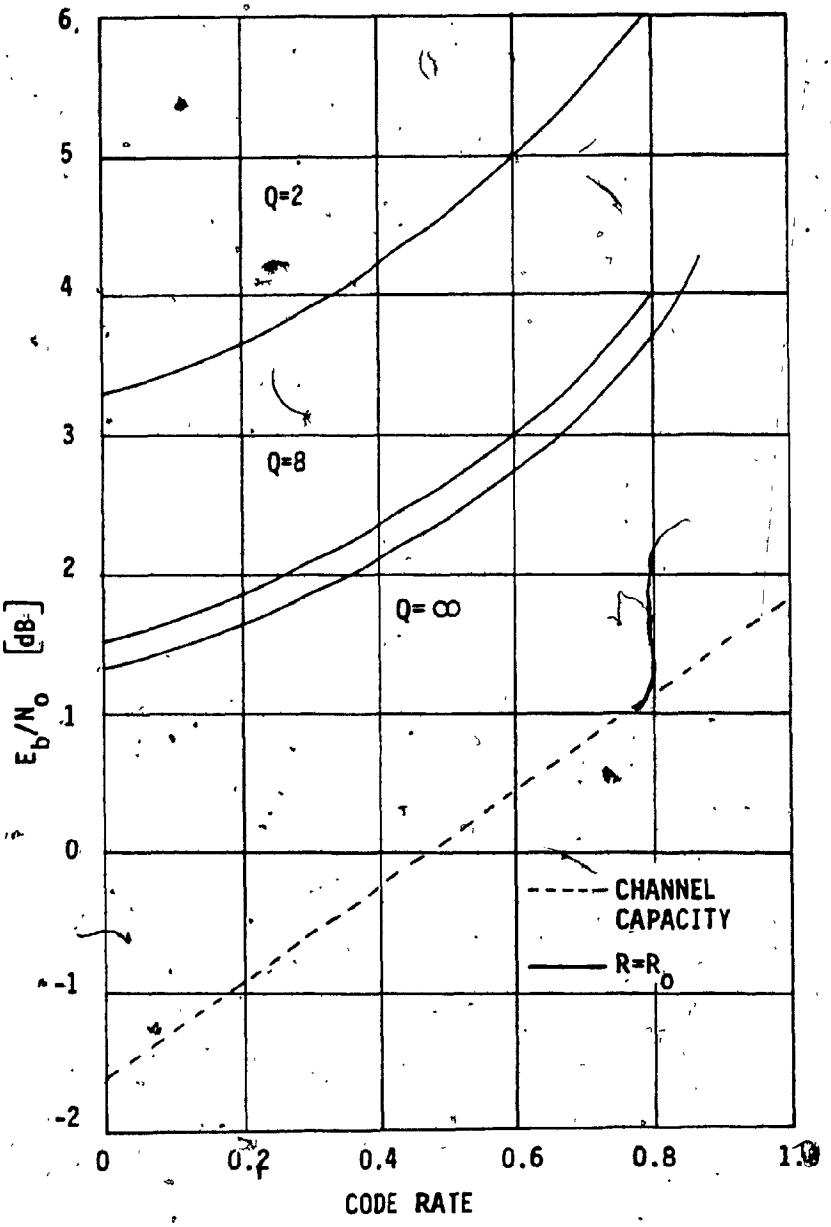

Fig. 4.2 $\frac{E_b}{N_o}$ required to achieve $R = R_o$ for binary signalling (from [4.7]).

rate 1/2 code. Thus, it is possible to obtain a net coding gain of at least 7.15 dB at $\overline{P_s} = 10^{-5}$ using a rate 1/2 code.

However, in Shannon's view, the channel parameters were regarded as fixed and the codes as variable. He also ignored the question of decoding complexity and delay required to achieve the coding gain. Naively paraphrased [4.8], Shannon's formulation asks every user to specify exact channel parameters, i.e. the time invariant average signal-to-noise level, the probability of error required, etc., and then the engineer finds a code of certain length and rate to meet the above specifications.

In the past decade, his formulation of the problem of analyzing the performance of various coding and decoding schemes has fallen out of favour. The modern engineering approach considers the channel to be variable and the code fixed, rather than vice versa. As it is very difficult to specify exactly the channel, because of its variation from time to time depending on numerous unpredictable factors such as the weather or the interference, it is now customary to begin with a particular ad-hoc choice (or a limited range of choices) of coding and decoding schemes. Then provide a curve or a set of curves showing the result of some sort of analysis or simulation of how well the proposed coding/decoding scheme will function against a variable level of average channel noise [4.8]. The decoding complexity, cost and speed factors are also considered while choosing a code (or a set of codes).

In the previous section code selection criteria for AFEC resource sharing techniques in Ka-band has already been discussed. One of the most demanding requirements is the high coding gain. Hence, in the following, only high performance coding techniques will be considered.

The high performance codes can be broadly partitioned into four categories:

a) convolutional codes (CC)

b) Bose-Chaudhuri-Hocquenghem codes (BCH),

c) Reed-Solomon codes (RS)

d) concatenated codes.

Convolutional codes are a subset of the so-called tree codes and were introduced by Elias [4.9]. Sequential decoders for convolutional codes were introduced by Wozencraft-Reiffen [4.10] and Fano [4.11]. Jacobs and Berlekamp [4.12] investigated the buffer overflow phenomenon, which turned out to be the primary limitation of sequential decoders.

Viterbi [4.13] introduced a new decoding algorithm which circumvented this difficulty at the cost of computational complexity that grows exponentially with the operational speed and constraint length. In order to cope with these limitations, Viterbi decoders now typically use short to moderate constraint lengths and operate at slow to moderate speeds. However, with parallel processing the decoding can be made faster and applied to high speed operation [4.7].

A general form of binary algebraic codes known as BCH codes were formulated mathematically by Bose, Chaudhuri and Hocquenghem [4.14]. Non binary algebraic codes known as RS codes were devised by Reed and Solomon [4.15]. The RS codes operate on characters (or short words) rather than on individual bits. These codes are quite extensively studied and efficient encoding/decoding algorithm have been developed.

It can be observed from Eq. (4.1) that increasing the code length reduces error probability or in other words increases the error correcting capability of the code. Thus coding gain is increased. However, as explained in [4.16], the complexity of coded communication systems grows exponentially with the increase in

block length for block codes (or with the constraint length for convolutional codes). Hence, instead of directly using very long codes, the idea of cascading two or more codes of less complexity to achieve highly reliable communications was first considered by Elias [4.17] and later by Forney [4.18]. These codes are known as concatenated codes.

So far, convolutional codes with Viterbi and sequential decoding, BCH, RS and different types of concatenated codes remain the major varieties of code in use for various satellite, microwave and deep space communication systems [4.19, 4.20, 4.21, 4.22].

In Fig. 4.3 and Table 4.1 [4.1, 4.7, 4.16], the codes that are usually employed in satellite communication and have a TCG exceeding 5 dB are shown. The codes are of simple to moderate complexity and hence are suitable for high speed operation.

Although most of the codes have a TCG exceeding 5 dB (low gain threshold) only a few have a TCG exceeding 9 dB (high gain threshold). This shows that there are many potential candidates for low gain applications and only a few suitable for high gain applications.

Since high rain fades are less probable than the low fades, low gain codes are required more often than the high gain ones. Hence the size of a resource pool depends mostly on the code rate of the low gain one. Moreover, average coding/decoding delay of the system also depends on the code complexity of the low gain codes. In order to reduce the resource sharing pool size and delay, it is important to have a high rate and less complex code for low gain applications. This makes the choice limited to codes with rate not lower than 1/2. A few representatives of these codes are given below:

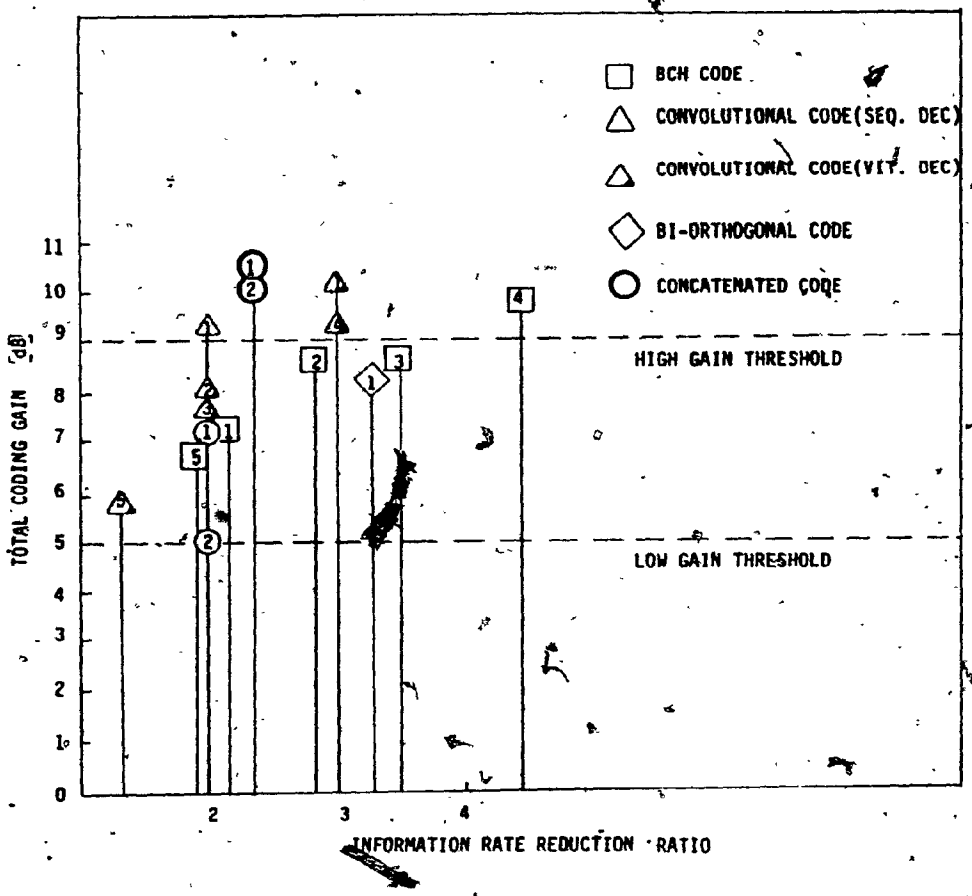

Fig. 4.3 Code performance at BER of 10^{-5}

Table 4.1 Code performance at BER of 10^{-5}

SYMBOLS	CODES	DECODING	TCG dB	NUMBER OF COMPUTATION/ INF. BIT
	BCH CODES			
1	(255,123)	HARD DECISION	7.01	2042
2	(255, 91)	HARD DECISION	8.4	2042
3	(127, 36)	HARD DECISION	8.5	1214
4	(127, 29)	HARD DECISION	9.7	1471
5	(127, 64)	HARD DECISION	6.34	811
1	(23,12)	HARD DECISION	5.0	30
2	(24,12)	SOFT DECISION	7.0	30
	CONVOLUTIONAL			
1	K= 7, R = 1/2	SEQ.(3 BIT)	9.2	128
1	K= 7, R = 1/3	VIT.(3 BIT)	10.17	128
2	K= 7, R = 1/2	VIT.(3 BIT)	8.1	128
3	K= 5, R = 1/2	VIT.(3 BIT)	5.3	32
4	K= 4, R = 1/3	VIT.(3 BIT)	9.1	16
5	K= 9, R = 3/4	VIT.(3 BIT)	5.55	512
	BI-ORTHOGONAL			
1	(16,5)	SOFT DECISION	8.05	272
	CONCATENATED			
1	(127,111)RS/(K=7, R=1/2 CONVOLUTION)	SOFT DECISION	10.4	2666
2	(63,55) RS/(K=7, R=1/2 CONVOLUTION)	SOFT DECISION	10.1	1010

1) Golay codes

2) some of the BCH codes

3) convolutional codes (Viterbi decoding)

Coding gain and decoding complexity increases with the code minimum distance [4.7]. A higher minimum distance means a lower code rate. Some of the codes which are suitable for high gain requirements and have a moderate rate (in the range from 1/3 to 1/2) are given below:

1) convolutional codes (sequential decoding)

2) convolutional codes (Viterbi decoding)

3) concatenated codes

Convolutional codes (sequential decoding) are eliminated from consideration because of their inherent problem of variable decoding delay and buffer overflow with signal-to-noise ratio fluctuations [4.7, 4.16]. Moreover, in a resource sharing TDMA environment the same coder/decoder will be shared on a time division basis by several sub-bursts during each frame. This requires flushing of the shift registers after each sub-burst. Due to large constraint length requirements this creates more redundancy [4.1].

As it stands, by choosing suitable low and high gain codecs which could operate in conjunction with each other, an AFEC scheme can be arranged. However, with a view to minimize redundant hardware and increase the use of built in hardware resources of the earth station a suitable AFEC scheme using a low gain (rate 1/2, constraint length 7) convolutional code and a high gain (rate 1/3, constraint length 7) convolutional code has been suggested in [4.23]. The

scheme can give a dynamic fade margin of 10 dB for a maximum information rate reduction of 3.

It is possible to realize a variable rate (rate $\geq 1/2$) convolutional code from the original rate 1/2 convolutional code with a minor addition of external circuitry to the codec [4.24]. This will allow a progressively adaptive rain counter-measure and efficient management of the resources.

Among all the codes given in Fig. 4.3 the (127,111) Reed Solomon/(rate 1/2, constraint length 7) convolutional code concatenation has the best performance (TCG = 10.4 dB). The code rate is also moderate. Hence, an effective AFEC scheme can be realized using the above code with the inner convolutional code used for low fades (TCG = 8 dB). For high gain requirements both the inner and outer code will be used in concatenation. It is also possible to incorporate the technique of variable rate inner convolutional code (as previously mentioned) to allow a progressively adaptive rain counter-measure.

In a Viterbi decoder an error event occurs whenever the correct sequence is rejected by the decoder in favour of its adversary at some node. The adversary must differ from the correct sequence in at least one branch, and may differ in many branches. Thus errors come in bursts, and typically a burst event affects more than one symbol of a RS code word. An interleaver is placed before the inner coder and a deinterleaver after the inner decoder.

For concatenated codes the interleaver /deinterleaver in between the outer and inner codecs acts as a buffer during switching of codecs. Hence, a little additional circuitry is required to adapt the codec to an AFEC application.

Concatenated codes have less overall complexity than a single powerful code of equivalent performance [4.25]. The reduction in complexity and the opportunity of using component codes alone or in combination to obtain variable gain and

higher utilization of hardware resources make concatenated codes very appealing for AFEC purpose.

In Table 4.2 the performance of some TDMA/AFEC compatible concatenated codes are illustrated. In all the codes the inner code is chosen to be a (rate 1/2, constraint length 7) convolutional code (Viterbi decoded) to meet the low gain requirement. For the outer code RS codes of different symbol sizes were used. Comparing Table 4.2 and Fig. 4.3 it is found that concatenated codes have better TCG than most codes of identical rate.

The AFEC scheme based on concatenated codes discussed above requires two different sets of codecs (Reed Solomon and convolutional). Because of the infrequent nature of rain attenuation these codecs are utilized in conjunction for only a small period (less than 0.1%) of time. Most of the time the TCG obtained from the convolutional code will be enough to counter the rain attenuation. Thus the scheme is not efficient in resource utilization and does not justify the increased earth terminal cost required to install two codecs and other related accessories. Moreover, both Viterbi and RS decoding require a large amount of computation implying decoding delay.

In Ka-bands, service to the customers will be abundant. In these bands the number of single channel users will increase largely along with high capacity trunk services. Expensive terminals will certainly discourage the small capacity users.

With a view to reduce complexity and cost we propose to use the same outer and inner codes. Thus, a single codec could be used repeatedly. We denote this type of two identical cascading codes as double coding. In fact double coding is a degraded concatenated code as the outer and inner codecs are the same.

In Fig. 4.4 a block diagram of an AFEC scheme using double coding is illus-

Table 4.2 Performance of concatenated codes at BER of 10^{-5}

OUTER CODE (RS CODE)	INNER CODE	OVERALL CODE RATE	TOTAL CODING GAIN [dB]	NUMBER OF COMPUTATIONS PER INFORMATION BIT.
(63,59)	RATE 1/2 CONSTRAINT LENGTH 7 CONVOLUTIONAL CODE (VITERBI DECODING) (TCG=8.1 dB)	0.47	9.56	582
(63,55)		0.44	10.1	1010
(127,119)		0.47	9.87	1134
(127,111)		0.44	10.4	2666
(255,239)		0.47	10.1	3246
(255,223)		0.44	10.56	9198
(511,479)		0.47	10.25	10718
(511,447)		0.44	10.7	35118

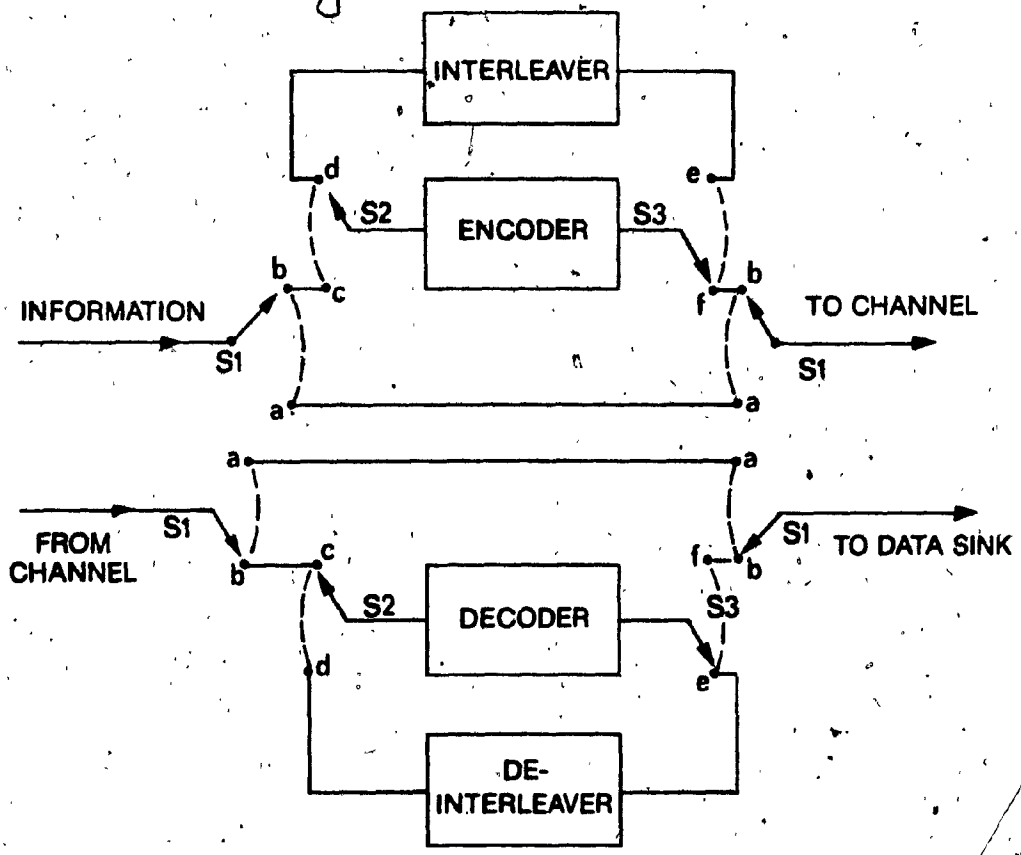

FOR NO CODING	S1 IN "a"
FOR SINGLE CODING	S1 IN "b"; S2 IN "c"; S3 IN "f"
FOR DOUBLE CODING	FIRST: S1 IN "b"; S2 IN "c"; S3 IN "e" NEXT: S2 IN "d"; S3 IN "f"

Fig. 4.4 Block diagram of double codec

trated. Besides codecs, the other important blocks shown in the figure are the interleaver and deinterleaver. Interleaving and deinterleaving are used to remove the channel memory.

For double coding, a block of information bits is encoded and stored in the interleaver memory. Subsequently, the stored bits are read out in a sequence determined by the interleaver and re-encoded. After double coding the bit stream is ready for transmission. At the receiving end the reverse process is performed by decoding, de-interleaving and decoding in succession.

In the case of single coding the bit stream is transmitted directly after the first coding.

Thus, by adaptively choosing single coding (for less protection) or double coding (for better protection) an AFEC scheme can be realized which offers efficient resource utilization and simplicity of application.

Details about this scheme will be given in the following chapter.

REFERENCES

[4.1] Adaptive Forward Error Correction Techniques - Miller Communications Systems Ltd., DSS Contract OST81 - 00249, 1982.

[4.2] Shannon, C.E., " A Mathematical Theory of Communication, " B.S.T.J, Vol. 27, 1948, pp. 379-423, 623-656.

[4.3] Shannon, C.E., Gallager, R.G., and Berlekamp, R.E., " Lower Bounds to Error Probability for Coding on Discrete Memoryless Channels, " Inform. Control, Vol. 10, 1967, pp. 65-103, 522-552.

[4.4] Massey, J.L., " Coding and Modulation in Digital Communication, " Telecommunications Seminar, Zurich 1974.

[4.5] McEliece, R.J., The Theory of Information and Coding, Addison-Wesley, 1977.

[4.6] Viterbi, A.J., " Spread Spectrum Communications - Myths and Realities, " IEEE Communications Magazine, Vol. 17, 1979, pp. 11-18.

[4.7] Clark, G.C., and Cain, J.B., Error Correction Coding for Digital Communications, Plenum Press, New York, 1981.

[4.8] Berlekamp, E.R., " The Technology of Error-Correcting Codes, "

Proc. of IEEE, Vol. 68, 1980, pp. 564-593.

[4.9] Elias, P., " Coding for Noisy Channels, " IRE Conv. Record, Pt. 4, 1955, pp. 37-46.

[4.10] Wozencraft, J.M., and Reiffen, B., Sequential Decoding, M.I.T Press, Cambridge, Mass. 1961.

[4.11] Fano, R.M., " A Heuristic Discussion of Probabilistic Decoding, " IEEE Trans. on Inform. Theory, Vol. IT-9, 1963, pp. 64-74.

[4.12] Jacobs, I.M., and Berlekamp, E.R., " A Lower Bound to the Distribution of Computation for Sequential Decoding, " IEEE Trans. on Inform. Theory, Vol. IT-13, 1967, pp. 167-174.

[4.13] Viterbi, A.J., " Error Bounds for Convolutional Codes and an Asymptotically Optimum Decoding Algorithm, " IEEE Trans. on Inform. Theory, Vol. IT-13, 1967, pp. 260-269.

[4.14] Bose, R.C., and Ray-Chaudhuri, D.K., " On a Class of Error Correcting Binary Group Codes, " Inform. Control, Vol. 3, 1960, pp. 68-79, 279-290.

[4.15] Reed, I.S., and Solomon, G., " Polynomial Codes over Certain Finite Fields, " J. Soc. Indus. Appl. Math., Vol. 8, 1960, pp. 300-304.

[4.16] Bhargava, V.K., Haccoun, D., Matyas, R., and Nuspl, P.P., Digital Communications by Satellite , John Wiley & Sons, 1981.

[4.17] Elias, P., " Error-Free Coding, " IRE Trans. on Inform. Theory, Vol. IT-4, 1954, pp. 29-37.

[4.18] Forney, G.D., Concatenated Codes, M.I.T. Press, Cambridge, Mass., 1966.

[4.19] Berlekamp, E.R., Algebraic Coding Theory, Mc-Graw Hill, New York, 1968.

[4.20] Lin, S., and Costello, J.R., Error Control Coding: Fundamentals and Applications, Prentice-Hall Inc. New Jersey, 1983.

[4.21] Michelson, A.M., and Levesque, A.H., Error-Control Techniques for Digital Communication, John Wiley & Sons, 1985.

[4.22] INTELSAT Study Contract, No. 191, Final Report, Cyclotomics 1981.

[4.23] Lee, L., and Strickland, S.G., Adaptive FEC - Final Contract Report, COMSAT Laboratories, INTEL 222, RCE 008, 1982.

[4.24] Yasuda, Y., Kashiki, K., Hirata, Y., " Development of Variable-Rate Viterbi Decoder and its Performance Characteristics, " Proc. of the 6 th ICDSC, 1983, pp. XII-24--XII-31.

[4.25] Odenwalder, J.P., " Optimum Decoding of Convolution Codes, " Ph.D Dissertation, University of California, Los Angeles, 1970.

CHAPTER FIVE

AFEC TECHNIQUES USING DOUBLE CODING

The concept of AFEC using double coding was introduced in chapter 4. In the present chapter double coding gain and interleaving requirements will be analyzed and the results of double coding simulation will be presented. Performance of double coding will be compared with other concatenated codes and candidate codes for AFEC double coding will be chosen. As an illustrative example a conceptual implementation of AFEC using Golay double coding will be discussed.

5.1 Double coding gain

The idea of double coding is to improve coding gain by increasing the error correcting capability of the overall code compared to single coding. The above can be achieved if the errors which the first decoder fails to correct can be corrected by the second one. However, in the received sequence decoded by the first decoder the following two cases may happen:

1) The number of errors are less than or equal to the error correcting capability 't' of the code. In this case, the decoder successfully corrects the errors and outputs the correct information block.

ii) The number of errors in a codeword are more than 't'. In this case, the decoded information block still contains error.

It is to be noted that for the second case if a code word is in error, it is not always necessary that the corresponding information block is in error. The errors may occur only in the parity block and thus there are no errors in the information block. As the second decoder will receive only the information block from the first decoder, the information block error rate and error pattern is of concern only. Denoting information block error probability by P_I the following can be derived [5.1]:

$$P_I = \sum_{j=t+1}^{n} \binom{n}{j} p^j (1-p)^{n-j} - \sum_{j=t+1}^{n-k} \binom{n-k}{j} p^j (1-p)^{n-j} \qquad (5.1)$$

where

p channel bit error rate

n code length

k information length

t no. of correctable errors

Similarly, the post decoding BER can be derived using

$$P_b \leq \sum_{j=t+1}^{n-t-1} \frac{j+t}{n} \binom{n}{j} p^j (1-p)^{n-j} + \sum_{j=n-t}^{n} \binom{n}{j} p^j (1-p)^{n-j} \qquad (5.2)$$

$$- \sum_{j=t+1}^{n-k} \frac{j+t}{n} \binom{n-k}{j} p^j (1-p)^{n-j}$$

However, for moderate to high rate codes the last terms in Eqns. (5.1) and (5.2) can be ignored.

If the two decoders are cascaded, the second one receives the output sequence of the first one directly. The two decoders being identical, the second one fails to correct most of the post decoding error pattern of the first decoder. It can decode correctly only if the number of erroneous bits within the span of a codeword is up to the correcting capability of the code. Failure of the second decoder is due to the post decoding error pattern (i.e. channel memory) at the output of the first decoder. It is necessary to break this error pattern or make the channel memoryless by randomizing the bit sequence before passing it to the second decoder. In an ideal case of randomization the second decoder input will be BSC with transition probability p_1. The value of p_1 is derived from Eq. (5.2). Once p_1 is known the output BER p_2 of the second decoder can be calculated by replacing p by p_1 in Eq. (5.2).

Thus, in the process of double coding $p \rightarrow p_1$ and $p_1 \rightarrow p_2$ where $p \geq p_1 > p_2$.

Here, channel BER 'p' depends on bit energy-to-noise ratio $(\frac{E_b}{N_o})$. For a coherent PSK modulation, an AWGN channel, and coding with no rate reduction the BER 'p' can be determined by [5.2]

$$p = 1/2 \operatorname{erfc} \left(\sqrt{r \frac{E_b}{N_o}}\right) \qquad (5.3)$$

where

$r = k/n$ code rate

$\frac{E_b}{N_o}$ bit energy-to-noise ratio

and $r \frac{E_b}{N_o}$ indicates reduction in bit energy-to-noise ratio due to coding.

It is to be noted that for low BER ($\leq 10^{-5}$) satellite channels can be modelled as AWGN. Hence, the errors at the input of the first decoder is assumed to be of random nature. As a result the random error correcting codes are generally used. If due to reduced bit energy-to-noise ratio channel errors occur in bursts, then a scrambler after the second encoder and a de-scrambler before the first decoder will be used to randomize the errors during double coding application.

For TDMA/ AFEC applications in order to keep the data transmission rate constant, the information rate to the encoder is reduced. The transmission power being kept constant, $\frac{E_b}{N_o}$ does not change between coding or no coding. Hence, the channel BER 'p' to be used in Eqs. (5.1) and (5.2) is given by

$$p = 1/2 \operatorname{erfc} \left(\sqrt{\frac{E_b}{N_o}} \right) \tag{5.4}$$

For normal operating conditions $p >> p_1$. This means the BER at the output of the first decoder is less than the channel BER.

The performance of double coding can be estimated from the knowledge of its component code performance. In Fig. 5.1 a graphical method of finding the performance bound of double coding using the bound of its components is illustrated.

According to the no coding (i.e. raw channel BER) and single coding performance curves, if the input BER corresponds to 'a' then the output BER will correspond to 'b'. Thus, the BER reduces from 'a' to 'b' without any change in signal-to-noise ratio (SNR). Assuming a perfect scrambling which renders the output memoryless, the BER corresponding to 'b' is equivalent to 'c' for no coding and will be the input BER for the second coding. Now, the BER at the output will correspond to 'd'. As SNR remained the same 'd' will be shifted to 'e'. Thus, as a result of double coding, the BER changes from 'a' to 'e'. Analogously, all other points of the curve can be drawn.

In Table 5.1 performance bounds for different double codes (which have a rate 1/2 component code) are shown, from which the following points are observed :

i) If a high gain component code is chosen, the first TCG obtained is greater than the additional TCG obtained due to second coding.

ii) If a low gain component code is chosen, the first TCG and the additional TCG obtained due to second coding is about the same in terms of dB.

The above phenomenon can be explained as follows :

The net coding gain for a high gain code is greater than that of a low gain code. But, gain due to reduction of the information bit rate (or time frame

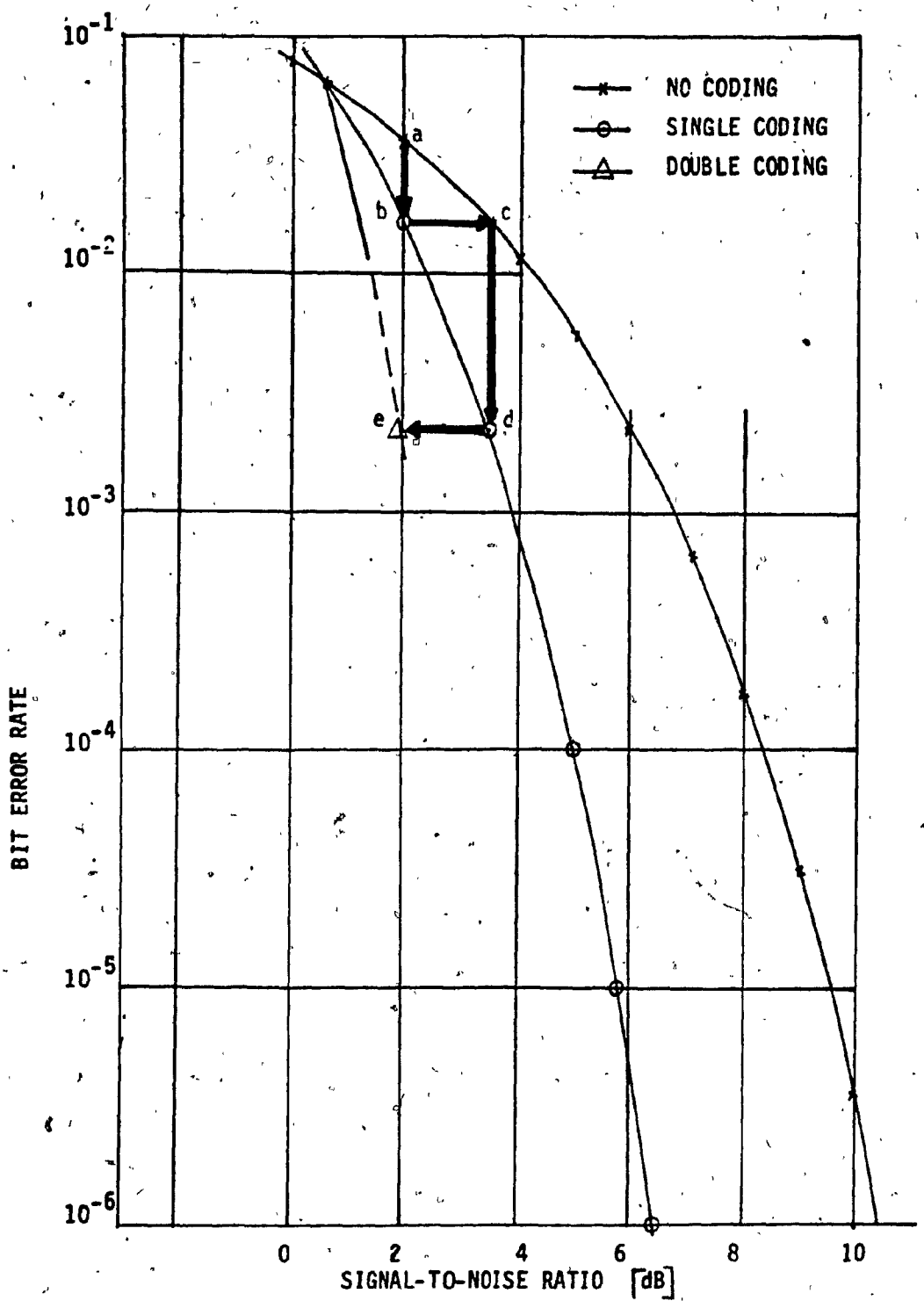

Fig. 5.1 Graphical construction of performance bound.

Table 5.1 Performance of double codes

Component code	Double code rate	TCG at a BER= 10^{-5} [dB]	Number of computations per information bit
(23,12) Golay	0.27	8.1	60
(31,16) BCH	0.27	7.6	418
(63,30) BCH	0.23	8.6	882
(63,36) BCH	0.33	8.0	776
(127,57) BCH	0.2	9.0	1742
(127,64) BCH	0.25	8.6	1622
(127,71) BCH	0.31	8.4	1502
rate 1/2, K=7 Convolution code (Vitebri decoding)	0.25	10.8	256

expansion) is almost the same for both the cases (because of the identical code rate). Hence the net coding gain constitutes a substantial part of the TCG for the high gain code. As the net coding gain obtained due to the second coding gets reduced, it causes a greater change in additional TCG.

It is seen in Fig. 5.1 that the performance curves of both the single code and double code intersect the no coding curve in the same place. However, the double coding curves are steeper than that of the single code. Thus, if it is possible to cascade more coder/decoders, the overall code performance curve should be steeper and tend to be parallel to the Y-axis. But, comparing the progressively diminishing additional TCG obtained at each successive coding, the multicascaded codes do not pose any practical interest.

The performance of double coding using the (23,12,t=3) Golay code was verified by computer simulation. The message block of 288 bits was first encoded into 552 coded bits. The bit sequence was then interleaved using a block interleaver of depth 23. The interleaved bit sequence was then re-encoded into 1058 bits.

The channel was simulated using a Gaussian noise distribution to corrupt the data bits. The corrupted data bits were then decoded, deinterleaved and decoded again in succession. The output is compared with the message bits to record the errors.

Fig. 5.2 shows the simulation model. In Fig. 5.3 simulation results of single and double code performance are illustrated. Using the graphical method of predicting performance curves for double coding (given in the previous section), the double Golay code was evaluated and illustrated in the same figure for comparison. It was found that the double coding performance obtained from simulation is in agreement with the prediction.

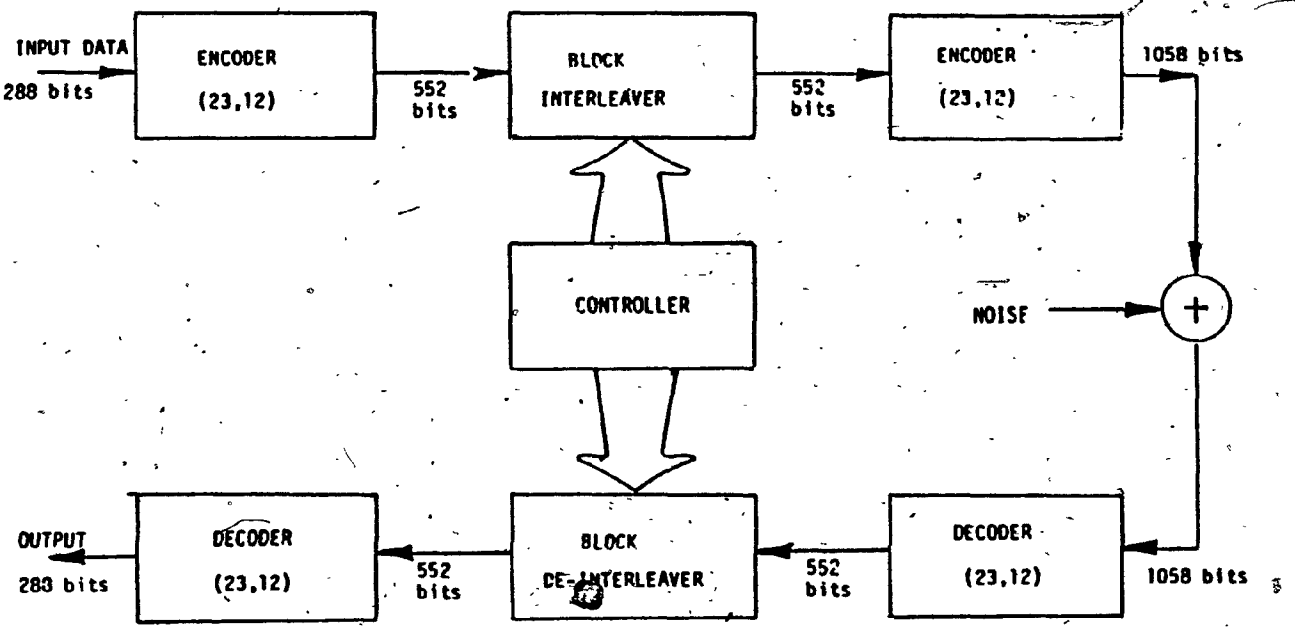

Fig. 5.2 Simulation model of double coding using (23,12) Golay code

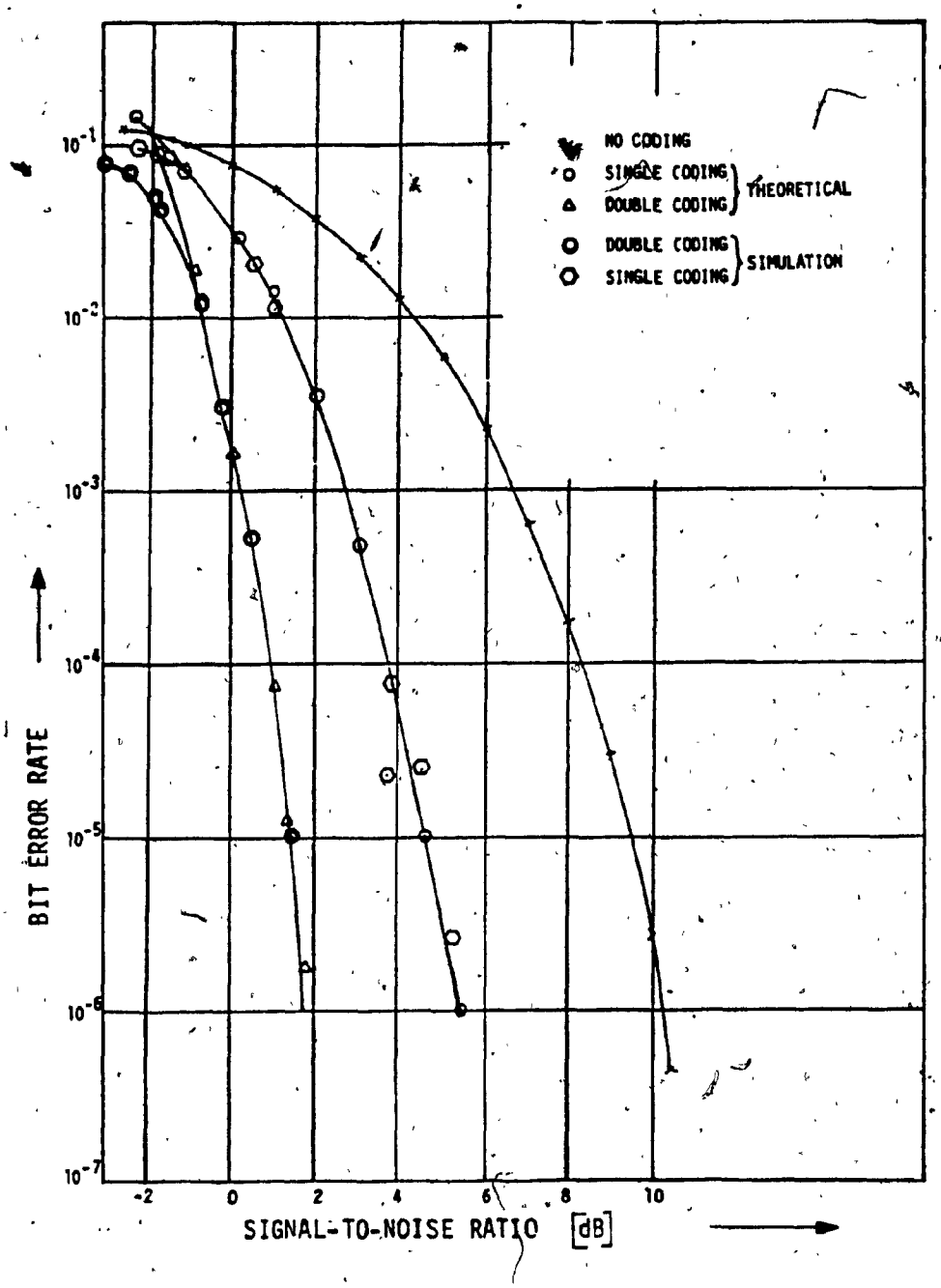

Fig. 5.3 Theoretical and simulation results for single and double Golay code.

5.2 Interleaver requirements

For double coding the information bits are first encoded, interleaved and encoded again before transmission. At the receiving end the reverse operation is carried out. Interleaving/deinterleaving is necessary to break the code memory at the output of the first decoder so that the second decoder can correct the errors made by the first decoder.

Interleavers can be classified into two broad groups [5.3]

i) block interleavers

ii) pseudo-random interleavers

For block interleaving the permutation or reordering of the sequence is a periodic function of time. A typical example of such interleaving involves taking the coded symbols and writing them by rows into a matrix. The symbols are read out by columns prior to transmission. For de-interleaving the received bit sequence is read into a matrix by columns and read out by rows.

For block interleavers, interleaving depth or the distance by which the two consecutive bits are separated after interleaving is fixed and determined by the number of rows in the matrix.

For pseudo-random interleaving the permutation is performed in a pseudo-random fashion. The interleaved bit sequence is chosen according to the sequence generated by the states of a maximal length feedback shift register. The feedback connections of the maximal length shift registers determine the order of sequence.

For a (n,k,t) code used as a component code, where

n code length

k information length

t number of correctable errors

the bits after the first encoder are interleaved such that no more than $\max\left\{ (t-1), 1 \right\}$ bits for the same codeword fall within an information block of k bits for the second coder. When $t > 2$, total number of elements from all the codewords which have more than one elements within the span of k bits, should not exceed t. This will ensure that if the first decoder makes an error in decoding $\max\left\{ (t-1), 1 \right\}$ codewords within an interleaving block, there will be at most $\max\left\{ t, 1 \right\}$ errors of the same codeword element at the input of the second decoder. In this situation, the output of the second decoder will be error free.

For block interleaving the above criteria can be satisfied by choosing an interleaving depth equal to a value which is a multiple of (buffer length/n).

For psuedo-random interleaving it is difficult to satisfy the above criteria. However, with an increase of buffer length (i.e. by interleaving long sequences), the random sequences are such that the above criteria are nearly fulfilled.

In Fig. 5.4 input vs. output error of the (23,12,t=3) Golay double code is shown for various depths of interleaving. The illustrated gain (which is taken as the ratio of BER_{input} to BER_{output} i.e. $\left(\frac{BER_{input}}{BER_{output}} \right)$) is normalized with

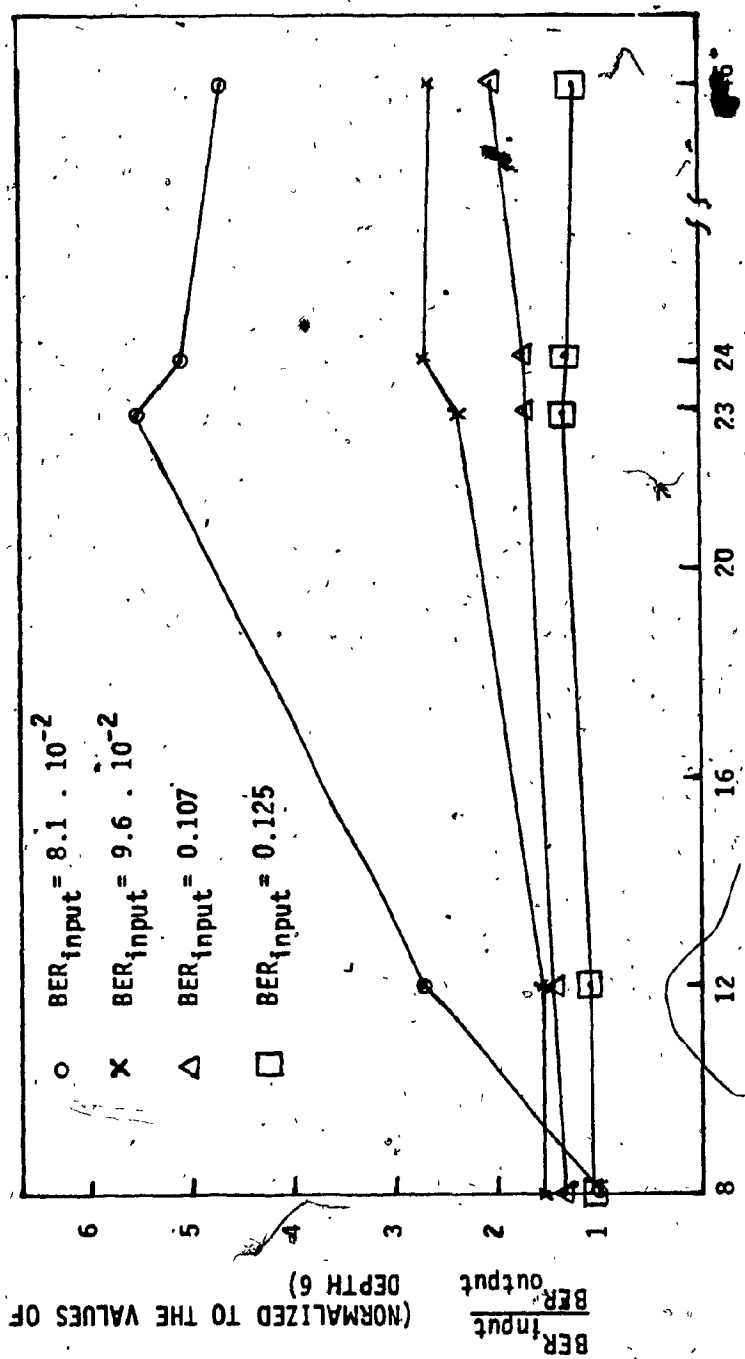

Fig. 5.4 Input BER versus gain for different interleaving depth

respect to the gain for interleaving depth 6. As can be seen, the gain increases with an increase of interleaving depth, and for a depth of 23 the gain is maximum. In this interleaving configuration at most one bit of the first decoded word can be in any codeword for the second code. If the first decoder fails, the error at its output which contains the message part is distributed among some of the 12 codewords of the second code. Thus, at the input of the second decoder errors occur randomly. The second decoder can only fail when four or more erroneous bits each contributed from an erroneously decoded first code are at its input. This is about the best that could be done.

In Table 5.2 the gain obtained for block interleaving of depth 23 (memory size 529) and that obtained from an equivalent pseudo-random interleaving (memory size $2^9 - 1 = 511$) is compared. For the latter interleaving, a slight degradation of code performance is observed.

Hence, for the present double coding (Golay code) scheme, a block interleaver of depth 23 seems to be the optimum choice.

5.3 Candidate double codes for AFEC

In Table 5.1 and Fig. 5.5 the TCG at a BER of 10^{-5} for different double codes discussed so far is summarized. Among block codes, the scheme using a (127,57) BCH code has the highest TCG (9.0 dB). However, the TCG for the scheme using (rate 1/2, constraint length 7) convolutional code (with Viterbi decoding) has an even better performance (TCG = 10.8 dB).

For the 'double coding' scheme using convolutional code, the first decoding uses soft decision decoding on the unquantized level output from the demodula-

Table 5.2 Input Bit Error Rate versus gain for block and pseudo-random interleaving.

BER_{input}	GAIN = $\frac{BER_{input}}{BER_{output}}$	
	FOR BLOCK INTERLEAVING OF DEPTH = 23	FOR PSEUDO-RANDOM INTERLEAVING ($2^9 - 1$)
0.124	1.98	1.93
0.111	3.75	3.48
$9.7 \cdot 10^{-2}$	8.02	6.47
$8.06 \cdot 10^{-2}$	32.38	22.29
$6.65 \cdot 10^{-2}$	297.67	70.03

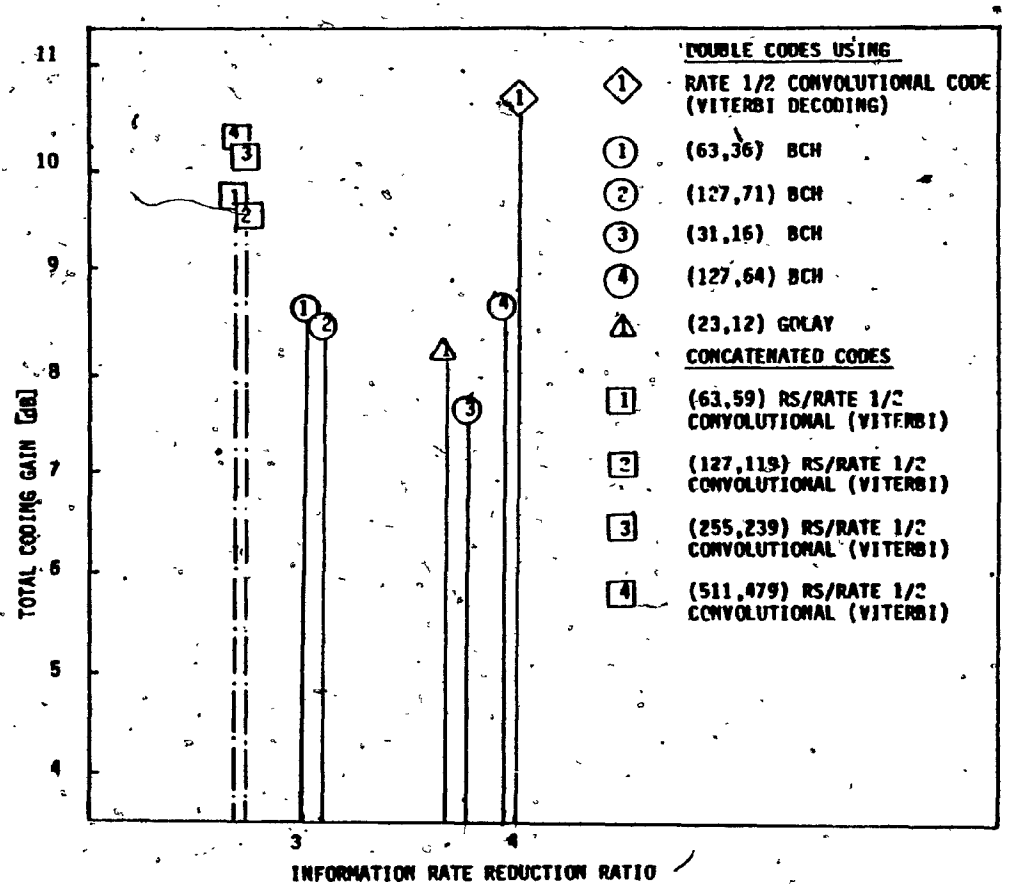

Fig. 5.5 Performance of double codes and concatenated codes of rate $\geq 1/4$

tor. The output of the first decoder is of fixed level (1 or 0), hence the second decoding is hard decision only. However, a Viterbi decoder equipped for soft decision decoding can be used for hard decision as well without any additional hardware.

The amount of decoding delay depends on the number of operations required multiplied by the time required to perform each operation. The basic unit of delay is the time required to perform an addition or shift a register. This basic unit is called computation [5.4]. Using the equations given in Appendix 5A the number of computations required to decode each information bit can be calculated. For a (127,57,t=11) BCH code the number of computations is 871. Where as, the required number of computations for (a rate 1/2, constraint length 7) convolutional code (Viterbi decoded) is $2^7 = 128$.

On the other hand, the double coding scheme using the (23,12,t=3) Golay code has moderate TCG (8.1 dB). The number of computations required for decoding of each information bit for single coding is 30, hence a substantial amount of savings in computations can be achieve in comparison to the earlier codes. But, the price to pay is reduction in TCG. It is expected that for the earth stations situated in less rain prone areas an AFEC scheme using Golay code could be very effective.

As found in Table 5.1 and Fig. 5.5, the TCG obtained for some double codes satisfy the high gain threshold (9.0 dB) required for the AFEC scheme. Performance of these codes is comparable to some of the best concatenated codes illustrated in Table 5.3. The concatenated codes have a higher overall code rate than the double codes, but the number of computations required per information bit for decoding of concatenated codes is also higher in comparison to that of double codes. For example, the number of computations per information bit required for

a (127,111) RS/convolutional code is 2794. It is far more than the number of computations (871) required to decode an identical rate (127,57,t=11) BCH code.

For high speed operation, parallel processing is required to reduce the decoding delay. In such a case the codes for double coding will require less additional circuitry as it has only one set of codecs. Whereas for concatenated codes which require two different sets of codecs additional circuitry will be comparatively more.

Considering the above facts, the advantages/ disadvantages of double codes compared to concatenated codes are summarized below in the context of AFEC applications.

Advantages

i) *Hardware simplicity*

ii) *Less number of computations required*

iii) *Efficient utilization of codecs*

Disadvantages

i) *Larger time frame expansion required because of low code rate*

Hence, double coding is most favourable for a resource sharing AFEC

scheme.

5.4 A conceptual implementation of an AFEC Golay double coding resource sharing scheme for high speed application.

The double coding AFEC scheme using Golay code has a moderate TCG with little coding/decoding delay (see Table 5.1). The Golay codes are simple to implement and suitable for high speed operation. In the following, the codec design and implementation will be discussed. Then the effective usable capacity of a double coding AFEC scheme using Golay code will be analyzed. Illustrative AFEC-TDMA system monitoring and control concepts will also be introduced.

5.4.1 Implementation of a high speed Golay AFEC codec

In the Golay code used, codewords of length 23 are obtained using the generator polynomial

$$g(x) = 1 + x + x^5 + x^6 + x^7 + x^9 + x^{11} \qquad (5.5)$$

and an additional overall parity bit is appended to make the codeword 24 bits long. The additional parity bit increases the code detection capability. Thus the extended Golay code permits detection of four errors and correction of up to three errors occurring anywhere within the codeword.

A. Encoder Implementation

The full hardware implementation of the Golay (24, 12) encoder is shown

in Fig. 5.6 and 5.7. As can be seen the modulo 2 summations and the generator polynomial g(x) are implemented by XOR gates placed between the storage elements of the parity generator shift registers. The logic 1 bit positions of g(x) determine the location of the individual XOR gates. To form the complete codeword the following is performed.

i) A block of 12 information bits is fed in, most significant bit (MSB) first, into one of the data storage shift registers. As the information rate is half that of the encoded data rate (i.e. clk out rate), 24 clk out periods are required to shift the 12 information bits.

ii) During the next 12 clk out periods the first set of 12 information bits is shifted out of the shift register and simultaneously fed to the parity generator and channel. As a result, at the end of the 12th clk out period, parity bit generation (11 of them) is completed.

iii) During the succeeding 12 clk out periods all 12 parity bits (including the appended overall parity bit) are sent to the channel.

While processes ii) and iii) are in progress another set of 12 information bits are simultaneously put into the second data storage shift register. Then the cycle is repeated with the new set of information bits.

B. Decoder Implementation

At the receiving end, information bits are recovered from the received sequence using syndrome calculation and table look-up to reduce the decoding

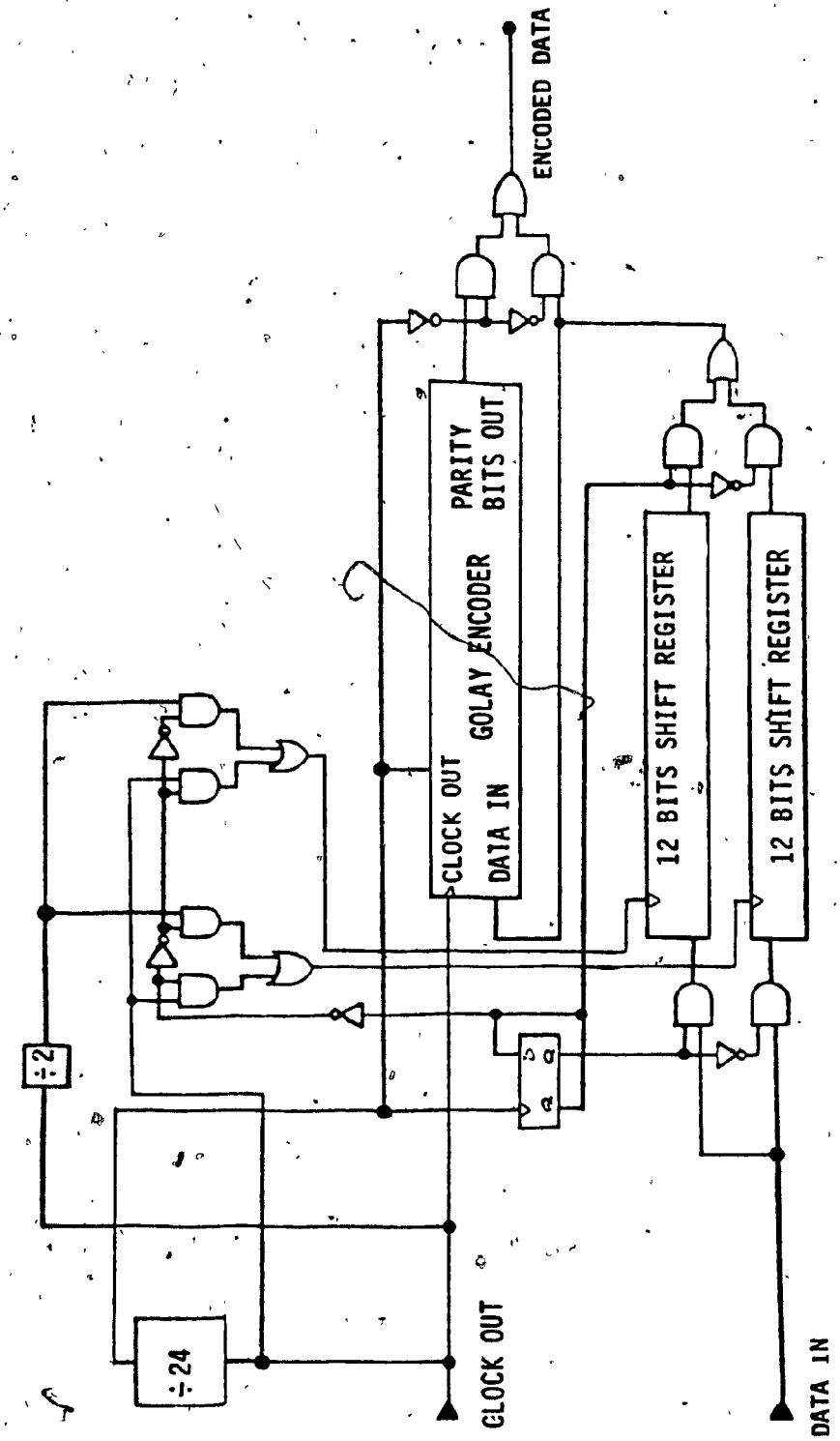

Fig. 5.8 (24,12) Golay encoder

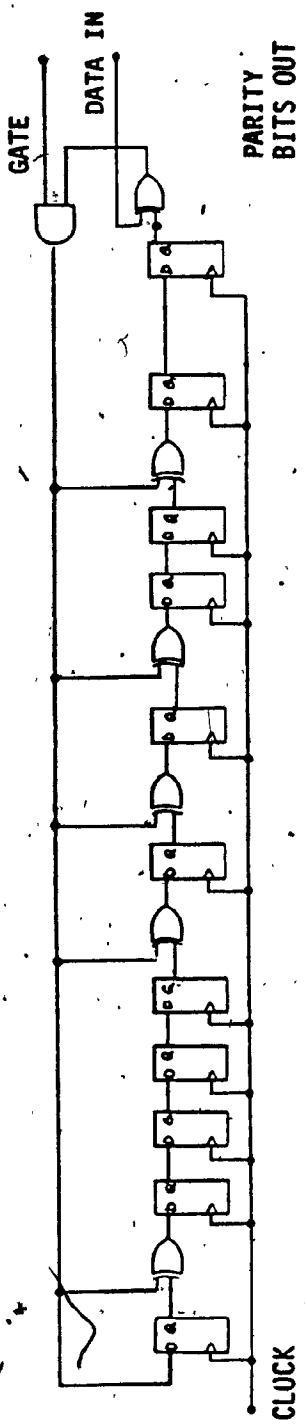

Fig. 5.7 Parity sequence generator for (24,12) Golay code

delay usually involved in Kassami [5.3] type decoding. As can be seen, the syndrome calculator is identical to the parity generator. The error pattern will identify the position of the erroneous bits. The decoder will correct the errors by inverting the information bits corresponding to the erroneous positions. However, the decoder fails when the number of errors exceed the correcting or detecting capability of the code.

Hardware implementation of the decoder is illustrated in Figs. 5.8 and 5.9. Decoding is performed in the following sequence.

i) The received codeword (24 bits) is shifted in sequence simultaneously into the received codeword shift register and syndrome calculator.

ii) At the end of the 24th clock period the syndrome will be ready. The syndrome serves as an address to the error pattern stored in ROM. The three preset counters are then loaded with the error location.

iii) After that, in synchronism with half clock rate, the first 12 bits are read out of the shift register and corrected according to the error location stored in the preset counters. At the end of 24 clock periods the decoding of the data is completed.

After the error pattern is located in ROM, the syndrome calculator is initialized to zero.

iv) As the data is shifted out of the received codeword shift register and corrected, the next sequence of 24 bits is shifted into the second received codeword shift register and syndrome generator.

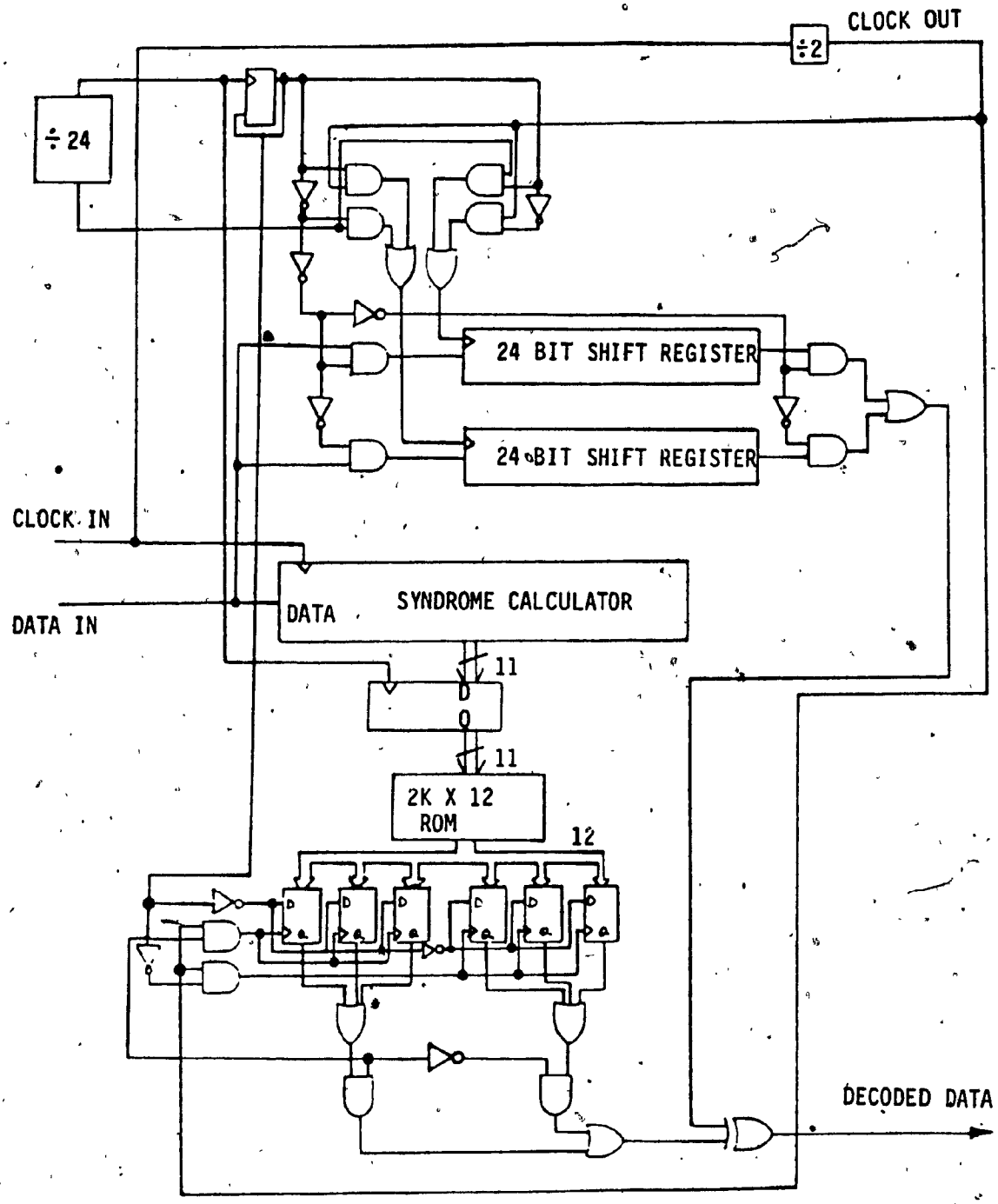

Fig. 5.8 (24,12) Golay decoder

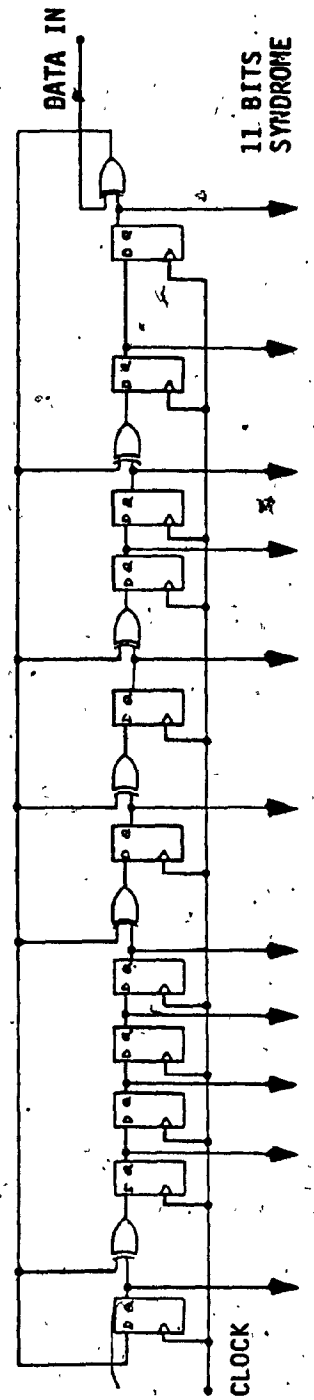

Fig. 5.9 Syndrome generator for (24,12) Golay code

The cycle of decoding continues in a similar manner.

For double coding applications the encoded words from the first encoder is stored and interleaved before being encoded again. Similarly, deinterleaving is performed at the receiving end before the second decoding. Implementation of the interleaver/deinterleaver has been studied in [5.3].

5.4.2 Monitoring and control subsystem

The proposed fade counter-measure scheme will have an impact on the design, operation and reliability of the overall TDMA network. In this section the system complexity is briefly discussed with emphasis on the following points :

Link Condition Monitoring

Power Control

Allocation of Resources

A. Link Condition Monitoring

Link condition monitoring is an essential factor for effective operation of the proposed AFEC scheme. Uplink and downlink conditions must be accurately and rapidly determined in order to apply appropriate rain counter-measures.

Previous study [5.5] recommended that a centralized architecture for monitoring is advantageous because of terminal costs, signalling overhead, and rain counter-measure system stability. In the centralized architecture, the master station monitors the bursts received from active traffic stations and then determines which of the traffic stations are suffering fades and require rain counter-measures. The link quality can be monitored with pseudo-error measurements for fast response. For example, a BER of 10^{-4} can be detected within 1 second [5.6].

B. Uplink Power Control (UPC)

In the proposed scheme uplink fade is assumed to be overcome by UPC techniques. Each earth station has a built-in UPC subsystem with pre-assigned power level steps.

As soon as the master station detects an uplink fade it informs the corresponding station to increase the RF transmitted power.

In case an UPC subsystem fails the master station commands the corresponding earth-station to shut off. The implementation of different UPC schemes was presented in [5.7].

C. Allocation of Resources

Once the master station detects a downlink fade, it sends a request to the Resource Assignment Controller (RAC) to assign necessary rain counter-measures from the available resource pool depending on the fade depth.

In the AFEC scheme RAC assigns codecs for the downlink transmission and allocates time slots from the reserved pool to accomodate the encoded bits.

Prior to the introduction of AFEC the RAC sends additional information to the affected earth stations regarding

i) Level of coding (low or high gain) to be used

ii) Preamble length

iii) Synchronization loop bandwidths

iv) Unique word detector threshold

v) Burst time plan (BTP), etc.

to allow possible adjustment and effective operation of the system under a degraded link condition.

The flow chart of RAC function is given in Fig. 5.10.

To increase the system reliability it is necessary to avoid multiple switching of rain counter-measure since each switching entails a number of changes in the traffic management. As the rate of fade variation increases with the intensity of rain, it is recommended that during the rainy period a higher gain codec be assigned for low fades to avoid switching for a short time as fade increases. This is particularly applicable for those earth stations situated in the rain prone region.

In general, the switching thresholds for codec application and withdrawal can be made different (i.e. hysterisis) so that fade fluctuations do not imbalance the system stability.

Carrier recovery, clock recovery, and unique word detection for burst and frame synchronization under fade conditions for TDMA systems have been investigated in [5.5]. Many results of this investigation are also applicable to our proposed scheme.

The proposed scheme requires that the system be capable of hitlessly responding within a short time to randomly occurring demands for resources to counteract the rain fades. For dynamic demand assigned (DA) TDMA systems the criteria is almost similar.

In DA-TDMA systems requests for new circuits to be established or an existing link to be protected are treated in a similar manner by system control. However, there are some minor differences between the requirement and operation of the proposed AFEC system under centralized monitoring and control with that of DA-TDMA.

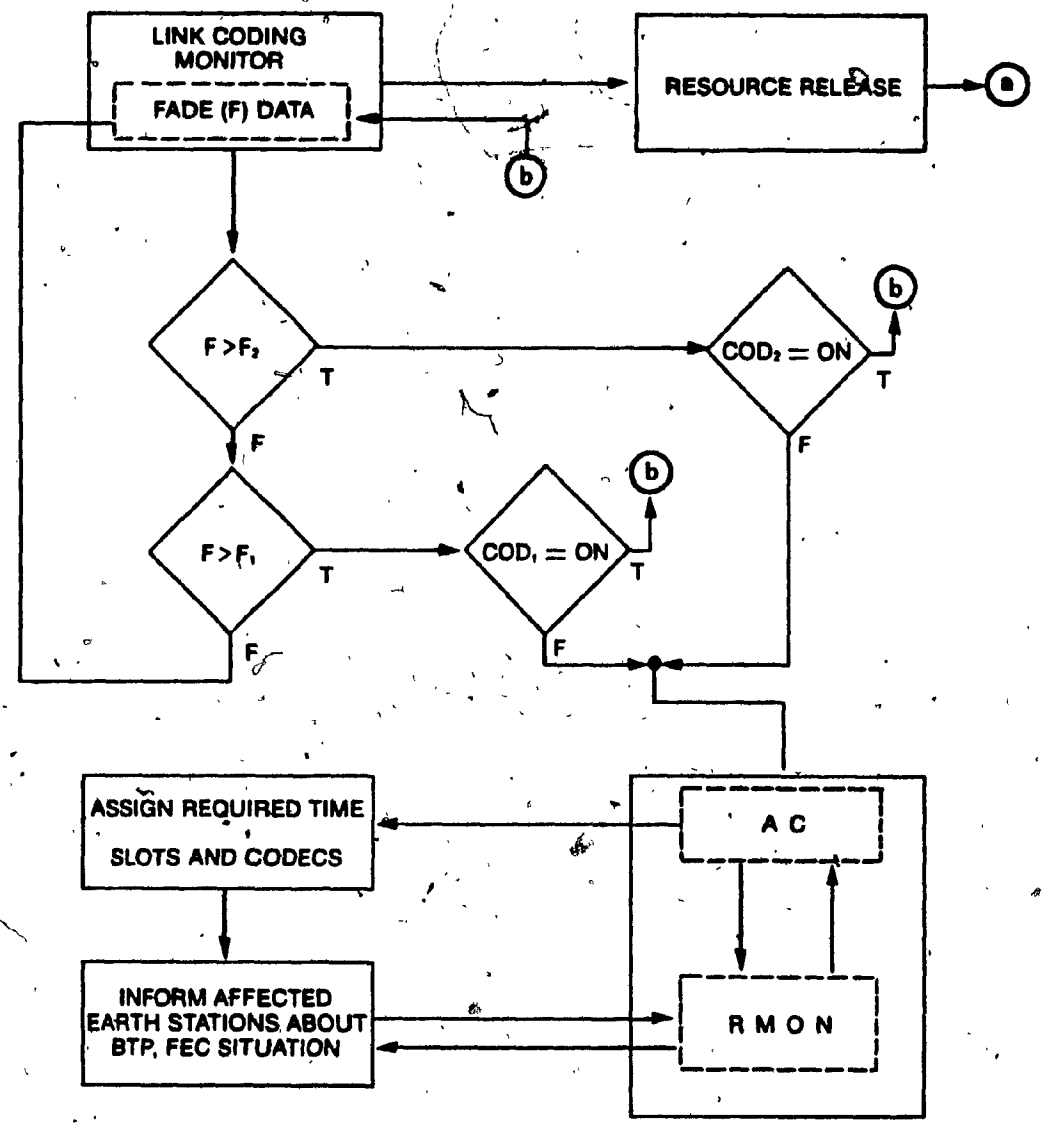

LEGEND:

AC	ASSIGNMENT CONTROLLER	RMON	RESOURCE MONITOR
BTP	BURST TIME PLAN	COD_1	LOW GAIN CODEC
F_1	FADE THRESHOLD FOR LOW GAIN CODE	COD_2	HIGH GAIN CODEC
F_2	FADE THRESHOLD FOR HIGH GAIN CODE		

Fig. 5.10 RAC function flow chart

i) Because of the continuous monitoring of fade, assignment of rain counter-measures is an automatic process and does not require a formal request.

ii) In a DA-TDMA system it is usual procedure that requests for capacity which cannot be satisfied immediately are placed on a queue of requests to be satisfied as the capacity becomes available. This 'call hold' does not degrade performance of the system. But, in the AFEC scheme, if the demand for rain counter-measures cannot be satisfied immediately an outage will occur.

Thus, DA-TDMA technology, with some minor changes, can effectively use the proposed AFEC scheme.

5.4.3 Analysis of the effective usable capacity of an AFEC scheme using Golay double coding

The Golay code can add 5 dB and 8.1 dB to the fade margin of an earth station in single coding and double coding applications respectively. Hence, the code can be used for two step AFEC resource sharing to overcome the rain attenuation of upto 8 dB above the built in fade margin. In the following, the effective usable capacity of Golay double coding scheme will be derived.

Denote the probability 'q' that a particular earth station experiences a fade depth between a and a', where a' > a. From Eq.(3A.15) it is known that

$$q = \alpha_{SDCF}\, \alpha_{SDF} \left(p(a) - p(a') \right) \qquad (5.6)$$

where

p(a) and p(a′): yearly average probabilities that rain attenuation exceeds a and a′ respectively.

α_{SDF} site diversity correlation factor

α_{SDCF} seasonal-diurnal correlation factor

Assuming the fades occur independently, the number of earth stations 'e' experiencing rain attenuation between a and a′ follows a binomial distribution

$$\Pr\left\{ \text{e out of N} \right\} = \binom{N}{e} q^e (1-q)^{N-e}. \qquad (5.7)$$

where

N total number of earth station

Denoting ($\Theta = e/N$) to be the fractional number of earth stations experiencing attenuation between a and a′, the mean and variance of the probability distribution of Θ is given by

$$y = E\{\Theta\} = q$$

and

$$\sigma^2 = \left[E\left\{\Theta^2\right\} - E^2\left\{\Theta\right\} \right] = \frac{q\,(1-q)}{N} \tag{5.8}$$

When $N \to \infty$ the variance $\sigma^2 \to 0$. As a result the fractional number of earth stations experiencing attenuation between a and a' equals q.

However, for large N the normal distribution may also be used for approximating binomial distribution. Therefore, as shown in [5.8]

$$\Pr\left\{ q - 3\sigma < \Theta \leq q + 3\sigma \right\} \approx 99.7\%$$

Using Eq. (5.6), the fractional number of earth stations experiencing attenuation of $a \leq A \leq a+5$ dB and $a+5 \leq A \leq a+8$ dB in the i-th climatic region (with 99.7% confidence) can be denoted as

$$\Theta_{1i} = \alpha_{SDF}\,\alpha_{SDCF}\left(p_i(a) - p_i(a+5) \right) \pm 3\sigma_{1i}$$

$$\Theta_{2i} = \alpha_{SDF}\,\alpha_{SDCF}\left(p_i(a+5) - p_i(a+8) \right) \pm 3\sigma_{2i} \tag{5.9}$$

The total number of affected stations in a system which require coding at any instant of time is denoted by

$$N_c = N \sum_{i=1}^{I} \left(\Theta_{1i} + \Theta_{2i}\right) m_i \tag{5.10}$$

where

N total number of earth stations in the system (which equals the number of traffic bursts as well)

l number of different climatic regions in the satellite coverage area

m_i fractional number of earth stations situated in the i-th region

The length of the resource sharing pool required in the TDMA frame to be used by the coded traffic can be derived as follows:

$$T_{RES} = N \Delta t \sum_{i=1}^{l} m_i \left[\left(\frac{1}{r} - 1 \right) \Theta_{1i} + \left(\frac{2}{r} - 1 \right) \Theta_{2i} \right] \qquad (5.11)$$

where

r code rate

Δt time allocated to each station

The resource pool can be effectively used by

$$N \sum_{i=1}^{l} m_i \left[\left(\frac{1}{r} - 1 \right) \Theta_{1i} + \left(\frac{2}{r} - 1 \right) \Theta_{2i} \right] \qquad (5.12)$$

pre-emptible traffic bursts during no rain fades.

The effective number of traffic bursts that can be accomodated is given by:

$$N_a = N \left\{ 1 - \sum_{i=1}^{I} m_i \left[\left(\frac{1}{r} - 1\right) \Theta_{1i} + \left(\frac{2}{r} - 1\right) \Theta_{2i} \right] \right.$$

$$\left. + \sum_{i=1}^{I} m_i \left[\left(\frac{1}{r} - 1\right) \Theta_{1i} + \left(\frac{2}{r} - 1\right) \Theta_{2i} \right] r \right\}$$

$$= N \left\{ 1 - \sum_{i=1}^{I} m_i \left[\left(\frac{1}{r} - r\right) \Theta_{1i} + \left(\frac{2}{r} - r + 1\right) \Theta_{2i} \right] \right\} \qquad (5.13)$$

The effective usable capacity of the system is given by

$$C_E = \frac{N_a}{N}$$

$$= 1 - \sum_{i=1}^{I} m_i \left[\left(\frac{1}{r} - r\right) \Theta_{1i} + \left(\frac{2}{r} - r + 1\right) \Theta_{2i} \right] \qquad (5.14)$$

For Golay code, r = 12/23. Hence, putting the value of ' r' in Eq. (5.14) the following is obtained:

$$C_E = \frac{N_a}{N}$$

$$= 1 - \sum_{i=1}^{I} m_i \left[1.39\ \Theta_{1i} + 4.31\ \Theta_{2i} \right] \qquad (5.15)$$

Thus, knowing Θ_{1i}, Θ_{2i} and m_i it is possible to determine the effective usable

capacity.

APPENDIX 5A

The amount of decoding delay depends on the number of operation required multiplied by the time required to perform each operation. The basic unit of delay is the time required to perform an addition or shift a register. This basic unit is called computation.

For BCH codes, the number of computations per information bit required to decode using the Berlekamp algorithm is given by [5.4]

$$N_c = N + 2m^2 - 2m + 7mt + 11t \qquad (5A.1)$$

where

t number of correctable errors

$N = 2^m - 1$ is the code length

The number of computations required using the Peterson algorithm is given by [5.4]

$$N_c = \frac{6N + 4t^3 + 15t^2 - 43t + 12tN + 24mt - 12m + 6}{6} \qquad (5A.2)$$

For RS codes, the required number of computations using the Berlekamp algorithm is given by [5.4]

$$N_c = 2N + 3mt^2 + 2t^2 + 13mt + 2m^2 + 16t - 2m \qquad (5A.3)$$

where

m symbol size

$N = 2^m - 1$ is the code length

Using the Gorenstein and Zierler algorithm the number of computations can be found by

$$N_c = \frac{6N + 6Nt + 4t^3 + 18t^2 - 43t + 24mt - 12m + 12}{3} \qquad (5A.4)$$

For convolutional codes with Viterbi decoding, the number of computations is given by [5.2]

$$N_c = 2^K \qquad (5A.5)$$

where

K = code constraint length

REFERENCES

[5.1] Yuen, J.H., (Editor), Deep Space Telecommunications System Engineering, Plenum Press, New York, 1983.

[5.2] Bhargava, V.K., Haccoun, D., Matyas, R., and Nuspl, P.P., Digital Communication by Satellite, John Wiley & Sons, New York, 1981.

[5.3] Clark, G.C., and Cain, J.B., Error Control Coding for Digital Communications, Plenum Press, New York, 1981.

[5.4] Simpson, R.S., Cain, J.B., A Study of Major Coding Techniques for Digital Communication , Final Report No. 101-102, NASA, NAS8-20172, 1969.

[5.5] Adaptive Forward Error Correction Techniques - Miller Communication Systems Ltd., DSS Contract, OST81-00249, 1982.

[5.6] Newcombe, E.A., and Pasupathy, S., " Error Rate Monitoring for Digital Communication ," Proc. of IEEE, Vol. 70, 1982, pp. 805-828.

[5.7] Ince, A.N., Brown, D.W., and Midgley, J.A., " Power Control Algorithms for Satellite Communication Systems ," IEEE Trans. on Communication, Vol. COM-24, 1976, pp. 267-275.

[5.8] Kreyszig, E., Advanced Engineering Mathematics, John Wiley and Sons, New York.

CHAPTER SIX

CONCLUSION

The rapidly increasing demand for satellite communication shows that conventional C- and Ku-bands will soon be saturated. As a result communication has to be carried out in higher frequency Ka-bands. The primary attraction of this band is the 2.5 GHz bandwidth available for communication purposes, which is five times that of either C- or Ku-bands. The large bandwidth can accommodate an increased traffic capacity. Moreover, in this band, because of the high frequencies involved, a large number of narrow beams can be generated with modest sized satellite antennas. Hence, frequency re-use will be possible by the generation of multiple spot beams, resulting in a manifold increase in the capacity of the geosynchronous arc [6.1].

Rain attenuation is a major factor in link condition degradation for Ka-band satellite systems. In the previous chapters rain fade situations in Ka-bands and its probable counter-measure schemes were studied. It was demonstrated [6.2] that in this band severe rain attenuation has seasonal and diurnal variation. Hence, maintaining high link availability requires a large fade margin but only for a small fraction of the overall time period. For example, in a typical earth station a fade margin of 11 dB is required to maintain a downlink availability of 99%. To increase the availability by another 0.9% (to 99.90%) the margin required is 20 dB. Whereas, to increase the availability by another 0.09% (to 99.99%), which is the standard for satellite links, the required fade margin exceeds 30 dB. As a consequence the conventional techniques of rain attenuation

counter-measure using dedicated resources of large fixed link margin or the alternative of widely applied site diversity are fully used only during occasional heavy rainstorms. Hence the measures are underutilized and not cost-effective, as a large portion of the system power is always kept on reserve, even when not required.

In search of a cost effective solution, adaptive rain attenuation counter-measure schemes were analyzed. These adaptive counter-measure schemes help to overcome rain attenuation at the time of its occurrence. Moreover, they will change adaptively with the intensity of attenuation.

In satellite systems each link has an allocation of three basic resources: power, bandwidth and time, which are used for information transmission purposes. The adaptive rain counter-measures, when applied, use a part of these resources, which reduces the link capacity. In order to maintain a constant capacity the idea of resource sharing was incorporated with adaptive rain counter-measure schemes. This was discussed in detail in this thesis.

Usually, the type of adaptive measures to be used depend on the multiple access scheme of the system. In this research, different multiple access schemes were studied. Considering the advantages of a TDMA scheme (flexibility and high capacity) compared to FDMA and CDMA, it was assumed that future satellites will predominantly use TDMA and have onboard processors. Hence, investigation was directed towards the evaluation of resource sharing adaptive rain counter-measure schemes suitable for TDMA applications. Implementation complexity, feasibility and performance of these schemes was compared. It was suggested that for uplinks power control techniques could be very effective in countering rain fade whereas for downlinks AFEC schemes associated with information rate reduction are most suitable.

Candidate codes for AFEC resource sharing schemes were investigated in this thesis, In consideration of the gain requirements, adaptive switching complexity and high speed operation, two AFEC schemes were proposed. The first scheme uses variable rate convolutional code and the second one uses RS/convolutional concatenated codes. The schemes have the potential to provide progressively adaptive fade margin of 10.1 dB and 10.4 dB respectively in excess of the system fixed fade margin.

However, the above schemes require two different codecs. For AFEC using a variable rate convolutional code, switching is done from a low gain (rate 1/2 code) to a high gain (rate 1/3 code) codec. For AFEC using a concatenated code, a (rate 1/2, constraint length 7) convolutional codec is used for low gain. For high gain, a (127,111) Reed Solomon code in conjunction with a convolutional codec is used.

Due to infrequent occurrences of large rain attenuation the schemes utilize their full resources only occasionally. In order to make efficient use of the shared resources of the system, an AFEC scheme using double coding was also introduced and its performance analyzed. For double coding application a single codec is used repeatedly for added gain.

It was shown that convolutional code and Golay code the double coding scheme can provide an adaptive fade margin of 10.8 dB and 8.1 dB respectively. Although concatenated codes have slightly better performance than double codes, hardware implementation and decoding complexity of the latter is significantly less.

Implementation complexity of a conceptual AFEC resource sharing scheme using Golay double coding was analyzed in light of time frame expansion, link condition monitoring, signalling, etc. It was concluded that the scheme can be

adapted to the present DA-TDMA system technology.

6.1 Suggestions for further research

Although the concept of resource sharing AFEC and performance of different schemes were extensively studied in this research, there are undoubtedly other interesting aspects which were not covered. Some suggestions for further research are :

Matched interleaving/deinterleaving

For double coding AFEC the interleaver/deinterleaver in the codec plays a very important role. It acts like a buffer and also breaks the memory of the first coder/decoder. Hence, it is required that the interleaver/de-interleaver be matched to the code length, post decoding error distribution etc. to obtain optimum performance. In this research, interleaving/de-interleaving is extensively studied for Golay code. For a block interleaver, double coding performance improved with an increase in interleaving depth. The optimum interleaving depth was found to be equal to the code length. The result applies for other block codes as well. However, interleaving/deinterleaving for double coding using convolutional codes has yet to be studied.

Implementation considerations of synchronized codec

In AFEC schemes it is assumed that a codec can be switched on and off or can be switched from one code rate to another under external command without interrupting the data flow. However, for each transition there is a variation in processing delay, change in the rate of information transmission, etc. Hence, in order to achieve lossless data transmission, the aspects of buffer requirements, variable clock rate, codec synchronization, etc. warrant further study.

Monitoring and control Signalling

Monitoring and control Signalling is essential for the successful operation of any AFEC scheme for satellite systems. A detailed study is required in this direction to come up with a feasible solution which is effective for all rapidly changing fade situations.

REFERENCES

[6.1] Hornstein, A., " An Integrated Design Approach to 30/20 GHz Trunking Systems ," IEEE Journal on SAC, Vol. SAC-4, 1983,pp. 589-599.

[6.2] Lin, S.H., Bergman, H.J., and Pursely, M.V., " Rain Attenuation on Earth-Satellite Paths-Summary of 10-year Experiments and studies , B.S.T.J, Vol. 59, 1980, pp. 183-228.